Prestressed Concrete Structures under Blast Loads

Tasch Samoray

School of Engineering

Thesis submitted for examination for the degree of Master of Science in Technology.

Espoo 24.8.2017

Thesis supervisors:

Prof. Jari Puttonen

Aalto University
School of Engineering

AALTO UNIVERSITY
SCHOOL OF ENGINEERING

ABSTRACT OF THE
MASTER'S THESIS

Author : Tsach Samoray

Title: Prestressed Concrete Structures Under Blast Loads

Date: 24.8.2017 Language: English Number of pages: 115

Department of Civil Engineering

Professorship: Structural Engineering

Supervisor: Prof. Jari Puttonen Code: RAK.thes

The design and analysis of protective structures and structural systems is a complex and challenging task.
The need for such structures being ever so greater, the paper is set out to challenge the assumption made by the Israeli Defense forces Home front commands directives regarding the use of high strength steel in the construction of structures to be used as sheltered spaces. High strength steel is very often used in the fabrication of prestressed concrete elements, which in turn are frequently used in the construction of large span structures.
The use of such technology is therefore effectively barred from taking place when it comes to protective structures in Israel.
The use of non-linear energy method based calculation for carrying out a performance based analysis of structures using advanced computer codes has relatively recently been implemented as a method of evaluation of structures ability to resist seismic actions.
This paper explores the possibility of using prestressed concrete systems to protect against air-blast loads and to compare such different systems performance to traditional RC structures, using the same method of analysis

Keywords: Prestressed concrete, Blast Load, Civil Defense, Performance Based Design

Contents

1. Introduction

Preface

The object of this thesis is to comparatively evaluate the performance of several pre-stressed concrete structural systems under blast loads.

The need for structures able to offer protection against an attack had existed for ages.

During the 20th century, with the advent military aviation and the development of advanced artillery, rockets and missile systems, as well as the prevalence of explosive charges used in urban guerrilla and terrorist attacks, the need for assuring the protective capability of public structures is never greater. The global urbanization trend is increasing the need for large public structures that may also serve as shelters against possible attack.

Pre-stressed concrete technology has existed for several decades and is a popular method for both the construction of large span and heavy load ceilings, as well as for bridges and other type of infrastructure.

In such structures, high strength steel is often used in order to properly utilize the tensioning force in the creation of a balancing load. Such steel is not as ductile as the steel used in ordinary strength reinforcement bars, commonly found in RC structures. This is assumed to limit the performance of the tensioned element under dynamic loads in general and blast loads in particular.

In addition, the different behavior in sectional response between different tensioning systems as well as the structural designs and layouts that they enable, cause structures that use different tensioning technologies to preform differently under blast loads.

These are the phenomena that this thesis is set out to investigate, using numerical calculation methods, and based on previous knowledge.

Motivation

According to UN statistics (Marc, 2016), it is estimated that 90% of war casualties in the 21st century are civilians. The undeniably increasing threat of terrorism, as well as the ongoing trend of warfare moving more and more from the battlefields of old and into urban settings, presents a challenge for 21st century engineers.

Examples for the threat of war entering cities can be found in mass at the war torn streets of Middle- Eastern cities and villages, as well as in North Africa and Ukraine. Once limited to areas of ongoing conflict such as Lebanon and Israel, Terrorism now brings the threat of bombs into western cities as well.

The need for protected spaces such as dedicated bomb shelters, in-house civil defense spaces etc. is expected to increase, not decrease in the upcoming years.

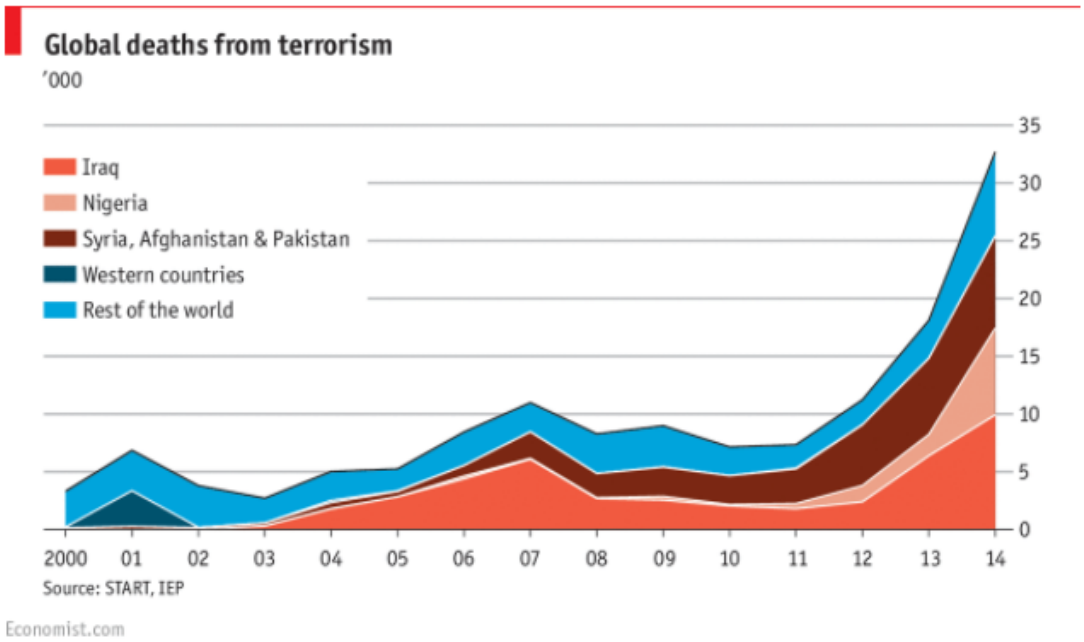

Figure 1 – Global deaths from terrorism Source: Economist.com

During my design work I have come across several instances in which civil defense considerations were a factor.

In one case, a railway bridge under design was requested to be tested for its capacity to withstand a truck bomb attack. The ~30m span bridge segment's superstructure consisted of two precast, post tensioned beams supporting the slab and the surface structure. This forced the designer to find a way to consider the effects of the blast on the prestressed superstructure.

The second case was of an underground station, which was also to serve in case of emergency as an ad hoc public shelter. The station's top slab was to be constructed in two stages, for reasons of traffic overhead. For that reason the casting of the slab had to be stopped close to the middle of the span. Moreover, the large span made it impossible for

normal reinforcement bars to be used without lapping. Reluctant to use lapped bars in a 100% lapping at mid-span, the design firm suggested using pre-tensioning for the structure, as it also seemed to be the natural structural solution for a large span bearing a large load. However, due to the IDF's home front command (IDF Home Front Command, 2012) regulations, the use of pre-stressing in civil defense structures was prohibited.

According to its regulations The IDF home front command prohibit the use of steel stronger than s-400 for the construction of main structural elements (beams, walls, ceilings) of shelters and other civil defense structures. The regulations specifically prohibit the use of cold drawn steel reinforcement from being used. The assumed reasoning behind the regulation is that the higher strength, cold drawn steel does not provide the ductility necessary for sufficient performance under blast loads.

Out of the belief that there is value in testing the claim that the mere use of higher strength steel in a cross-section is not enough to predict inferior performance under blast loads, this research is carried out.

Upon primary consideration, as mentioned before, the possibility of having lapped reinforcement in a structural element, especially cases in which 100% lapping (common when using premade steel meshes) is expected to yield lower ductility in the relevant cross sections and may worsen the resistance capacity to blast load of the structure.

Even in the case of using mechanical couplers to splice the reinforcement bars it is shown <> that only a 10-15% elongation is achieved, which is similar to that of s-500 steel and even higher strength steel.

Moreover, (US DoD, 1990) dedicated a chapter to the use of precast prestressed elements. It also includes a basic calculation example of a prestressed double Tee element.

While expressing the difficulty involving such a design, specifically the limitations in ductility, the smaller maximal elongation of the steel at rupture and the allowance for small deflections only, **the manual does not prohibit the use of such elements or of such steel.** Moreover, it does not demand or even recommend the use of mild steel reinforcement as additional bending reinforcement, with the exception of rebound reinforcement. This is evidence to challenge the notion that using pre-stressing in shelter construction should not be necessarily prohibited.

Prestressed concrete had several advantages due to the very nature of the technology. It allows the introduction of loads opposing gravity loads and deflection control. It also enables the efficient use of high strength concretes and even more so, the use of high strength steel in order to produce more compact sections.

From a structural mechanics stand point, the more compact and flexible the section, the more likely it is to resist large dynamic loads successfully, compared to more massive, under-reinforced sections. This is of course depends on its strength and deformability.

Naturally, such sections are also expected to be more efficient since less of their load bearing capacity is wasted on their own self weights. In addition the reduction in the

structures overall size will also likely lead to a reduction in cost. Also, when properly designed, the combination of high quality concrete and deflection control using pre-stressing allows increasing the element's service lifespan.

As mentioned before, Pre-stressing allows and enables the use of longer, continuous reinforcement. This is to be seen as an advantage over mild steel reinforcement bars and especially meshes, which often are lapped when the spans grow larger, due to their limited length, due to limitations of fabrication and transport.

The disadvantages in the use of prestressed concrete are however also important to consider; the high strength concrete used may be more brittle in case of concrete of nominal strength higher than 50/55 (EN). This however may be possible to mitigate to a degree using confinement, as the Mander model (Reddiar, 2009) shows. Concrete confined with reinforcement is not only expected to fail at a higher stress than otherwise, but is also expected to sustain a larger ultimate strain.

The steel is also limited to about 3.5% -4% elongation at rupture, in case of high strength strands (ISO 6934-4, 1991). This is potentially expected to reduce the ductility of the sections and therefore the flexural deformability of the structural element overall. Moreover, mild steel behaved differently when the loads are introduced very rapidly; reducing the advantage the high strength steel has due to its strength. While this is true, it is also worth mentioning that new steel fabrication methods replacing cold drawing is producing reinforcement that exhibits improved elongation.

Stronger prestressed steel is also more vulnerable to corrosion and heat. In the case of attack scenarios involving massive heat shock loads (as with explosions involving Liquefied petroleum gas), it is undoubtedly a disadvantage, especially if not mitigated using mild steel in conjuncture.

Another possible disadvantage of prestressed concrete is that, by its very nature, introducing additional loads to the structure. The fear of a localized failure due to extreme loading may cause a failure cascade due to the internal pre-stressing forces in the element is believed to be the cause of an intuitive reluctance to use pre-stressing where such accidental damage can occur. This is especially true in the case of unbonded strands or cables. The idea that a rupture in the reinforcement can lead to a violent release at the anchorage points and following damage is often mentioned. The fact is, however, that local damage can be sustained using lateral mild reinforcement, additional reinforcement in the direction of the strands and redundancies in the static scheme of the structure.

In conclusion, the need for the investigation of pre-stressed concrete structures is not only relevant since such existing structures might come under attack regardless, but also there is reason to believe that using proper design practices, the resistance of structures constructed using prestressed concrete may be sufficient to the point that a blanket prohibition of it no longer makes sense.

2. Blast as a structural load

Nature of the problem

An Explosion is defined as a sudden and rapid release of energy.

There are different types of explosions – physical, chemical or nuclear. Physical explosions can occur due to a rapid release of gas from a ruptured pressure vessel. Nuclear explosions caused due to a nuclear chain reaction and great the energy it involves. Chemical explosions are caused by a powerful, rapid exothermic reaction. Such a reaction may be the oxidizing of fuel or the separation of an unstable molecule.

An example of chemical explosion is that which is caused by the combustion of liquefied petroleum gas. Such reactions are very energetic and create a long thermal pulse. Explosive compounds are classified according to their role in the detonation process and the velocity in which the reaction front moves within it.

Primary explosives are easy to react and usually used as an initiator of the secondary explosive. Secondary explosives require a higher temperature and pressure to detonate. Some explosive devices may involve a tertiary explosive, following the same principle.

Classifying explosive materials according to reaction velocity separates them into high and low explosives. Low explosives are those in which the reaction travels at a subsonic velocity, and are used as propellants. Low explosive deflagrate rather than detonate. Two examples for low explosives are nitrocellulose and cordite.

High explosives are those of which the explosive shock front is supersonic. These explosives usually possess a shattering quality, the measure of which is called "brisance". High explosives are those who are usually used for weapons as well as for demolition.

While examples for high explosives are many, and include TNT, dynamite, RDX, HMX, ANFO and many others. (Ngo, Mandis, Gupta, & Ramsay, 2007)

This paper focuses on the effects caused do to the blast loads imposed on structures due to the detonation of high explosives.

Explosions can be classified as either unconfined or confined, according to the location in which they occur in relation to a confining structure or environment.

The unconfined explosions are further classified to:

1. Free air burst explosion – takes place in mid-air and reaches the target directly, without any amplification due to being reflected
2. Burst explosion – takes place above the target, so that the blast wave reaches the ground before it reached the target, and therefore is amplified.
3. Surface burst explosion – takes place close to or at ground level.

According to (US Department of Defense, 2014), the distinction between a burst explosion and a surface burst explosion is having the latter take place beneath the height of a one or two story building, i.e. 3-6 meter above ground level.

This paper is focused on unconfined explosions exclusively, and furtherly upon burst explosions specifically.

When a high explosive detonates, the explosive material is converted into dense gas, high in pressure and temperature. About one third of the material detonates, while the rest deflagrates and does not contribute to the formation of the blast effect. Pressures immediately behind the shock front can exceed 300 kilo bars, and temperatures may exceed 3000 ^{0} C. The expanding hot gases are creating a shock wave which expands outwards from the explosive material and towards the surrounding air.

The shock wave travels outwards, reflects off the ground and impinges on surrounding structures, which are later engulfed by it. As the wave travels onwards, it becomes less energetic, longer in duration and slower (TM 5-1300, 1990) The pressure within the shock front is known as the "incident pressure".

When the pressurized air particles in the shock front reach a barrier, they are pressured onwards by the particles moving behind them, increasing the pressure inflicted on the barrier. This is known as "reflected pressure" and is always higher than the incident pressure, in extreme cases by up to a factor of 10 (Swisdak, 1994). As a general rule, the stiffer the target is, the greater the increase factor due to reflection will be.

Once the shock front has been reflected off the obstacle, the obstacle is subjected to the under-pressure wave that follows behind the shock front, creating what is known as the "negative phase". The negative phase is less intense than the positive phase, and is also usually longer in duration.

The negative phase tends to be more significant the further away the target is from the charge. It also depends heavily on the geometry of the problem – the dimensions of the target as well as the shape of it and the angle of incident.

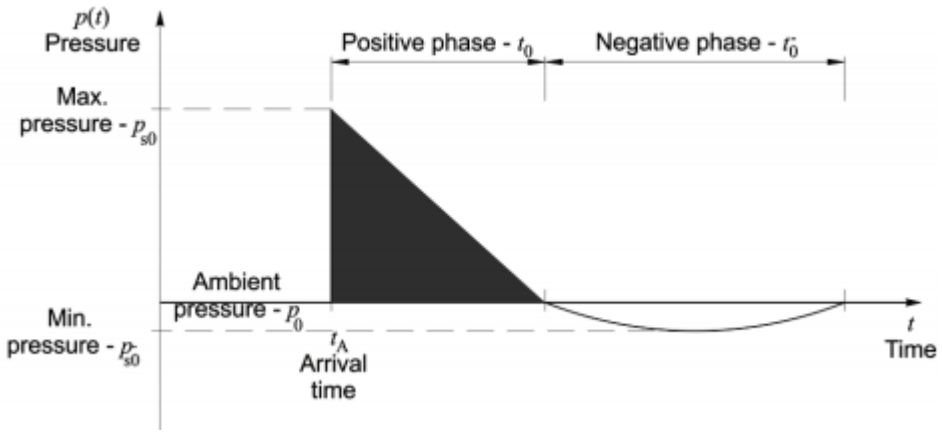

Figure 2 – Incident pressure time – history (Draganić & Sigmund, 2012)

Humans are in danger of suffering the negative effects of a blast loads when exposed to it, which include overpressure effects, injury inflicted by fragments and shock effects, whether carried by air or by ground. Combined with that is the danger imposed by secondary effects such as structural collapse, fire and smoke.

Data concerning human survivability of explosions exists and is used in order to evaluate the causalities resulted from any given attack scenario.

Blast theory

Research to measure, quantify and predict the loads imposed on structures due to blast loads had begun near the beginning of the 20th century, with the bulk of the research carried out during the mid-20th century. The research is still ongoing today.

Blast load prediction methods relied on semi-empirical methods, i.e. the loads imposed on a structure by the detonation of a charge would be predicted using existing experimental data, by looking up a similar case, not based on a complete analytical model, but relying in part on analytic principles.

In recent years and following the rapid development of computer technology, computer methods and CFD (computational fluid dynamics) programs have been considered and researched as a possible prediction method (Ngo, Mandis, Gupta, & Ramsay, 2007) (Rigby, Blast Wave Clearing Effects on Finite-Sized Targets Subjected to Explosive Loads, 2014).

Scaling laws were first theorized by Hopkinson (1915) and Cranz (1926), are a key concept for the semi empirical method. The idea is that since the blast energy is dissipating in all 3 directions, some of the effects of a certain charge at a set distance can be similar to those created by a larger charge at a further distance or of a smaller charge at a closer distance.

This gives birth to the concept of "scaled distance", which is calculated as:

$$Z = \frac{R}{W^{1/3}}.$$

Equation 1

with Z being the scaled distance, R the distance to the target and W the weight of the charge.

Since different explosives have different energy densities as well as other characteristics (blast velocity, brisance), they have to be converted into a TNT equivalent charge weight.

This is done usually by applying a conversion factor, although systems of correction factors accounting for various resulting effects (arrival time, duration etc.) also exist.

Name of explosive	TNT equivalent mass factor	
	Peak pressure	Impulse
TNT	1.00	1.00
C3	1.08	1.01
C4	1.37	1.19
CYCLOTOL	1.14	1.09
OCTOL 75/25	1.06	1.06
TETRYL	1.07	1.05
HMX	1.02	1.03
AMATOL	0.99	0.98
RDX	1.14	1.09
PETN	1.27	1.11

Figure 3 - Example of a conversion table for TNT equivilant weight. (Karlos & Solomos, 2013)

Formulas for predicting the blast effect characteristics were developed during the mid -20th century, mostly as means to predict loads imposed due to nuclear explosions, in terms of TNT equivalence. Friedlander (1946) had developed a simple expression for the incident pressure wave over time:

$$p_r(t) = p_{r,max}\left(1 - \frac{t}{t_d}\right)e^{-b\frac{t}{t_d}}$$

Equation 2

Formulas for predicting the peak incident pressure by way of scaled charge were developed by Brode (1955), Newmark and Hansen (1961), Kinney (1985) and Mills (1987).

The Brode and Newmark and Hansen expressions were found to be less accurate for conventional explosions, since they were originally developed for estimating nuclear explosions. (Karlos & Solomos, 2013)

Perhaps the most often used set of prediction formulas was based on the Kingery-Bulmesh (1984) research, which was used in the creation of the TM-5-1300 manual.

The Kingrey – Bulmesh predictions are defined by a series of charts, which also include value predictions of peak incident pressures and reflected pressures.

The charts also allow for the prediction of time of arrival, positive phase duration, shock wave speed and blast wavelength.

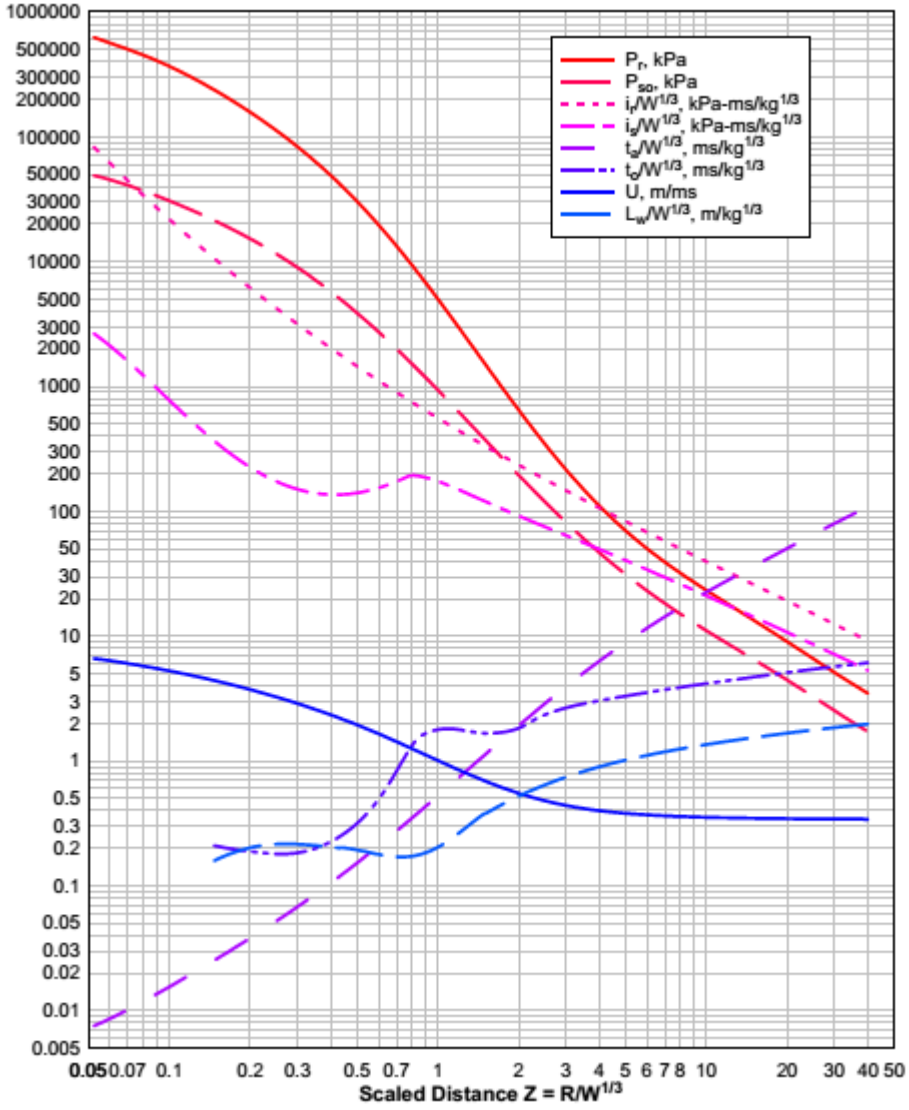

Figure 4 - Blast load parameters for the positive phase , free air burst of a spherical charge (Karlos & Solomos, 2013)

The function and resulting effects of an Explosive charge depend on its shape and the location of the detonator, which affects the direction in which the detonation wave travels both within and away from the explosive mass.

While the original research and manual included only effects caused by a spherical charge, with the detonator placed at the center of the charge. Later manuals such as UFC 3-340-02 (2008) included other types of chrages, such as the very common cylindrical charge.

The effects of the shockwave being reflected off the ground and other hard objects can be somewhat considered by applying factors, as well as the possible absorption of energy by other objects. However, in order to consider these in a more accurate manner, more complex methods of analysis must be used.

As mentioned, blast wave – structure interaction is complex and requires an elaborate numerical analysis in order to be considered in an accurate fashion. Instead, usually the target structure is considered infinitely rigid as a safe-side assumption.

Furthermore, in order to consider the type of response the structure will have, its fundamental natural period (the inverse of the lowest natural frequency) needs to be calculated and compared to the total duration of excitation. If the structure has a much longer natural period than the duration of the load by a factor of 4 or more (which is the most common case), the load is considered impulsive.

If the loading time is similar to the natural period of the structure, the loading will be more sensitive to the maximum pressure values; until in theory will reach the quasi-static state.

As mentioned, since most structures have a fundamental natural period that is much longer than the loading duration (which is measured in milliseconds), the load will normally be considered impulsive. (Karlos & Solomos, 2013)

The load definition algorithm according to the UFC -3-340-02 is as follows:

1. Determine the weight if the charge, distance and relation to the target and distance of the charge from the ground
2. Apply a safety factor of 20%
3. Select the points upon which pressure should be calculated, and calculate the (scaled) distance from the charge, angle on incident and distance from the ground and the edges (for clearing effects)
4. Determine the explosion parameters - scaled impulse, Peak overpressure, length of the positive phase, blast wave velocity and time of arrival. For scaled values, multiply with the cubic root of the charge weight to obtain absolute value.
5. Determine the value of the peak reflected pressure and impulse for the front façade (facing the charge)
6. Calculate the clearing time using the speed of sound and the geometric parameters for each point
7. Determine the fictitious (simplified) parameters - positive phase duration, reflected pressure, negative phase duration, and peak negative pressure.
8. Repeat the process for the side and back facades
9. Apply the time-history loads calculated for each point.

The load time history is simplified into two triangular wave phases, positive and negative, of a dynamic impulse equal to that predicted by the relevant curve for an exponential decrement.

$$t_{of} = \frac{2i}{p}.$$

Equation 3 – Fictitious phase duration for a simplified triangular load

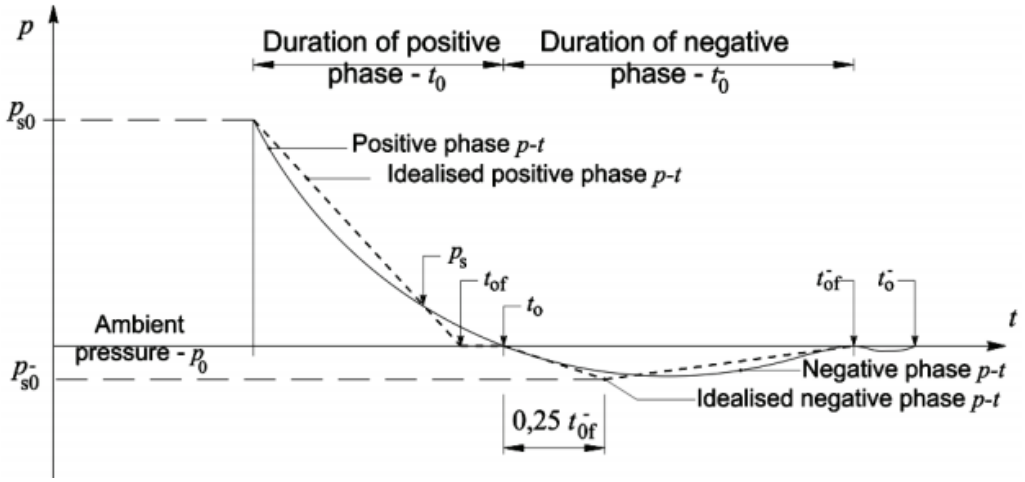

Figure 5 – Simplified time-history load (Draganić & Sigmund, 2012)

The angle of incident affects the reflected pressure in a non –linear way, as described in this figure:

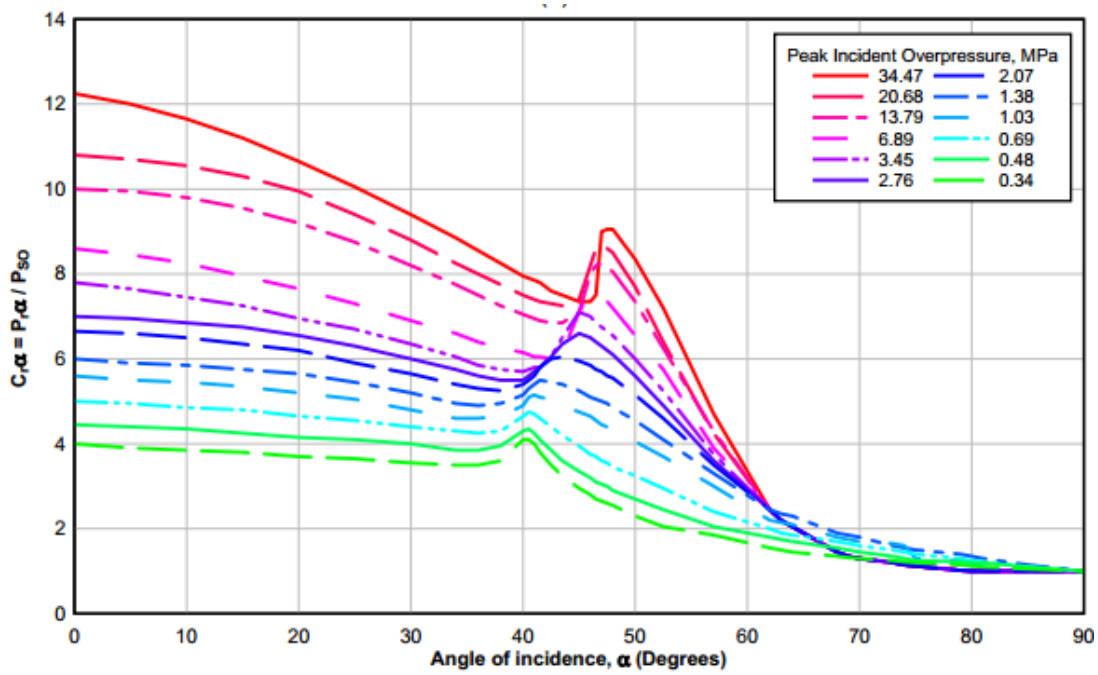

Figure 6 – Pressure increase factor die to reflection or large pressures (Karlos & Solomos, 2013)

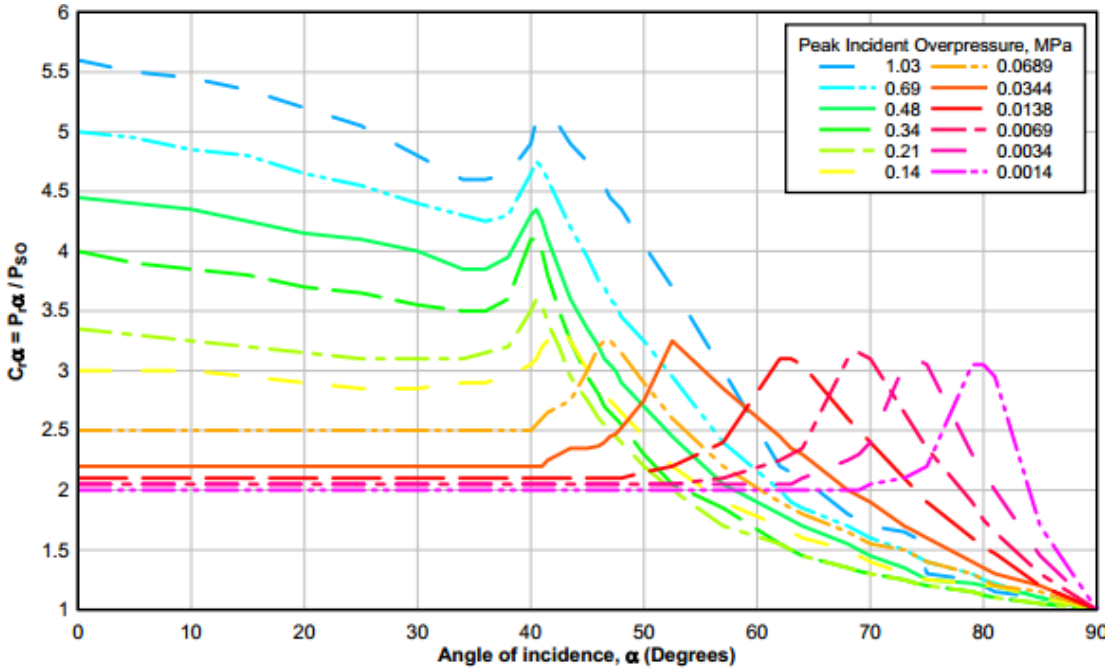

Figure 7 - Pressure increase factor die to reflection or small pressures (Karlos & Solomos, 2013)

The subject of wave diffraction and clearance effects has been studied extensively by Rigby (2014), comparing clearance effects from the semi empirical predictions and numerical simulations to experimental results.

The negative phase is very small both in scale and in effect for small scaled distances, and may be neglected. As the shock front progresses, the negative phase increases compared to the positive phase, but decreases in absolute terms.

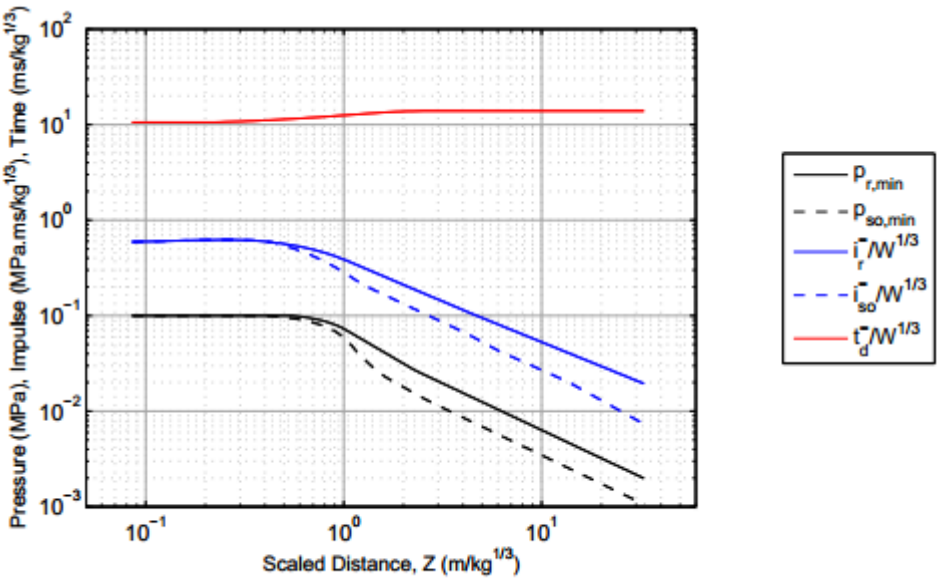

Figure 8 - Negative phase parameters, free air burst (Karlos & Solomos, 2013)

Rigby's research found some of the semi empirical results to be satisfactorily accurate, amongst his other findings (Rigby, Blast Wave Clearing Effects on Finite-Sized Targets Subjected to Explosive Loads, 2014).

State of the art

At the moment there are a few levels of work in the context of structure resistance to blast loads.

Experimental research work is carried out to quantify different effects of blast loads trough experimental work. Though vast amounts of empirical data exist, the mere complexity of the phenomena and its practical relevance keeps research relevant. Such research includes the effects of explosions on foundations (Rigby, 2014).

Research of structural systems via numerical studies is a different avenue of research. The detailed modeling of structural elements in order to simulate their behavior under high strain rate loads is a difficult task to due to the complex behavior of materials under such loads.

The purpose is to enable the focus on a small part of a larger structure, leaving computing power to model complex local behavior such as material non-linearity. Apply different dynamic increase factors to different fibers of a section at different sections, as they strain at a different rate; consider steel-concrete bonding effects and more.

Currently, several documents exist describing the theory of protective structure design and the loads imposed on structures by blast loads. This includes an official EU document, a UN document and several academic papers of various origins. However, all of those draw heavily upon the US department of defense UFC 3-340-02 (2008) guide, which was updated in 2014, or its predecessor, the TM 5-1300, TM 5-855-1 and ESLTR-87-57.

The UFC3-340-02 unifies the design criteria for all U.S. armed forces and is used by many others. It contains information regarding blast effects of structures, equipment and humans, detailed explanations of the blast phenomena, experimental data for a variety of types of explosives, different target geometries, structure behavior, calculation principles and examples and more. It is by far, the most detailed document available at the moment discussing the subject of blast loads on structures.

There is also a UFC 3-340-01, which deals with the effects caused by conventional weapons directly. However, it is difficult to obtain since it is covered by the Arms Export Control Act, and is marked as "for official use only" by the American DoD. Under said law, it only made available to U.S. government and their contractors.

Another document is the Structural Design for Physical Security—State of the Practice Report (ASCE, 1995). This book also draws heavily from the TM 5-1300 guide regarding explosive loads, but is less focused on the subject and deals with other types of threat.

Books and publications on the subject include "Towards the Modelling of Blast Loads on Structures" (Miller, 2004), a thesis which discusses the state of the art in blast prediction at the time written, the Vector-Blast software and its verification.

While estimating the effects of blast loads using manual, single degree of freedom calculations and utilizing charts is possible for simplified problems, it is now far more common to use computer programs for the purpose of such an analysis.

Such programs can be separated to blast load prediction programs that only calculate the time-history loads using semi empirical functions (similar to the data obtainable from charts) and those that utilize numerical methods to calculate the effects on the structures.

The latter include programs in which the structure is considered stiff and only use CFD (computational fluid dynamics), and those in which the pressure field calculation is coupled with the structural dynamics calculation. Usually, the calculation is one-way coupled, since the structural deformation has only a small effect on the pressure field. However, as mentioned before, consideration of the structure's ability to deform often decrease the overall effects and will potentially prevent an overestimation of the loads.

VecTor-Blast is a somewhat dated program (2004) that is based on the TM 5-1300 manual to calculate the pressure profiles on targets. While simple, it is quite effective and was successfully validated against experimental data (Miller, 2004).

Other programs that include explosive load definition modules and CFD include: BlastX (SAIC, 2001), CTH (Sandia National Laboratories, 1993-2016), FOIL and SHARC (Applied Research Associates) (Ngo, Mandis, Gupta, & Ramsay, 2007).

CONWEP (US Army, 1987) is a program that uses semi empirical data from U.S. DoD experiments to calculate blast loads resulting from conventional weapons such as missiles, rockets, land mines, artillery shells and even small arms. It is used in conjunction with structural mechanics programs to analyze the weapons effects on the structure. Unfortunately, it is too only available for use by U.S. government and its contractors.

Programs that are capable of coupled analysis include DYNA3D (LLNL. 1976), LS-DYNA (LSTC, 1978-2015) and ABAQUS (ABAQUS INC, 1978-2016).

Both ABAQUS and LS-DYNA include specific modules for blast load modeling, and combined with other non-linear and DEM modules are very capable codes. Both not only can analyze the blast wave propagation through the environment, but also consider non- linear behavior such as yielding, failure, particle behavior and more.

Both programs are used for high- complexity analysis of various scenarios, including sub terrain effects and underwater explosions. Both programs also interface with CONWEP, which makes them very relevant and popular tools for blast load analysis.

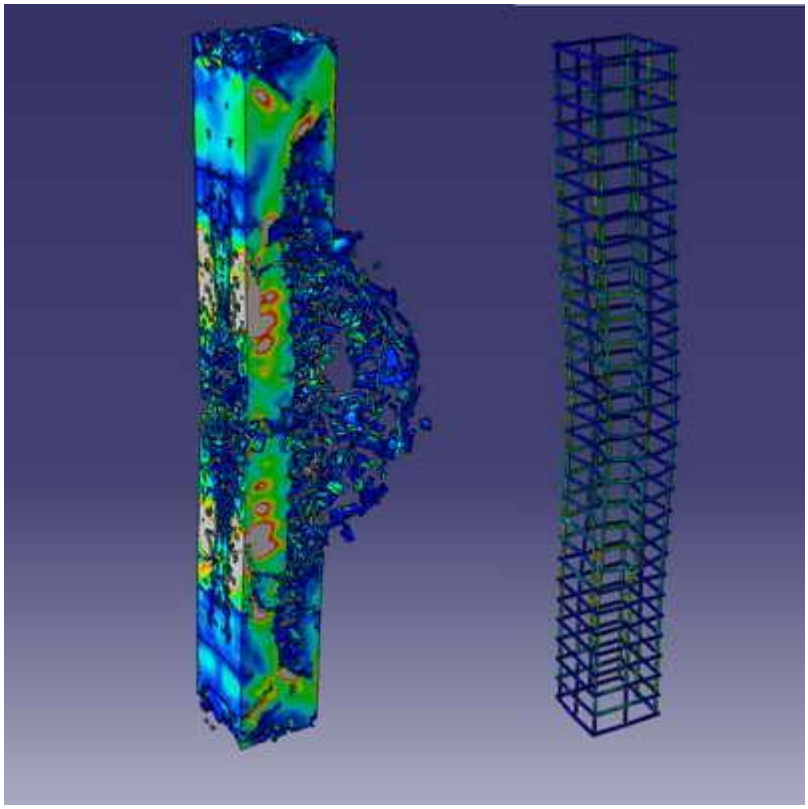

Figure 9 - RC column analysis using ABAQUS. Source - http://www.ikb.poznan.pl/piotr.sielicki/

"Blast Loads on Structures- Empirical Approach" (Lablanc, Adoum, & Lapoujade, 2005) deals with the possibility of predicting blast loads using the LS-DYNA computer program. The paper shows good correlation with the semi empirical data, validating the method of using LS-DYNA to predict blast loads.

AIR3D (Cranfield University, 2006) is another program that is capable of such calculations, yet lacks a graphic user interface (GUI) and therefore is not as usable. ProSAir (Prosair Technologies, 2015) is a successor that has a GUI and uses CFD to analyze blast wave propagation in complex environments and on complex structures.

COMSOL Multiphysics (COMSOL Inc., 1986-2017) is a code capable of coupled fluid dynamics – structural mechanics interaction analysis. Though it has no module dedicated to the definition of blast loads, those can be defined using its Fluid-structure interaction module.

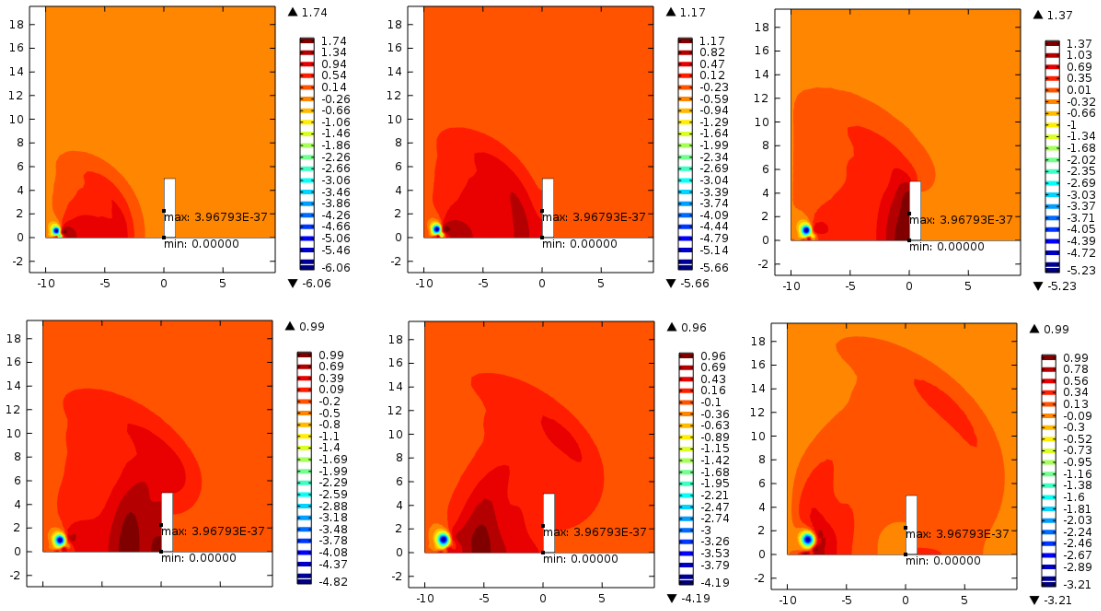

Figure 10 -Blast reflection and diffraction, COMSOL Multiphysics

While not optimized for that purpose and being somewhat limited in capabilities compared to other CFD – CSM capable codes, COMSOL opens up different possibilities, since it enables combining different physical models. One possible example may be a combination of the chemical module in the prediction of explosive charge effects, when combined with other customized functions perhaps.

First principle programs that use semi-empirical data to define load profiles on structures are limited in their capability to account for complex patterns of wave propagation, such as reflection, refraction and absorption by other elements of an environment, limiting the possibilities in terms of attack scenario complexity. However, due to the relative simplicity of the code, load definition functions based on semi empirical data can be (and are) incorporated into complex structure mechanics codes that allow for the modeling of complex, nonlinear structure and element behavior.

CFD programs often may lack the capability to account for complex structure behavior such as cracking, yielding, P-Delta effects, failure of structural elements and loss of structural mass. They can however analyze complex environment and often, in case of programs like LS-DYNA and ABAQUS, consider the load reduction effects due to structural response, even in a non - linear manner. Furthermore, since the CFD programs calculate the pressure fields created under the blast loads, they may also be used to evaluate danger zones and evaluate the risk to human life for every attack scenario. Therefore, it seems that in order to get the best of worlds, a very demanding and complex code needs to be used in order to explore a combination complex attack scenario and complex target structure behavior.

Another possibility bay be to combine the results obtained from a CFD – based code and use it for dynamic load definition in a structure-mechanics code that can handle complex structural behavior.

Extreme Loading (Applied Science International, 2004-2017) aka ELS, is perhaps the most suitable tool for defense-oriented analysis of structures. Using the Applied Element Method (AEM), it offers much better flexibility in the modeling of structures under a variety of catastrophic loading, such as earthquakes, wind loads, impact loads and blast loads. The program is also used for the planning of controlled demolition operations as well as for forensic analysis purposes. Using AEM, the elements do not have to remain attached to one another at the nodes. In fact, elements can be eliminated as well as boundaries in the analysis process. It also includes a dedicated blast load module based upon the semi-empirical data from the up to date UFC 3-340-02 manual. While it can be used to evaluate resulting pressures directly, it can also evaluate the velocity and energy of potentially life-threatening debris, making it a potentially effective tool for threat assessment.

The program incorporated non-linear structural analysis features such as crack propagation analysis, inelastic behavior, P-Delta effects. It can also calculate the effects of collision between demolished structural elements and those that are still intact.

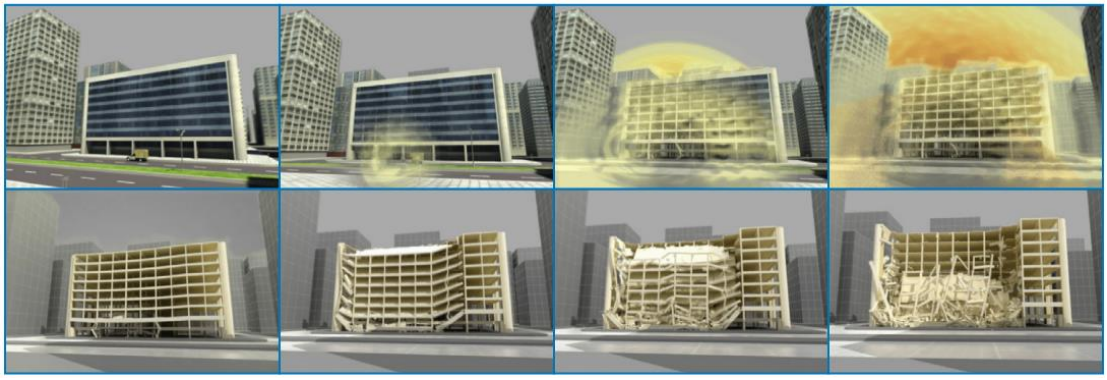

Figure 11 - ELS simulation of the A.P. Murrah building. Source – ASI case study of the Oklahoma city bomb.

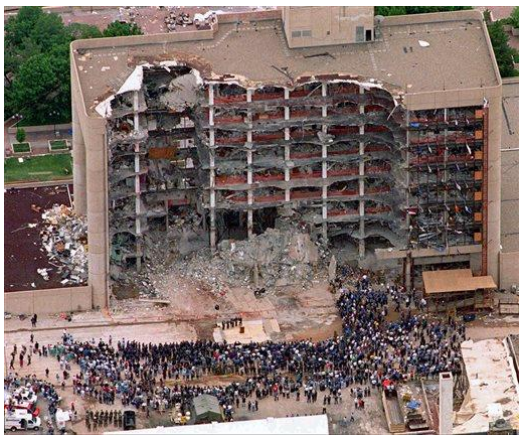

Figure 12 - The A.P. Murrah building, Oklahoma city 1995. Source - ksn.com

Computer programs use different mathematical methods for the fluid dynamic calculations:

- Finite Element Method (FEM)
- Discrete Element Method (DEM)
- Particle Blast Method (PBM)
- Corpuscular Method (CPM)

While the particulars of each method is worthy of further discussion, it is beyond the scope of this paper (Teng, 2016).

3. Numerical Study Description

Chosen Method of Analysis

Several approaches were considered for the analysis of prestressed structures under blast loads.

Detailed analysis of a single element was the first option considered. It would have involved a detailed model 3D model of a beam, with stresses calculated in all directions (by using non-linear solid elements) and wound require a complex interaction model between the concrete and the embedded reinforcement within. It would also include a complex system for varying the stress-strain curve for each element according to the time derivative of its strains (for the effects of the dynamic increase factor). This out have enabled a close up inspection of the forces and stress distributions developing within each part of the element.

This option was abandoned for 3 main reasons:

- Technical difficulty – the necessary code for such an analysis is very complex
- Lack of input data – the data for the variation in each stress development behavior under high strain rates (bonding strength. Reduction in ductility) is lacking
- Narrow scope – such an analysis would only enable the study of a single element due to high complexity, and will therefore limit the scope of investigation

The second option considered was an investigation of structural systems under blast loads using an AEM program, enabling the consideration of failure mechanisms, progressive failure effects etc.

This method had the added advantage of having been validated against a large amount of real world data. However, this was also abandoned since the only suitable code (ELS) was more difficult to obtain and would have been time probative to study all the relevant functions. Also, the added features if the code brought up a concern as to the ability of it to accurately model the effects of pre-stressing in its different forms.

The selected approach was therefore to use a familiar and available code, and to model an entire structure in order to compare different structural systems. Midas Civil was selected for its availability and for its capability of modeling PSC elements of different types effectively. It also is capable of inelastic analysis of structural components in a non-linear time history case, usually used for seismic design of supporting elements of bridges (substructure and pile foundations)

The consideration of non – linear behavior is important since it was anticipated that at least some of the blast loads will cause large deformations, cracking and yielding of the reinforcement. The only way to effectively consider the different behavior of reinforced sections would be through some type of inelastic analysis.

Despite being capable of fiber analysis, the function was not utilized, since it is incapable of considering pre-stressing effects and is suitable only for RC elements.

The selected method of definition was by using a moment- curvature skeleton curve for each section. The consideration of nonlinear effects only for one degree of freedom (DOF), which is vertical bending, was to simplify the analysis and spare resources, although vertical shear was also considered to be combined at one point, to add a failure mechanism.

The idea of adding inelastic shear to the model was abandoned, since it is assumed that shear failure is straight-forward. If the shear resistance capacity of a section was exceeded, it would be seen clearly in the analysis results. The effects of shear failure would be relevant for analysis beyond that when utilizing AEM, which would enable the consideration of secondary failures, progressive collapse of multiple floor slabs etc.

It was decided to use grillage models to simulate the two way behavior of the slabs, since it was expected that under large loads the slab will work mostly in the direction in which it is reinforced, and the effects of torsion would be negligible. Results from grillage elements were compared to those obtained from using plate elements (DKMQ). P-M interaction effects were also neglected, since the membrane forces expected to develop due to both the normative loads and the blast load are comparatively small. The second order effects such as tension-membrane at large displacements were not considered, out of a need to simplify the model.

In order to study the behavior obtain the required, a section response program was required. Such a program would not just calculate the ultimate capacity of each section, but would have to also produce a curvature- moment curve that would be then approximated and used as an input for the FEM program inelastic hinge analysis module. MIDAS Civil does have an inbuilt function that enables section response analysis, but it is limited to simple RC sections.

Response 2000 is a program that was developed at the University of Toronto. It is capable of both RC and PSC section non-linear analysis, i.e. calculates the stresses in the concrete and reinforcement by using a stress-strain curve, and not using "Whitney's block" approximations. It also outputs a curvature-moment curve for each section. It is, however, limited in one important and relevant way – it does not enable the modeling of un-bonded strands in the section.

Therefore, a calculation code was developed based on PTC Mathcad to produce the necessary data. The sheet considers arbitrary section shape, as well as any number of tensioned cables/ strands. Mild steel is, however lumped into equivalent sections at each side. The stress in the concrete is calculated based on the curve presented in the EN 1992.1.1.2004 code, modified for concrete strengths obtained from 10x10x10 cm test cubes.

The force at each strand or cable is calculated from the strain at its ordinate, while Bernoulli's assumption of linear strain is kept. A bi-linear yield model is used for both high strength and mild steel. For bonded strands it is assumed that the strain in the steel is the one resulting from the pre-stressing (minus the losses from shortening, concrete creep etc.), plus the additional strain from bending action at the ordinate.

For the un-bonded strands, the bending strain for the strand's ordinate is corrected by a factor to consider slippage effects. The factor varies according to load distribution and the location of the section within the span. For simply supported beams, the correction factor would be 1 for pure bending (no correction), 0.2 for evenly distributed loads and 0.1 for point loads at mid-span, for the mid span section. The analysis assumes the conservative value of 0.05.

Concretes of different strengths can be combined for composite section analysis. Tensile stresses in the concrete are considered to be zero. For each section, analysis had to be carried out for both bending directions, since the elements are expected to deform in both directions due to the rebound effect from the blast Partial safety factors were implemented according to EN 1992.1.1.2004 for steel and concrete.

Table 1 - Partial Safety Factors

Material	**Value**
Concrete	1.5
Mild Steel	1.15
High Strength steel	1.15

Dynamic Increase Factors were assumed according to TM 5-1300.

Table 2 - Dynamic Increase Factors, TM 5-1300

Material	Value
Mild reinforcement bars (bending)	1.17
Concrete (bending)	1.19
High Strength Steel (bending)	1
Mild reinforcement bars (shear)	1.1
Concrete (direct shear)	1.1
Concrete (compression)	1.19

The failure criteria were defined as one of the typical RC/ PSC modes of failure:

- Flexure failure
- Direct shear failure
- Support / punching shear failure

Flexural failure can occur by one of 3 sub modes – steel yield, concrete failure in compression and steel tensile failure. Each sub mode is considered and coded into the section response calculation sheet.

Shear failure has 2 sub modes – concrete diagonal failure and steel stirrup yield. These sub modes are considered using EN 1992.1.1.2004 based calculation sheet. Local spalling and bleaching are not considered in this model.

Normative loads (self-weight and tensioning loads) are calculated as standard static loads. The self-weight of structural elements are calculated automatically by the program, according to the volume of the element and the unit weight of the material assigned to it. For grillage models, only elements in one direction were assigned weight.

The tensioning loads are defined by using a software module that is specifically designed to consider different types of tensioning methods (pre tensioning, bonded and un-bonded post tensioning and external). The mass data for the dynamic analysis is derived from the self-weight loads. No other dead loads were defined.

The basic data for the strands (section area, material, friction loss coefficients etc.) is entered. Cable / strand geometry is defined and the tensioning force at the jack is entered.

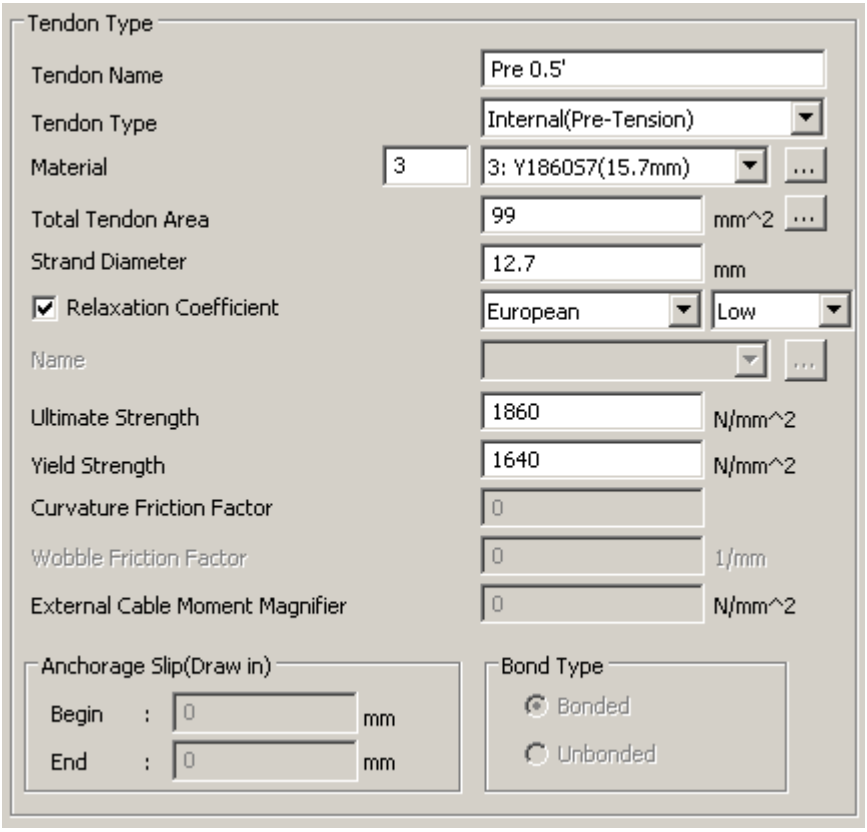

Figure 13 - Program Input Data for a 0.5 inch pre-tesioning Strand

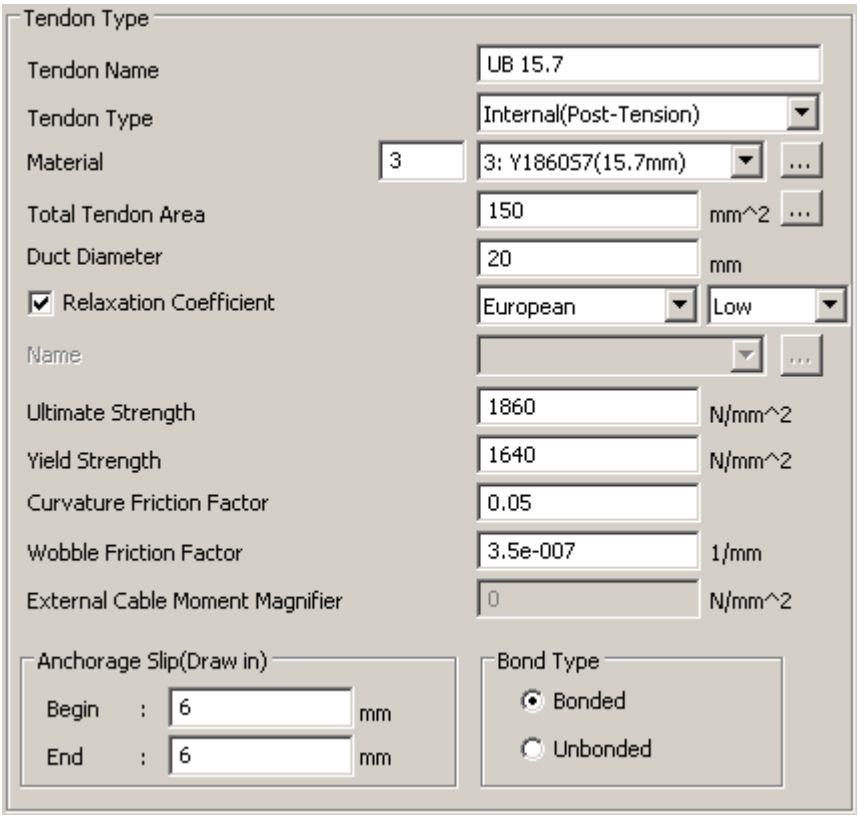

Figure 14 -Program Input Data for a 15.7mm Unbonded Strand

The program calculates the immediate loses and formulates the equivalent load vectors. These are used in a staged analysis that also considers the effects of concrete creep and shrinkage (according to the calculated stressed at each stage) and from that and relaxation data, calculates the residual tendon force.

Creep, shrinkage and relaxation are all calculated by the module according to the selected code, which in our case is the European, i.e. Eurocode.

As a part of the base for analysis, the natural period of the structures was estimated for its un-cracked, linear phase by using eigenvalue analysis. This enables the characterization of the blast load behavior as an impulsive load, as well as helps establish the duration required to be analyzed using time –history analysis.

The blast loads are defined for each scenario using the time history profiles obtained from the first principle VecTor-Blast program, and using it to define the time-history loads in the FEM program MIDAS Civil. The loads were calculated for each node group.

The VecTor-Blast program uses the structure geometry, charge weight and location in relation to the structure and the ground, to calculate the pressure load profile at any requested location.

In the FEM model, the FEM loads were defined for the roof elements only, neglecting the actions inflicted upon the sides of the structure, as well as any effects caused by the shock wave acting in the foundations through the soil.

The pressure is modeled as a set of time – history point loads, acting at each node group. The time history analysis is defined as subsequent to the static loads defined for the normative loads.

The time history analysis is a nonlinear, direct integration, transient state analysis. The nonlinear analysis is a given, since inelastic behavior is to be considered in order to account for the different section behaviors – cracks, yielding and concrete non-linearity in compression.

Direct integration is required since modal methods are based on the structure's linear dynamic modes, which cannot account for the non-linear behavior previously mentioned. Since the problem is transient in nature, a transient analysis is required.

It is using the constant acceleration method (central difference method for time integration), since it had shown itself to be stable at the relevant time step. The duration of the analyzed time is determined to be twice as long as the natural period of the structure, in its un-cracked state. This is to allow maximum deflection in both directions and to also get an idea of the structure's post-blast vibration decrement. The time step selected is $5*10^{-4}$ seconds, or one half of a thousandth of a second.

This is to properly consider the time-history loads while avoiding numerical damping. This was also ensured by comparing the results with those obtained using much smaller time steps, such as 10^{-6} of a second. Such comparison had shown no increase in the calculated resultants.

The elements used are beam elements (with Timoshenko shear deformation considered), that are then over-ridden by using inelastic distributed hinges. The distributed hinge response is determined according the curvature calculated at 5 integration points along the element. The flexibility matrix for the beam element is determined through integration over these points according to their hysteretic condition, and then reversed to obtain the stiffness matrix. In essence, the number of integration points determines the number of terms used in the Gauss-Lobatto integration.

Each hinge is defined by a skeleton curve, which is defined, as mentioned previously, as an idealized, tri linear model of the sectional response curve (curvature-moment) calculated (Analysis for Civil Structures, 2015). The base location for the strength calculations is assigned the middle of each element, for symmetry.

The tri linear approximation of the sectional response curve is defined by the base un-cracked stiffness of the structure, with modification factors applied at the relevant moment values, reducing the stiffness for any additional curvature deformation.

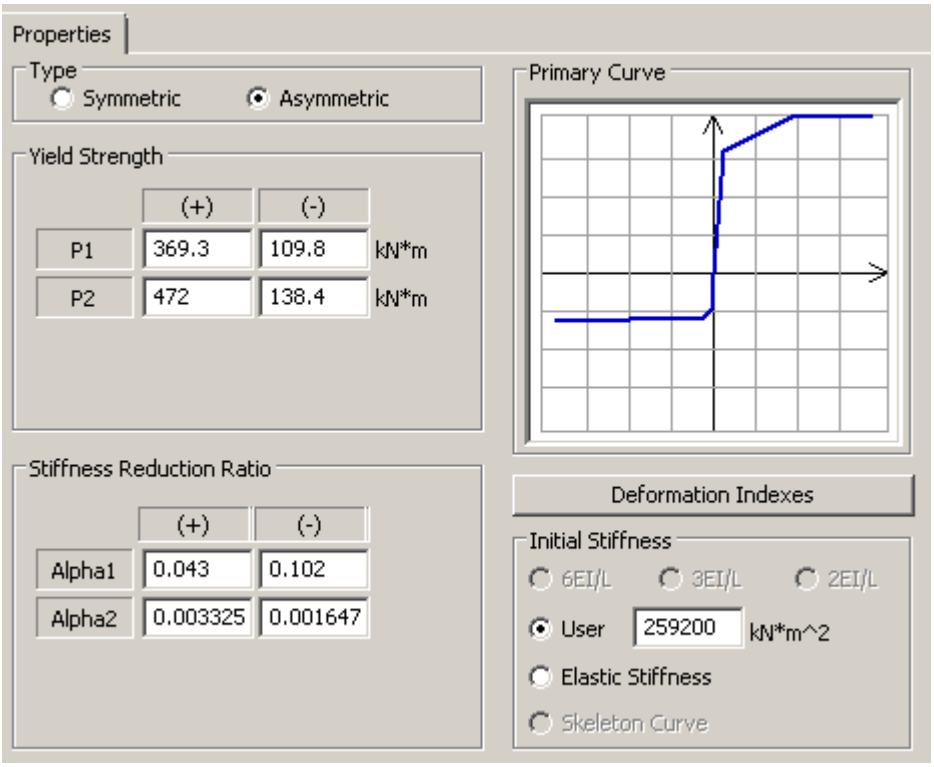

Figure 15 - Example: Skeleton Curve Definition

The hysteretic model selected is a degrading trilinear model.

The rational being that a trilinear model is necessarily adequate for modeling the typical response curve, which comprised of 3 stages: linear un-cracked, cracked without yielding, and post yield.

The choice of a degrading model is in order to describe the anticipated loss of stiffness in the section due to cracking at a dynamic setting, which can cause spalling, local de-bonding and loss of material within the concrete cracks.

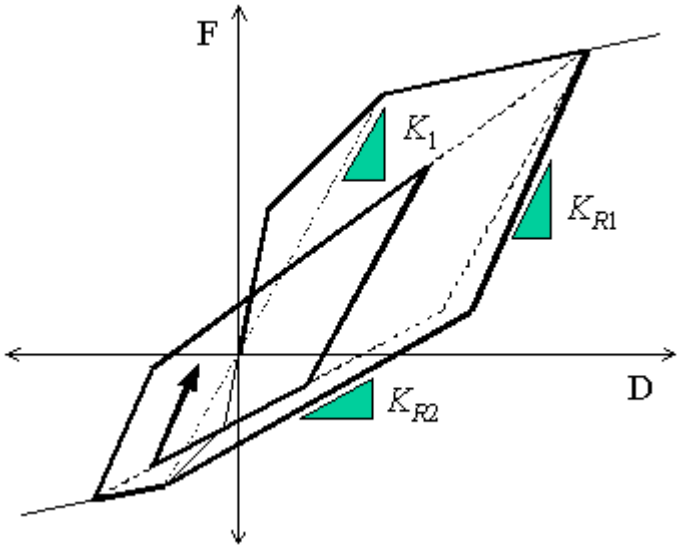

Figure 16 - Degrading Tri-linear Hysteretic Model source: MIDAS

While it is not thoroughly investigated in this paper, it is believed that while this model is more suited for the analysis than other hysteretic models, the effect of any hysteretic model on the result is small due to the short load duration and small number of oscillations, compared to, for example, seismic loads.

The damping method selected for the wall elements, for which inelastic hinges were not defined, is strain-energy based, where the damping rate is 5%, as accepted for RC structures when considering seismic actions. It is also applied to the linear phase of the inelastic elements.

Blast scenario definition

As described in (Karlos & Solomos, 2013), the first stage of any blast – resistance analysis of a structure begins with the definition of an attack scenario.

While EN 1991-1-7 offers a limited reference to the subject of accidental explosions, there is no available code that defines the attacks scenario to be considered for each structure.

Attack scenario definition is therefore left to the owner/operator of the structure and the advising body to decide and define.

In (FEMA 426, 2003) and (FEMA 427, 2003) , the subject is discussed at length. Measures of mitigating risk are described through design considerations, secondary measures to distance an attacker from the target, support systems and emergency service response. However, no distinct algorithm to select an attack scenario is given.

While probabilistic risk assessment models have been suggested and explored (Stewart & Netherton, 2006), it was found that a complete risk assessment analysis would require difficult to obtain data regarding past conflicts and attacks, which places it well beyond the scope of this paper.

Therefore, in order to select a suitable, non-arbitrary attack scenario, it had to be constructed as a scenario which is both to the structural element investigated, and applicatory to the primary motivation. Since the original motivation was related to the Israeli Homefront command's directives regarding shelter space construction and design, it is logical that the attack scenario would be considered according to threats present to that country first, and then perhaps expanded.

During the 2006 conflict with the Shiite organization Hezbollah, an estimated 3970~4200 rockets were fired into Israeli territory. The vast majority of these rockets were 122mm and 107mm Grad rockets, Originally a Soviet design. Only 457 out of the estimated 4000 were larger, heavier rockets, such as the 220mm and 302mm rockets that exist in the organization's arsenal. The rockets are used as an area-weapon, in order to disrupt routine and cause chaos in the Israeli cities. 907 of these rockets landed on and near buildings of different types. During the conflict, about 2000 dwellings were damaged, and 53 Israelis died (Rubin, 2007).

Beginning in 2001, rockets and mortar shells have been fired from Gaza into Israeli territory by the Islamist Organization Hamas, as well as by other organizations.

Figure 17 - Rocket Strike Damage, Sderot, Israel source: JNS.org

Between 2001 and 2006, 1600 rockets have been fired from Gaza, most of them improvised and local production rockets (the rocket threat from Gaza 2000-2007, 2007). During the same time, more than 2500 mortar shells were used against Israeli targets. Beginning 2006, the local production rockets were phased out and replaced with Iranian made 122mm rockets, as well as some other, heavier rockets. Between 2006 and 2014, more than 11000 rockets were launched into Israel from Gaza, then majority of which were the 122mm rockets (IDF, 2015).

While arguable, it seems that the standard to beat when considering civil defense threats against Israel is the BM-21 rocket. The enormous worldwide proliferation of 122mm rockets of various productions makes it a relevant threat for any other place as well.

While various payloads exist for the 9M22U BM-21 "Grad" rocket, the typical HE warhead is of 21 kg of composition B (60% RDX and 40%TNT) (Dullum, 2010).

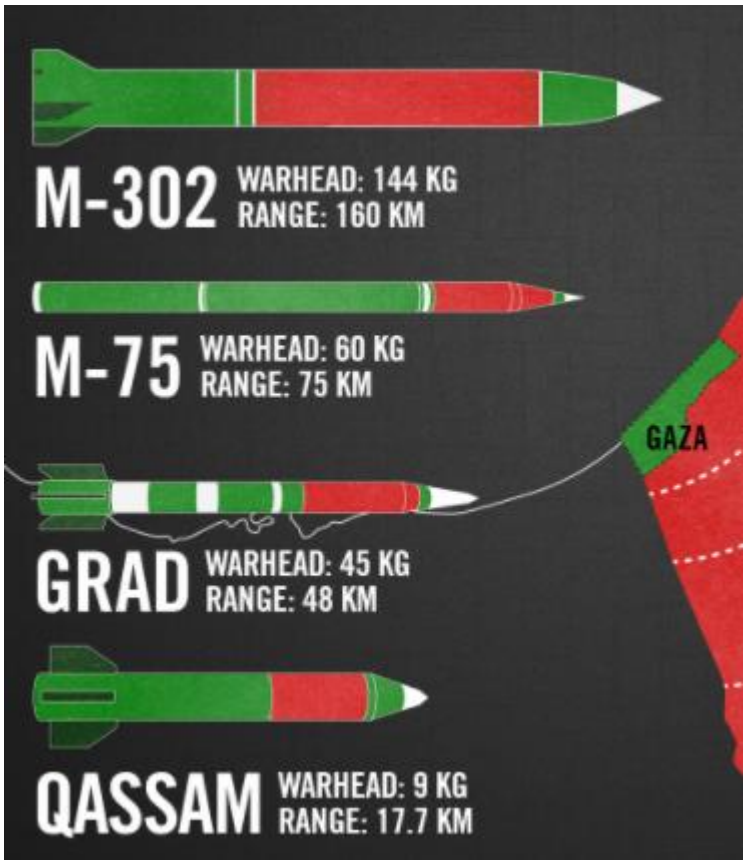

Figure 18 - Rockets Used By Hamas source: idfblog.com

It has been decided to investigate two more scenarios. If the BM-21 rocket is to be used as a reference case for the common threat, a second, less severe case will represent the minimal requirement, and a third, more severe case will represent a worst-case-within-reason scenario.

For the second case, the 81mm mortar shell was selected. As mentioned briefly before, it had been used extensively against Israeli targets. It is also an extremely common weapon used by many militaries and non-military organizations around the globe. The variety of ammunition for the mortar is vast. Several charge weights and types exist along with non-explosive payloads. The AR-M81 shell was selected as an example of a general use HE round. The charge weight is 750 grams and the explosive type is again, composition B (Bulcomers, 2014).

Figure 19 -AR-M81 81mm Shell source: bulcomersks.com

For the third, extreme case, the 250 kg general purpose bomb was selected. While heavier weapons exist within the circle of threat and have been in fact used before, it is the weapon used to assess and design protective structures to military specifications.

The MK82 bomb is one example of such weapon. It houses a charge of 202 kg of Tritonal (8-% TNT and 20% aluminum powder) explosive.

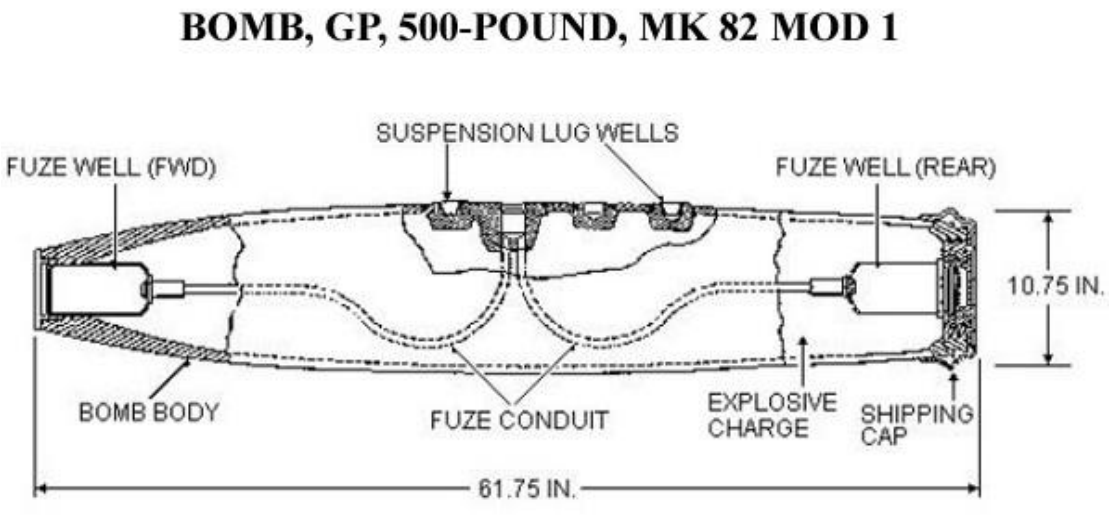

Figure 20 - MK-82 Bomb Source: uxoinfo.com

In order to simplify, the effects of the charge encasement, charge shape and location of the detonator were not considered, and all cases were calculated as spherical charges.

For the investigation to be as suitable to examine the tensioned elements, the scenario was defined so that the loaded element will suffer the effect of the air blast directly.

Since tensioning is used mostly in ceilings and beams, the investigated elements are horizontal. For an external air- blast to effect the ceiling directly, it has to take place someplace above the structure.

The attack scenario is therefore defined as a situation in which each of the above mentioned weapons strikes a building that is situated right next to the investigated, above ground shelter.

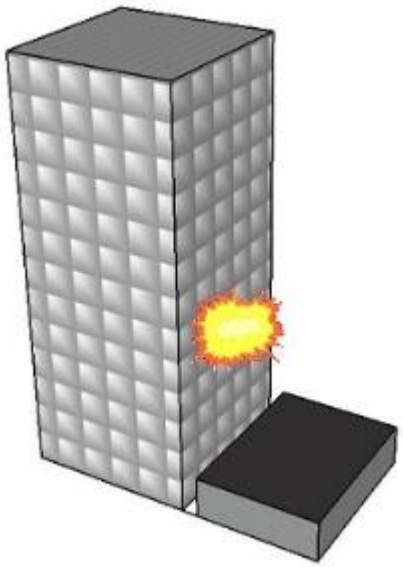

Figure 21 - Scenario Layout: Airblast over an Above Ground Shelter

For reasons of data availability for the equivalent distance and result significance, the vertical distance between the target upper level and the impact point varies between 5 meters for the first (mortar shell) scenario and 10 meters for the second and third (rocket, GP bomb) scenarios.

A worst case assumption is made that after detonation, a downwards traveling shock front will be formed by the direct pressure wave combined with the wave reflected from the impacted building's outer wall. While in reality some of the energy will be absorbed by the impacted structure, a safe side assumption is made to consider as if the entire blast wave is reflected.

The required result suggested for the examined structures to maintain for each attack scenario is:

- In the case of the 81mm mortar shell, the structure will not lose serviceability
- In the case of the BM-21 rocket, the structure will not be damaged beyond repair and will offer protection against the down-falling debris
- In the case of the MK82 bomb, there will not be any catastrophic failure and the structure will offer some protection against down falling debris

In order to validate the suggested method of analysis, the method was implemented for the known and well-studied case of the 1995 Alfred P. Murrah building in Oklahoma City.

The basis of comparison for the validation is the LS-DYNA investigation of column G24 carried out by (Ngo, Mandis, Gupta, & Ramsay, 2007) and the data presented at (FEMA 277, 1996). The G24 column was analyzed using Response 2000 and its response curve was extracted. For that purpose, a ballpark estimation if the permanent loads was also calculated. The resulting response moment-curvature diagram was approximated and entered to a simple model of the column using MIDAS Civil. The Blast load was calculated using VecTor-Blast based on the data in the FEMA report, in order to compare it to the approximated curve in both sources.

Finally, the model was loaded and analyzed, and the results compared to those presented in the FEMA report and to those obtained by using LS-DYNA.

Subject structures

The selected structure is a large public structure, which may be ordinarily used as an auditorium or a public event venue, yet doubles as an above ground shelter when needed. The measurements of the examined structure are 12x16 meters, with a net clearance of 4 meters. The measurements were determined so that PSC systems would be relevant in terms of span, while a comparison to RC would still be possible. Another consideration was to enable a two way action in systems capable of such action, giving them a small advantage over systems that do not.

Finally, the height of the structure was defined at 4 meters as to enable its use as a meeting hall or a public event venue. The thickness of the walls was defined to offer minimal rotational restraint acting as a boundary for the ceiling systems, while keeping it functional as a shelter, complying with the IDF Home front Command's directive for shelter spaces used by schools. The wall thickness was therefore set to be 25 cm.

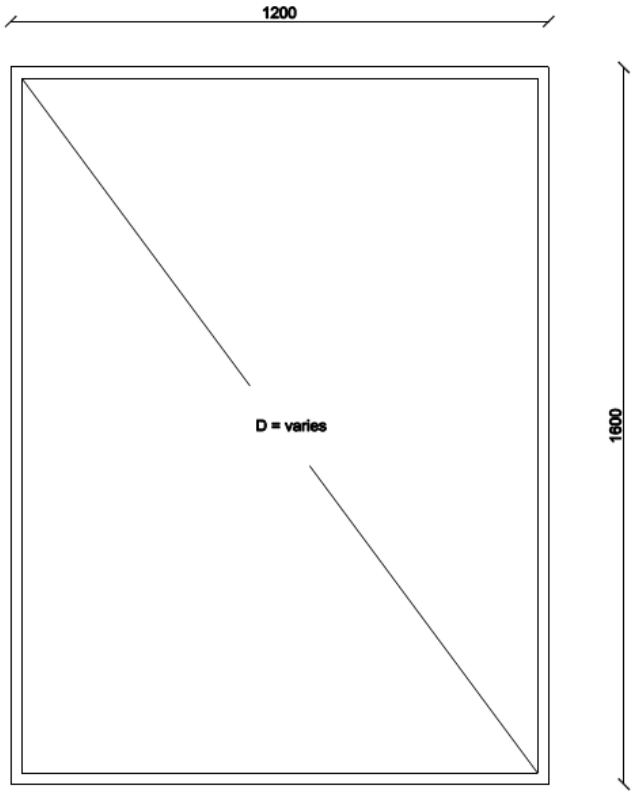

Figure 22 -Plan View of theExamined Structure

The sections for each system were designed so that they would be able to carry the self-weight of the structure, in addition to a superimposed vertical load of 5kN/m^2.

This design load does not represent a live load specific to any structural specification or code specific for shelters. It was set so that in addition to preforming against normal loads as a roof, it would stand a chance to perform as shelter.

The first system used as a base for comparison is a two-way, reinforced concrete system. The concrete type was selected was C-30/37 equivalent, since it is very common in RC buildings and infrastructure. The bars are spaced 20cm apart. The specifications for the construction of shelter spaces specify a maximum spacing of 10 cm for the internal and 20 cm for the external reinforcement in every direction, for the purpose of reducing the danger of injury due to spalling concrete.

The directive is not relevant to the analysis, since the model does not consider spalling directly, and therefore was not implemented.

While shear reinforcement could have been added to improve shear resistance to blast loads, the predetermined aforementioned loads did not indicate a need for shear reinforcement to resist the normative loads, and therefore such reinforcement was not added.

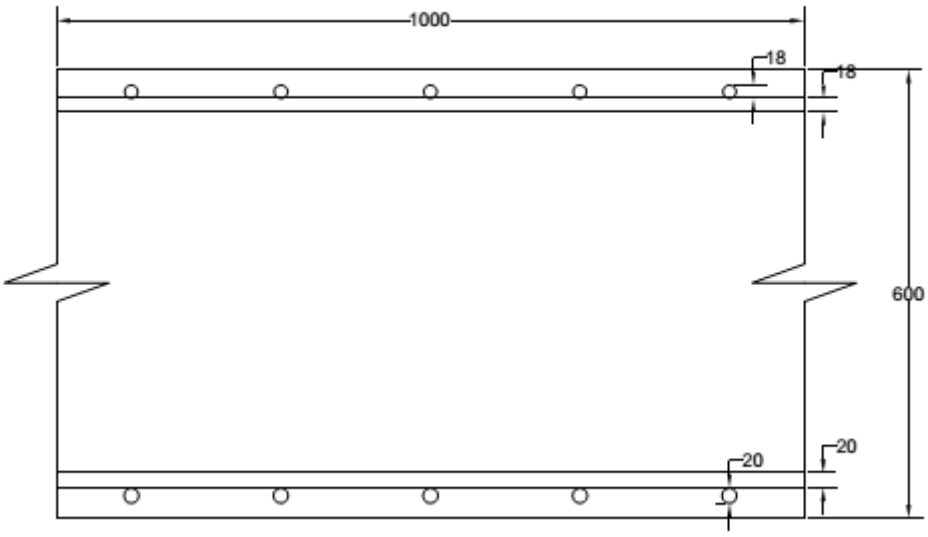

Figure 23 – Reinforced Concrete Slab Section

The second system examined is a prefabricated hollow core slab system.

This is one of the most commonly used systems for large span and heavy loads bearing ceilings. It is considered a cost efficient method for quick construction. The pre-fabricated elements are produced using pre-tensioning and each contains a number of tensioned strands the type and number of which is determined according to the span and the ceiling's service and design loads.

Since there is no significant mechanical connection between the elements, the system can only work in the direction of the elements, as a one way system. Since the thickness of the topping is only 5cm, there is only a minimal amount of room for reinforcement in the lateral direction. Such reinforcement was excluded from consideration in the analysis for simplicity, but is recommended for constructive reasons. A thicker topping layer, as well as additional shear connectors protruding from the prefabricated element into the topping layer could make the system stronger, but for the purpose of the comparison, the design remained within the standard specifications.

The thickness and design of the element selected for use in the examined design was determined according to the tables presented in the Ashcrete Catalog. The catalog was selected for being accessible and for the high amount of technical detail it provides for each product (Ashcrete, 2010).

The A-358-12 element was found suitable for the 12m span. It is arguably a fair compromise – having the maximum number of strands of the 35cm thickness elements.

It can be rightfully claimed that a thicker element would offer better protection, yet since the original estimate (based on span, load and section stiffness) was for a 40cm thick

tensioned element, the 35cm element + 5 cm topping was selected as a reasonable and likely representor of that particular type of system. In order for the system to be able to sustain the rebound effect from the blast, the 5 cm of topping have been reinforced with 6 mild steel bars 12mm in diameter, for each 1.2 meter wide element. Concrete types are 35/45 for the prefabricated element and 20/25 for the topping.

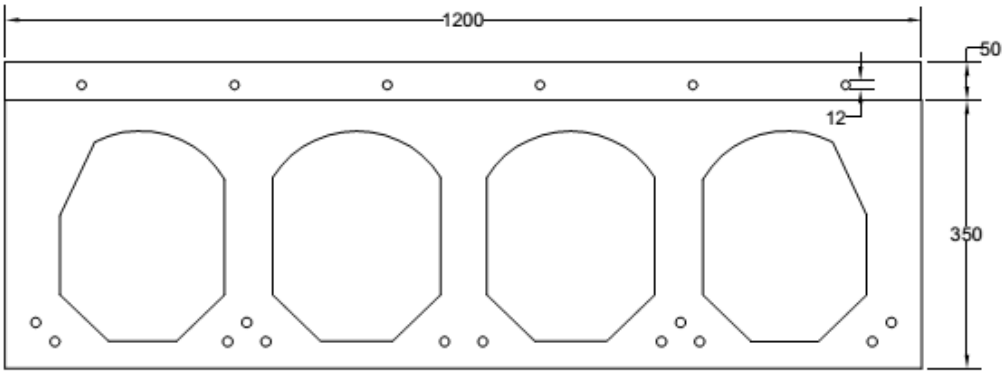

Figure24 - Precast Hollow Core Slab Element Section

The third system selected is a slab reinforced with unbonded mono-strands that are post tensioned. The strands are not straight but droop from a higher position at the supporting wall to a lower position at the mid-span area.

The suggested system involves a 15.7mm un-bonded stand running through the slab inside a PVC pipe. The thickness of the slab was determined to be 45 cm using the same evaluation method as before, and validated for service and design states. The strand geometry was also examined at the same time, by observing the stresses in the concrete at service state.

Additional bottom reinforcement was added for the purpose of complying with the requirements of IS 466 for fire safety. The concrete used for the slab is 35/45 strength concrete.

For reasons similar to the ones mentioned in regard in the RC section, the slab was not shear reinforced. The possible effects of shear reinforcement can, to some degree be, be contemplated without having these effects directly modeled.

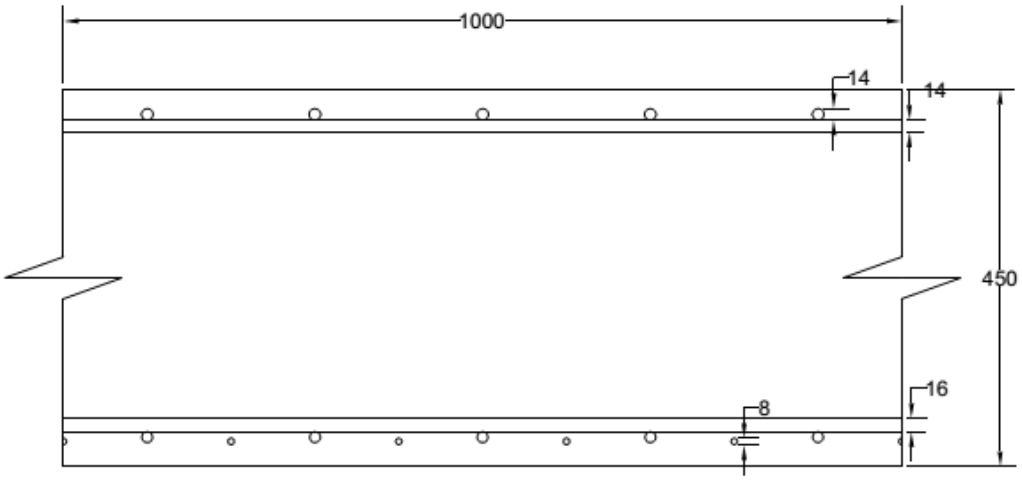

Figure25 - Unbonded Monostrand Reinforcement Slab

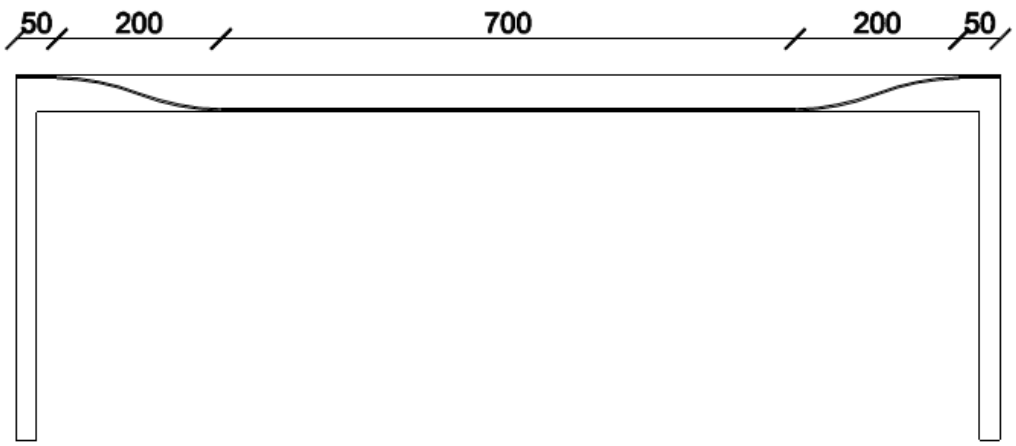

Figure 26 - Unbonded Strand Geometry

The strand geometry as shown in figure 26 is of a double curvature type, moving from 3.5 cm central ordinate (measuring from the slab's bottom) to 41.5 cm ordinate, with a 3m curvature radius.

Model attributes

As previously described, the structures were modeled as simple box structures.

The walls have been modeled using DKMQ shell elements. In order to simplify the behavior, no openings were modeled. The different ceilings were modeled using a Timoshenko beam with distributed inelastic hinges, with the reference location for resultant calculation in the middle of each element. Maximum element size was set to 1 meter. The prestressed hollow core slab elements were not connected in the transverse direction, neglecting the weak mechanical connection between the components.

The RC slab and the post-tensioned slab models are grillage models, neglecting the torsion effects in the slabs. The boundary conditions for the model are vertical ideal supports, combined with supports in the direction perpendicular to each wall. No constraints were placed against rotation in any direction. This was determined in order to simulate the effects of a foundation and base slab that are absent from the model, while keeping the model as simple as possible.

The time history loads were calculated for each node group, such group being a line of nodes that is an equal distance from the impacted structure. The effects load variation and decrement in the perpendicular direction was therefore neglected.

Table 3 - Material Properties

Material	Elastic Modulus [GPa]	Poisson's Ratio	Weight Density [kN/m^3]
C25/30 concrete	31.5	0.2	25
C30/37 concrete	32.8	0.2	25
C35/45 concrete	34	0.2	25
S-400 steel	205	0.3	76.98
Y1860S7 steel	195	0.3	76.98

Material properties presented in Table 3 are the default values defined in the MIDAS program, in accordance with EN 1992.1.1.2004

4. Method Validation

In order to validate the method, a 3 part process was carried out:

- Model validation – using the same modeling method in a known case
- Section Calculation validation – by comparing the results of the Mathcad sheet to those obtained by a well-known code
- Grillage validation – comparison of the grillage model results to those obtained from a shell element model

Model validation

The case of the Alfred P. Murrah is a well-known, thoroughly investigated case in which a truck bomb was used to attack a structure.

The 3200 kg, ANNM charge (equivalent of ~1814 kg of TNT) created a ground blast 4.3 meters from the structures façade, resulting in 168 dead and over 680 injured. An entire portion of the 9 story structure had collapsed. 3 weeks after the bombing, FEMA deployed the Building Performance Assessment Team (BPAT) which carried out an extensive forensic study of the structure that included visual inspection, interviews, sample tests and a post collapse evaluation using structural plans and material (FEMA 277, 1996).

An inelastic hinge model was created and the results were compared to those presented in the FEMA report.

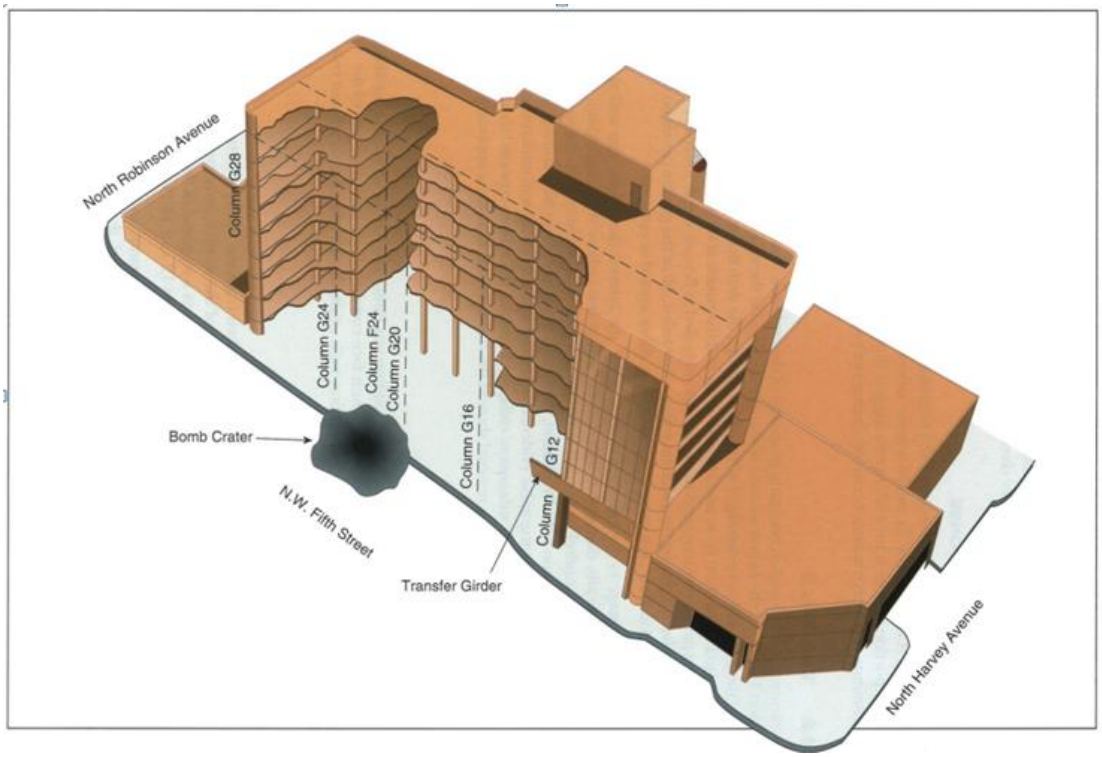

Figure 27 – Post Failure Layout, Alfred P. Murrah Building. source: FEMA 277

Furthermore, the results were then compared to the ones obtained by an LS-DYNA study in (Ngo, Mandis, Gupta, & Ramsay, 2007)

A model of the 6.4 meter G24 column was created using MIDAS Civil.

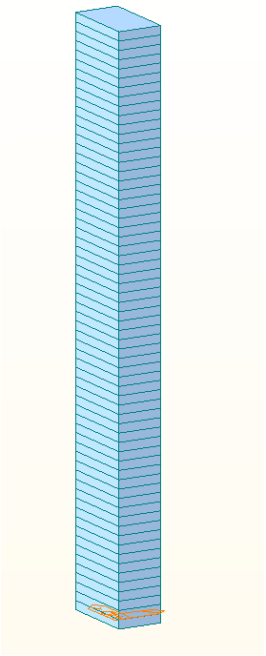

Figure 28 - Column MIDAS Civil Model

The model was created using the same beam elements used in the research grillage models. The length of each element was 0.1 meter. The boundary conditions for the column are pinned-pinned, as it was in the two other sources.

First, the vertical loads in the column due to permanent and live loads in the structure were calculated using the data presented in the FEMA report.

	Specimen B	Specimen H
Size	#8	#5
Design Yield Stress (thousands of pounds per square inch)	60	60
Measured Yield Stress (thousands of pounds per square inch)	71.8	65.2
Yield Load (thousands of pounds)	56.7	20.2
Ultimate Load (thousands of pounds)	84.9	33.3
Ultimate Stress (thousands of pounds per square inch)	107	107
Elongation (percent)	9.8	11.1
Gage Length	7-7/8	7-3/4
Modulus of Elasticity (thousands of pounds per square inch)	28,500	28,500

Figure 29 - Steel Sample Properties - FEMA Report

	Core Identification No. 3	No. 5	No. 7
Nominal Maximum Aggregate Size (inches)	3/4	3/4	3/4
Concrete Age at Test (approximate days)	Not Stated	Not Stated	Not Stated
Moisture Condition at Test	Dry	Moist	Moist
Orientation of Core Axis in Structure	Not Stated	Not Stated	Not Stated
Diameter 1 (inches)	5.70	5.71	3.26
Diameter 2 (inches)	5.68	5.71	3.25
Average Diameter (inches)	5.69	5.71	3.25
Cross-Sectional Area (square inches)	25.42	25.63	8.30
Length Trimmed (inches)	10.3	7.6	6.4
Length Capped (inches)	10.6	7.9	6.6
Weight in Air (pounds)	22.2	16.7	4.5
Weight in Water (pounds)	12.7	9.7	2.6
Density (pounds per cubic foot)	146.4	149.5	147.3
Loading Rate (pounds per square inch per second)	35	35	35
Maximum Load (pounds)	107,500	177,500	46,000
Uncorrected Compressive Strength (pounds per square inch)	4,230	6,930	5,540
Ratio of Capped Length to Diameter (L/D)	1.86	1.38	2.03
Correction Factor (ASTM C42)	0.989	0.945	1.000
Compressive Strength Corrected for L/D (pounds per square inch)	**4,180**	**6,550**	**5,540**
Fracture Pattern	Shear	Conical	Columnar
Compressive Strength Corrected for L/D and for Cylinder vs. Core Ratio (pounds per square inch / 0.85)	**4,920**	**7,710**	**6,520**

Note: Core No.1 had a vertical crack before testing. Core No. 5 had a 4½-inch piece of #4 reinforcement bar with 1 ½-inch cover running transversely 4 inches from the top surface of the core.

Figure 30 – Concrete Sample Properties - FEMA Report

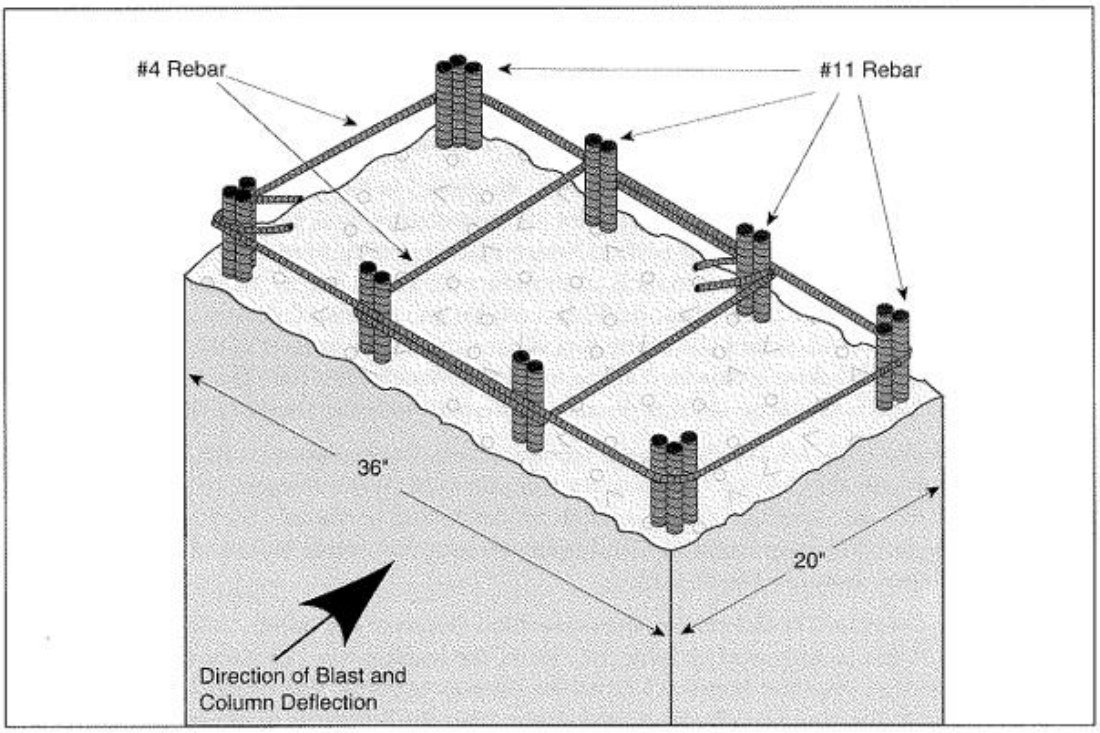

Figure 31 – G24 Column Section, FEMA Report.

The total axial force was estimated to be 3134.3 kN, in addition to the self-weight of the column. This load was modeled as a static point load. It was also used in obtaining the response curve for the section.

The elastic hinge properties were obtained by analyzing the section described in the FEMA report using the Response 2000 program.

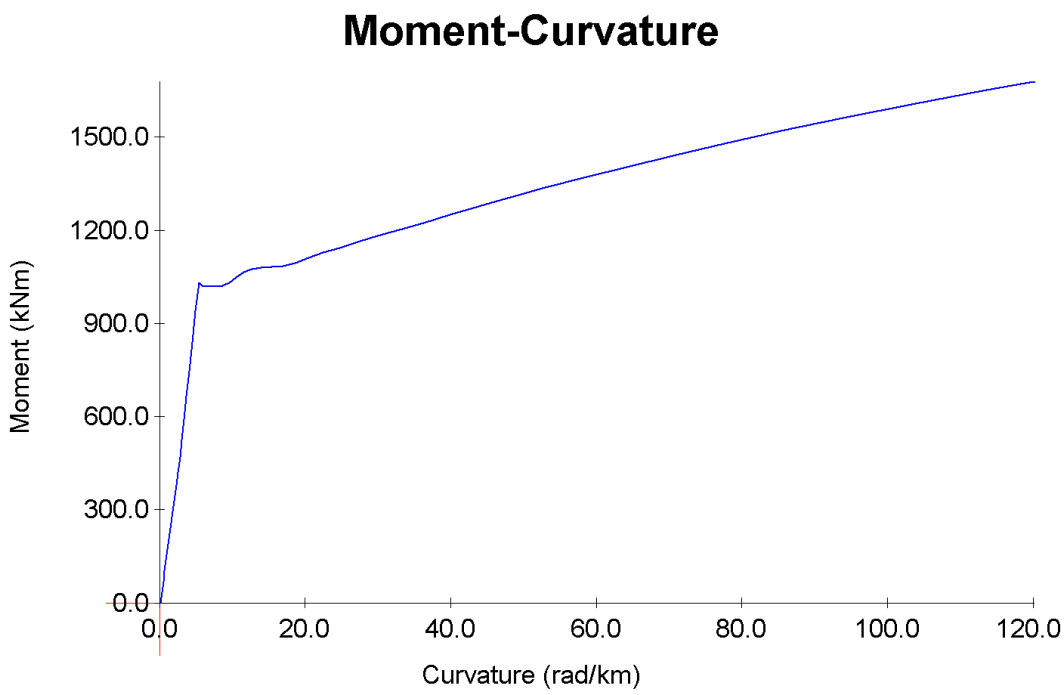

Figure 32 -Curvature-Moment Curve, G24 Column. Created using Response 2000

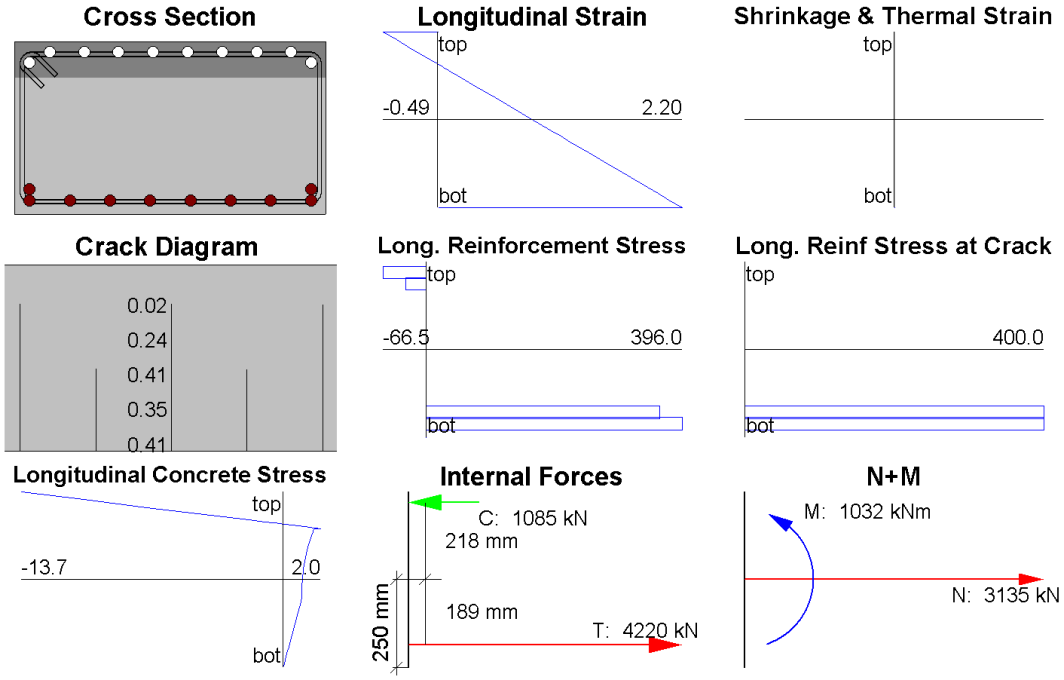

Figure 33 - Response 2000 Output for the G24 Column Section, at the yield point

A skeleton curve was created as an approximation of the curvature-moment obtained and was used to model the inelastic hinges.

The shear capacity of the structure was calculated using the same EN1992.1.1.2004 based sheet, converted to 10x10x10 cm concrete nominal strength, as well as using Response 2000. While Response 2000 uses an advanced model based on the Modified Compression Field Theory for its calculations, the code based sheet is essentially identical to manual calculations

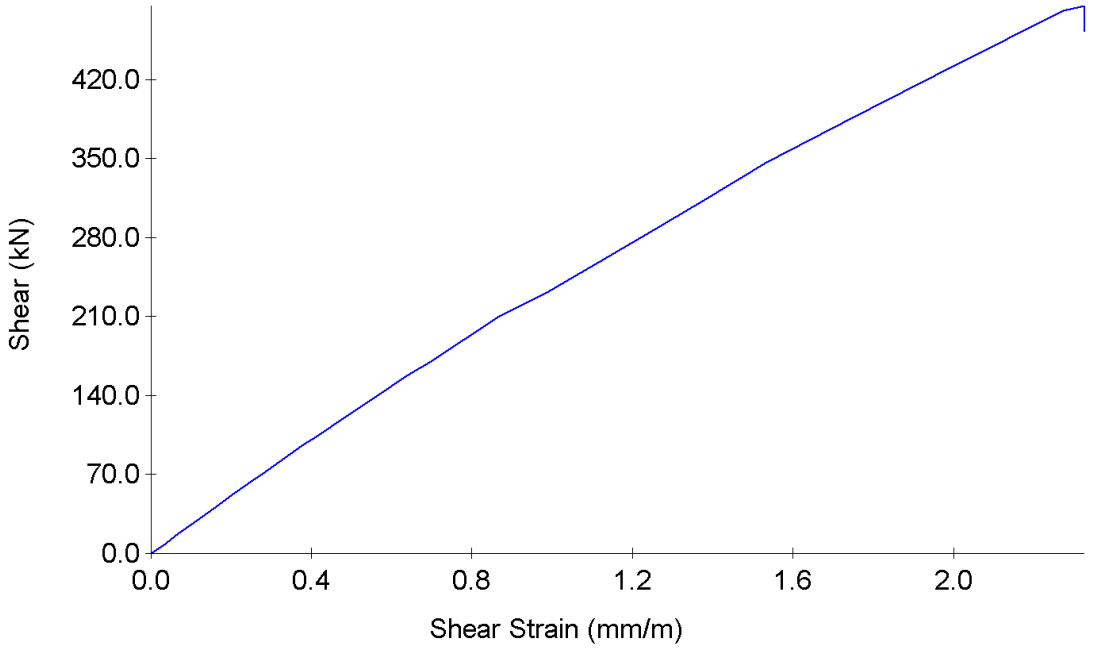

Figure 34 - Shear Capacity Analysis, G24 Column. Created using Response 2000

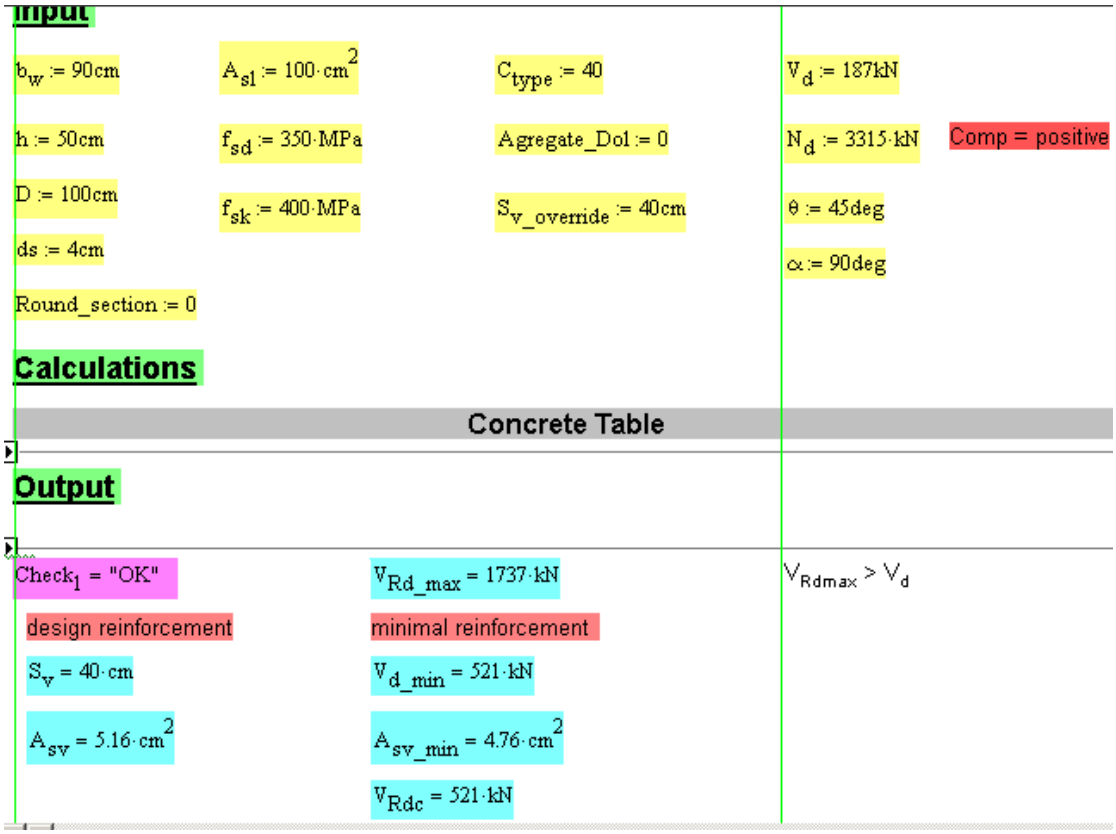

Figure 35 – shear capacity calculation according to EN code

The code calculation predicts shear reinforcement yield at 187 kN. The concrete's shear capacity is estimated at over 500 kN. However, it is clear that it was not the case, since the column was in fact sheared off.

The ligature spacing (step distance between stirrups along the direction of the element) being 40cm and therefore clearly sub-standard, may have something to do with it. The FEMA report states that the ultimate shear capacity is found to correlate to an average shear stress of 52 PSI, which translates into 166kN. If so, it seems that Response 2000 tends to over-estimate the shear capacity of the section.

Time history loads were defined according to the simplified load presented in the LS-DYNA study. The LS-DYNA study presented a simpler load than the one presented in the FEMA report. However, the loads are similar both in terms of peak pressure and in total impulse. The load was also cross-checked using the VecTor-Blast program

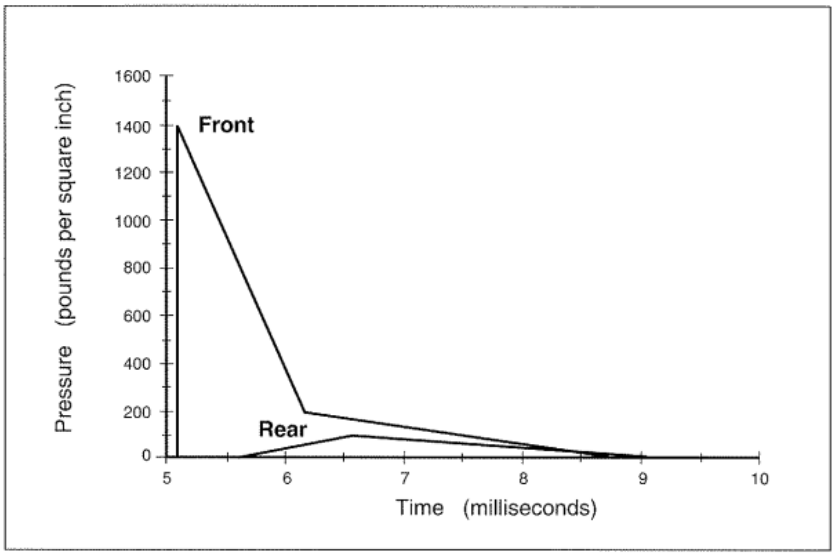

Figure36 - Time History Load, G24 column, FEMA 277

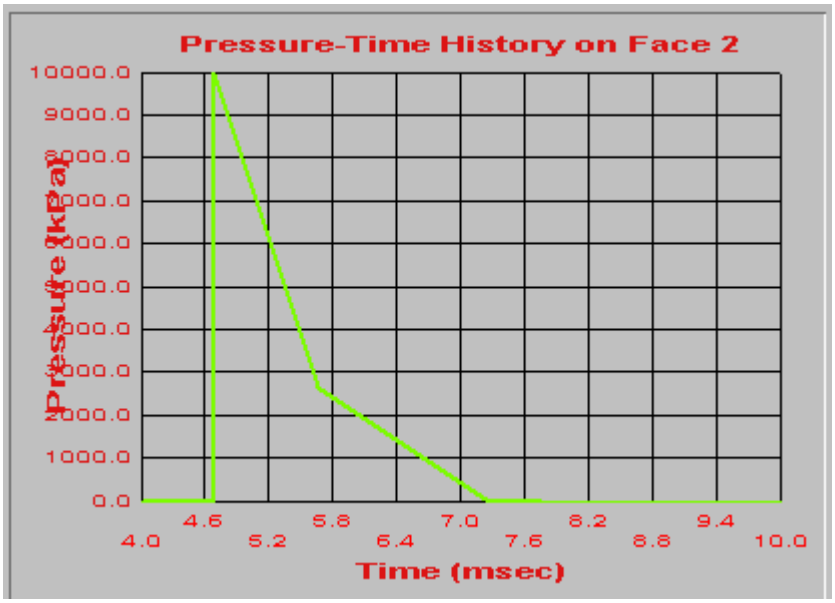

Figure 37 - Time History Load, G24 column, VecTor-Blast Analysis Output

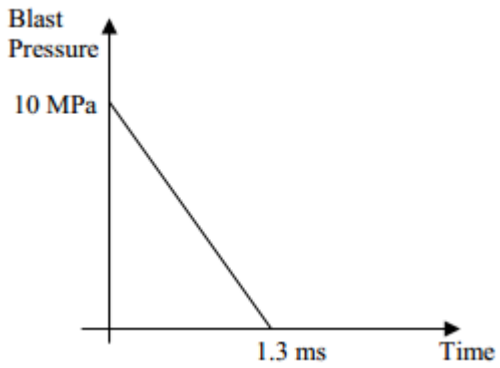

Figure 38 - Time History Load, G24 column, LS DYNA Study (Ngo, Mandis, Gupta, & Ramsay, 2007)

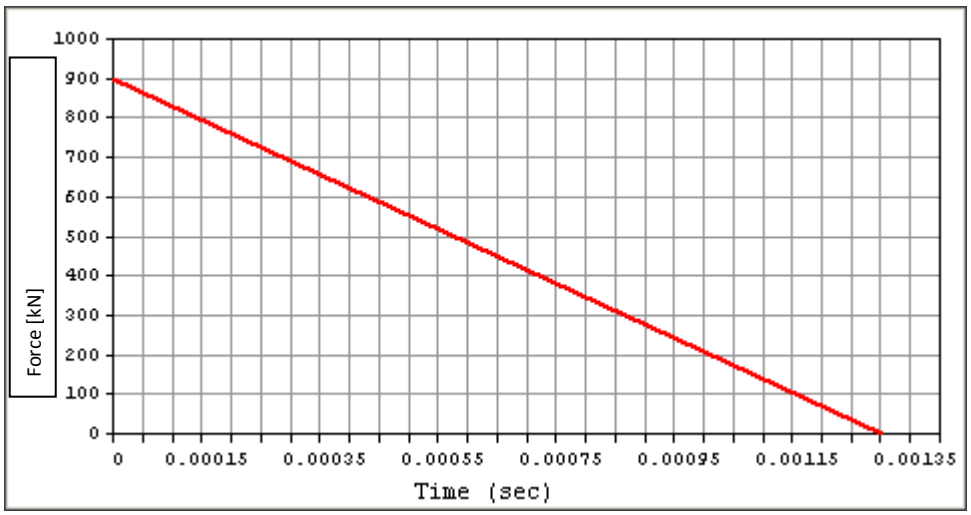

Figure 39 - Time History Load on the Column, MIDAS Civil Input Data

The force was calculated according to the time-history pressure acting on the 90cm wide side of the column, pushing in the column's weak direction.

An Eigenvalue analysis was carried out in order to characterize the load

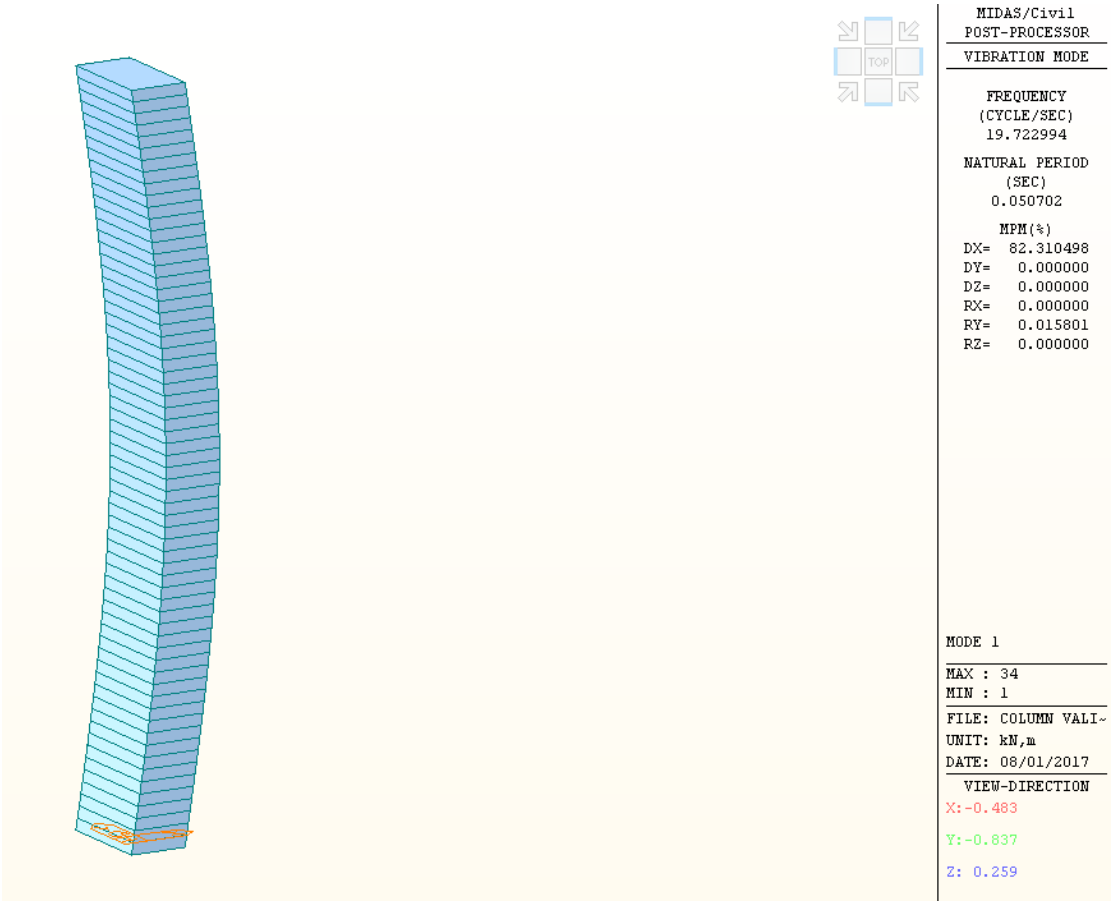

Figure 40 - Eigenvalue Analysis Result - G24 Column

The ratio between the column's natural period and the duration of the load indicates clearly an impulse controlled load. A time step of 10^{-5} second was selected for the analysis, since the loading duration is so very short, and so to avoid possible numerical damping.

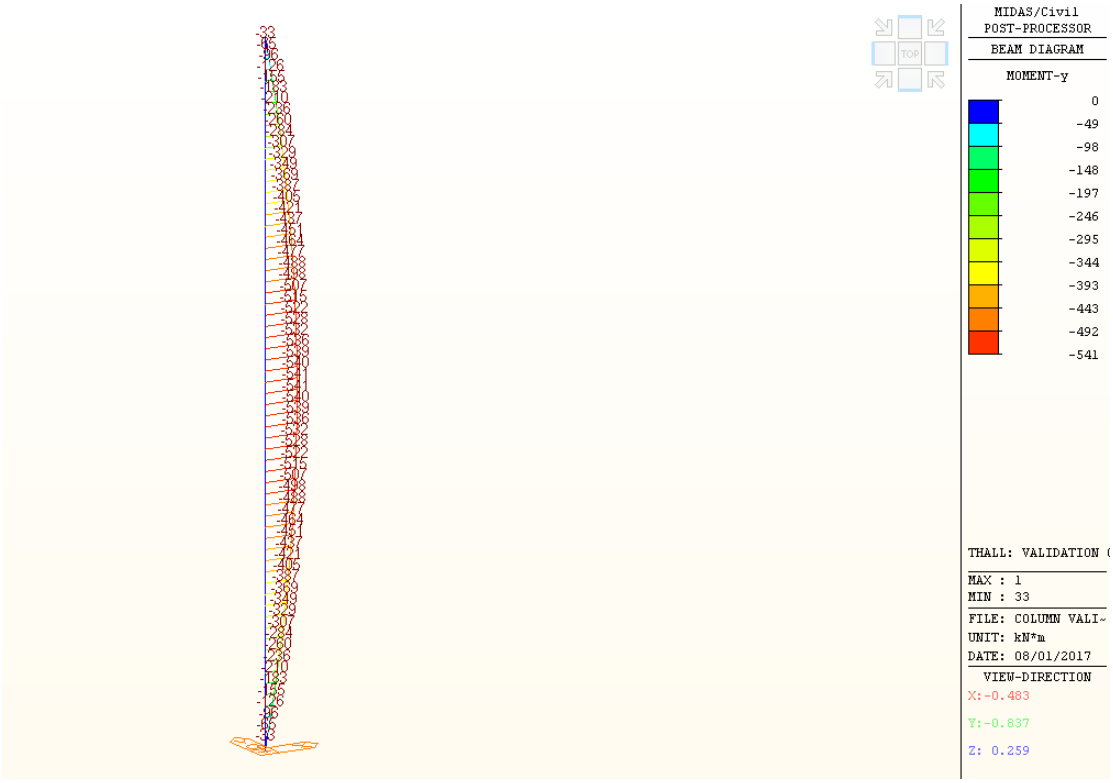

Figure 41 - Moment Envelope Resultant, G24 Column, Time History Analysis [kNm]

In is clear from the result that the column was adequately reinforced to sustain the moments resulting from the blast.

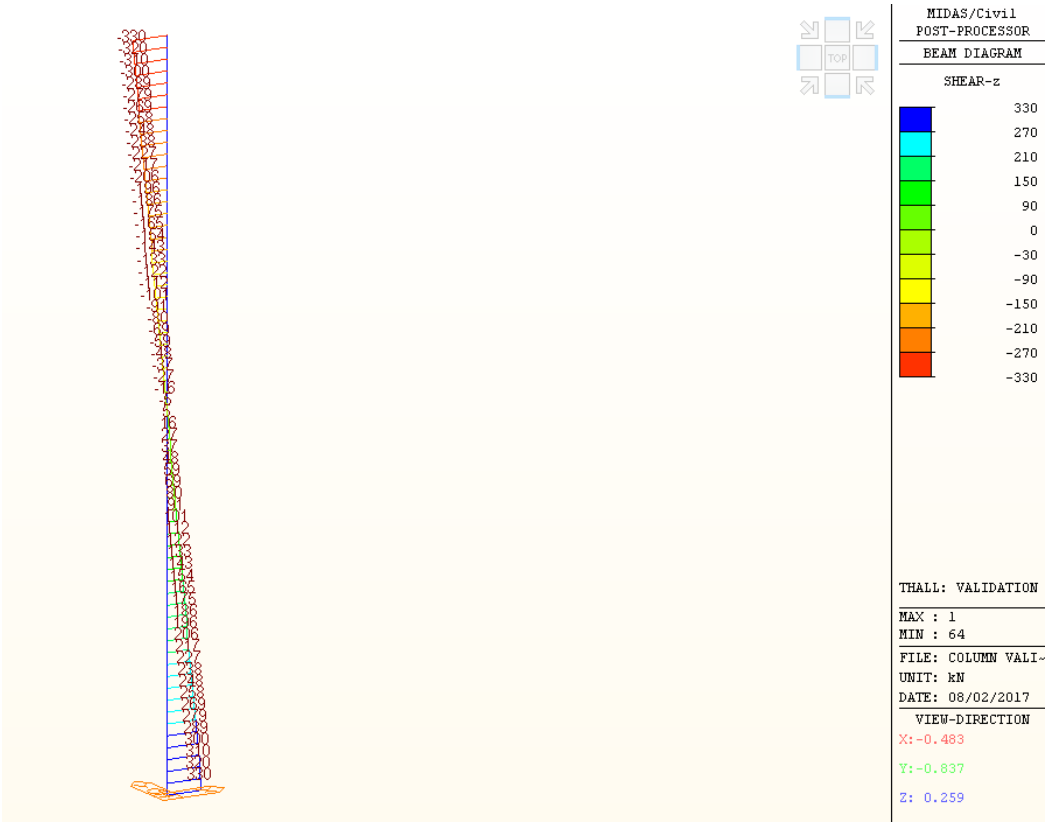

Figure 42 - Shear Envelope Resultant, G24 Column, Time History Analysis [kN]

The output shows that the shear force in fact exceeded both the capacity value obtained from the FEMA report, and the capacity calculated using the code.

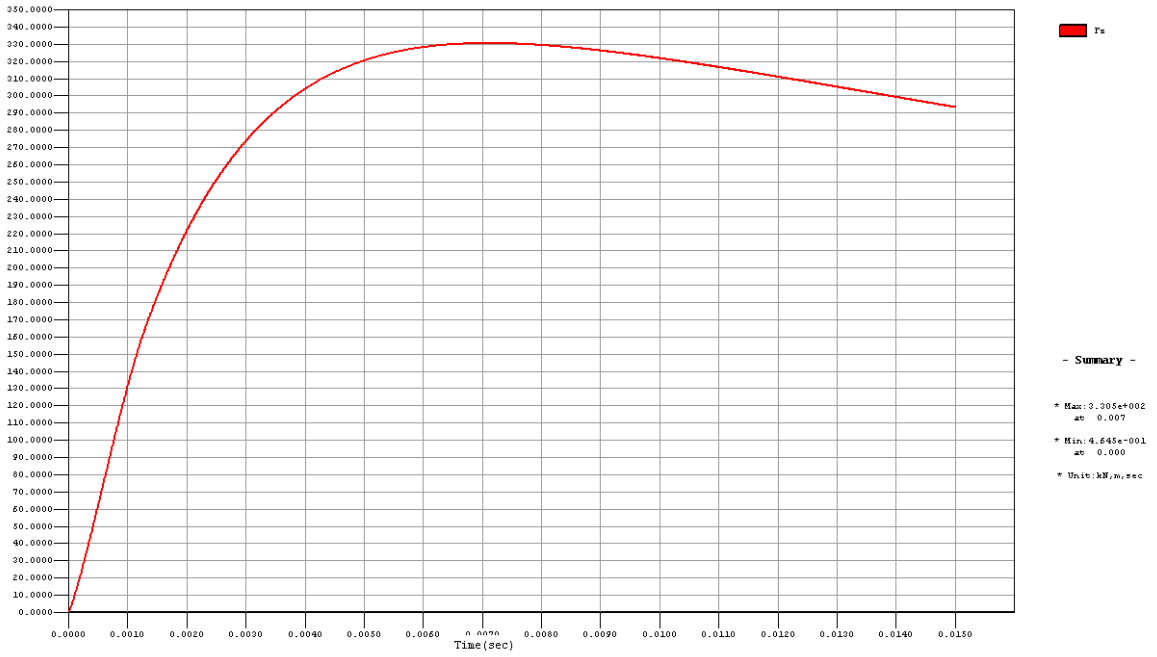

Figure 43 - Time History Output - Shear at the Base of the Column [kN]

When the shear behavior is factored into the analysis, the failure pattern correlates to the one found in previous studies

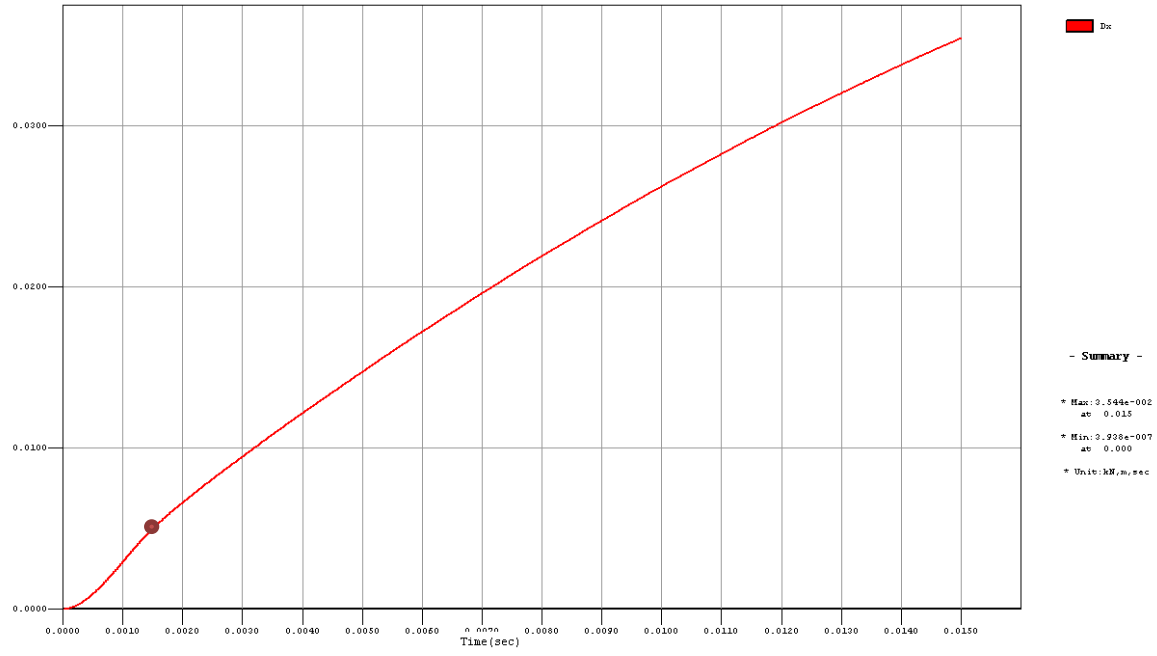

Figure 44 - Time History Output - Displacement at the middle of the Column [m] point of shear failure is marked by a red circle.

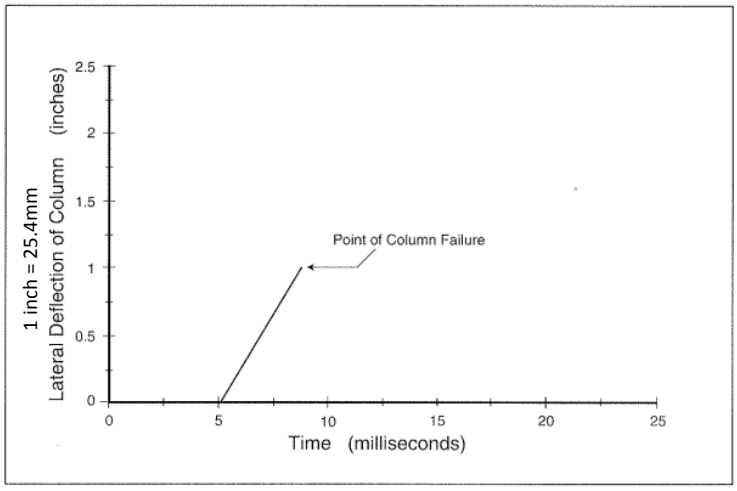

Figure 45 - Time-Displacement Graph, FEMA 277

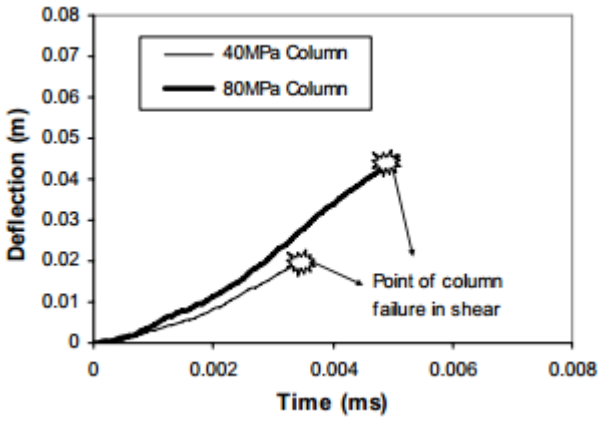

Figure 46 - Time-Displacement Graph, LS DYNA Study (Ngo, Mandis, Gupta, & Ramsay, 2007)

The displacement at the time of failure was found to be 4 mm, significantly smaller than the FEMA report (2.54cm) and the LS-DYNA study (2cm). The failure was also quicker to develop in the inelastic analysis. 1.3 milliseconds comparing to 2.5 milliseconds in the FEMA report, and 3 milliseconds in the LS-DYNA study.

However, considering the immense complexity of the problem and the vast room for assumption as well as the variation is the analysis approach, these results are actually relatively close. It also corresponds to manual approximations.

Section Calculation validation

While a more thorough study is necessary in order to truly validate the results from the Mathcad section response calculation sheet, it was thought to be helpful to at least present a few examples of comparison with results obtained through a well-accepted code.

The example selected is a mid-span section of a pre-stressed concrete beam.

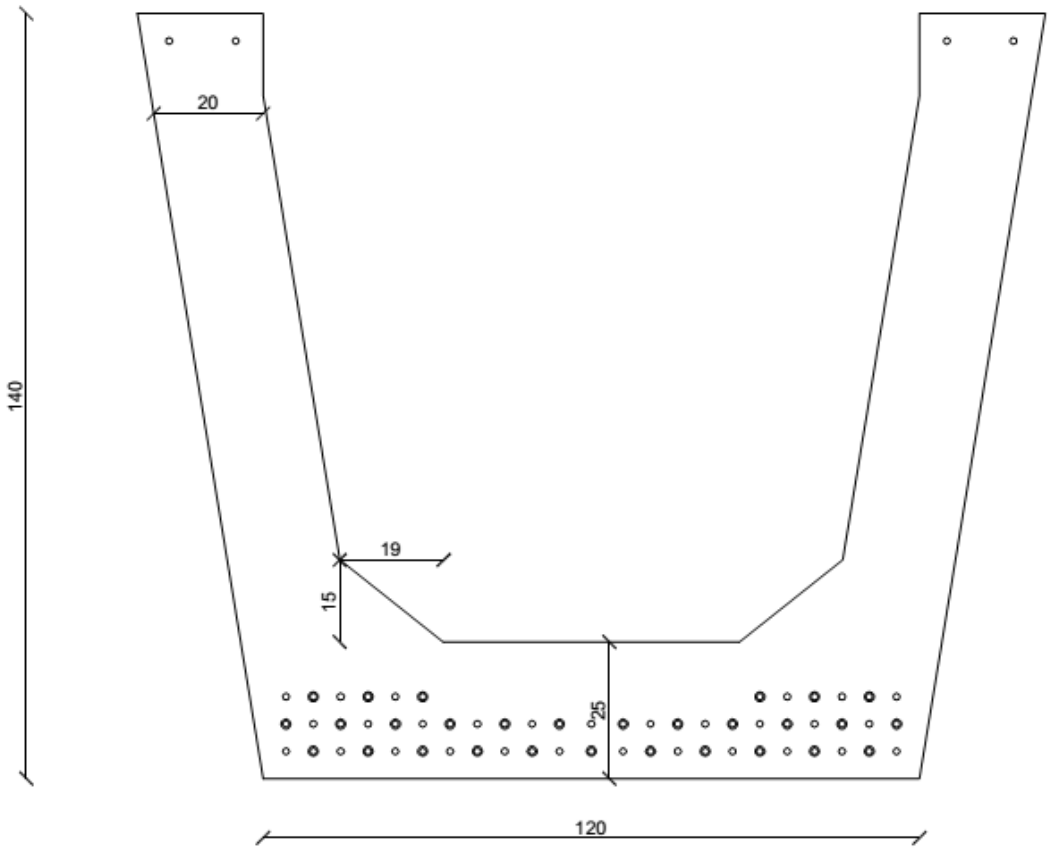

Figure 47 - Section Analysis Example Section. 1.4m PSC beam. Web Thickness: 20cm. Bottom Flange Thickness: 25 cm.

The section response was evaluated using both the Mathcad sheet and Response 2000.

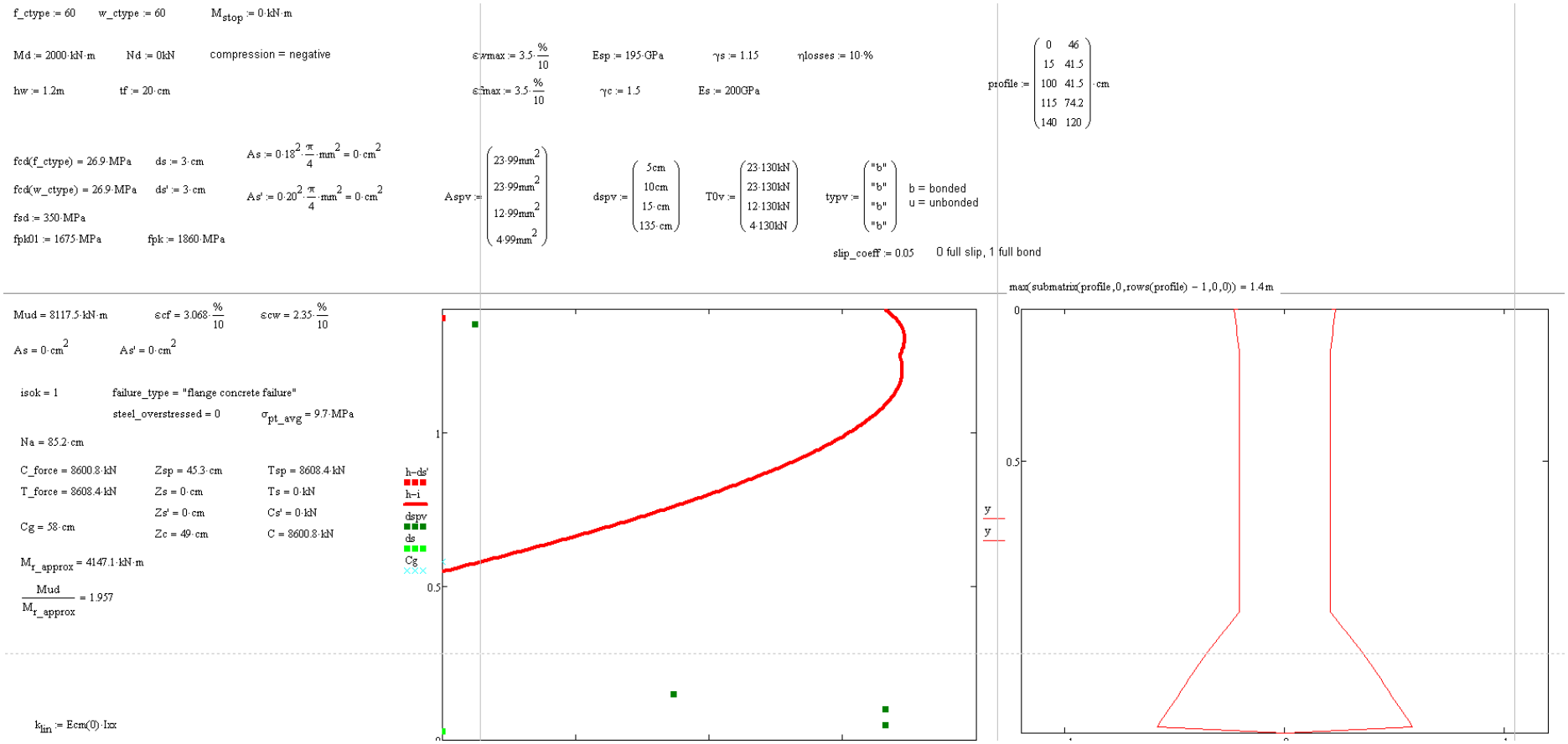

Figure 48 - Pre-stressed Beam Calculation Sheet– Validation Example

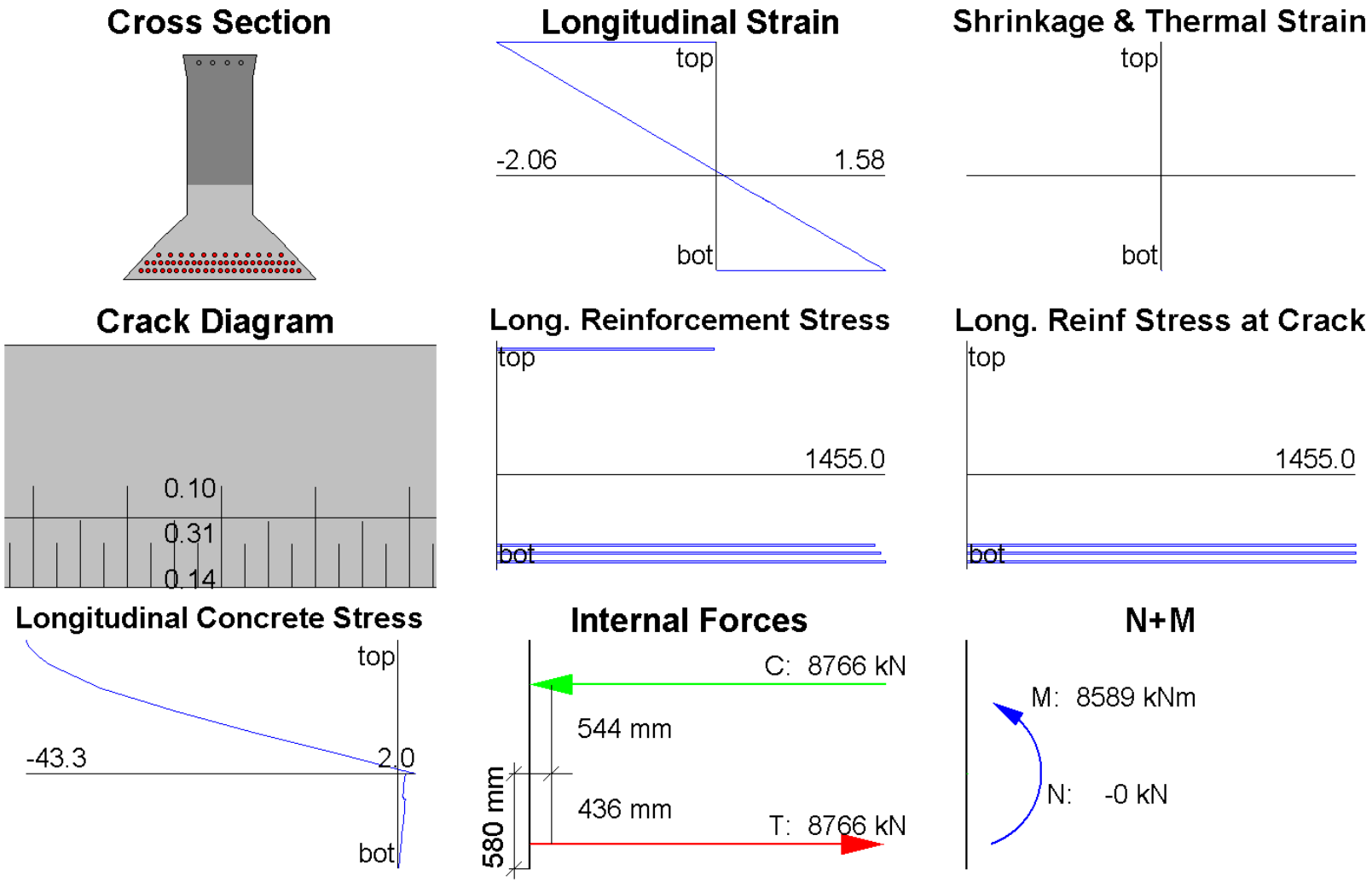

Figure 49 - Pre-stressed Beam Response 2000 Output– Validation Example

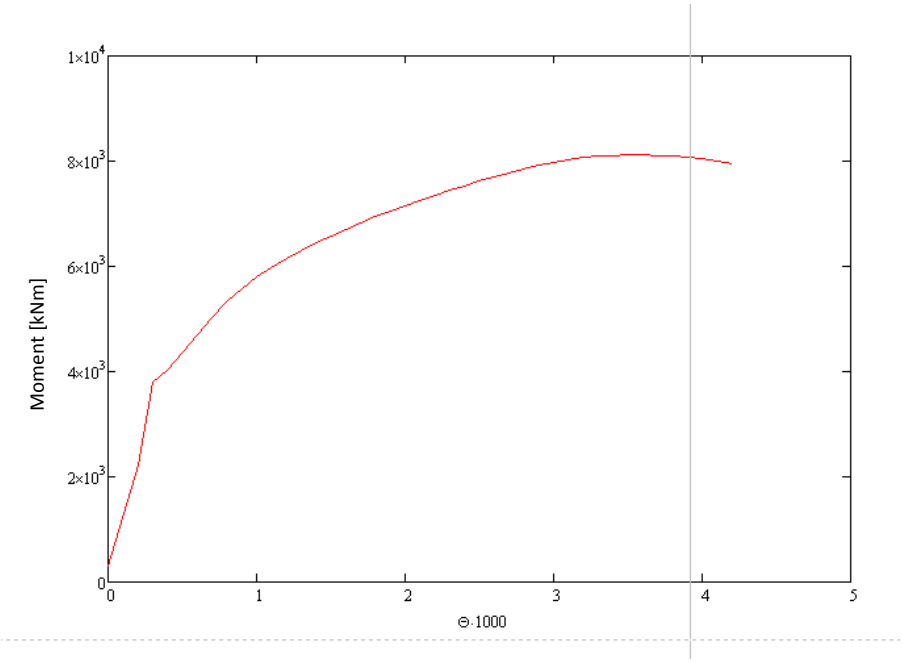

Figure 50 - Curvature-Moment curve, Mathcad Sheet

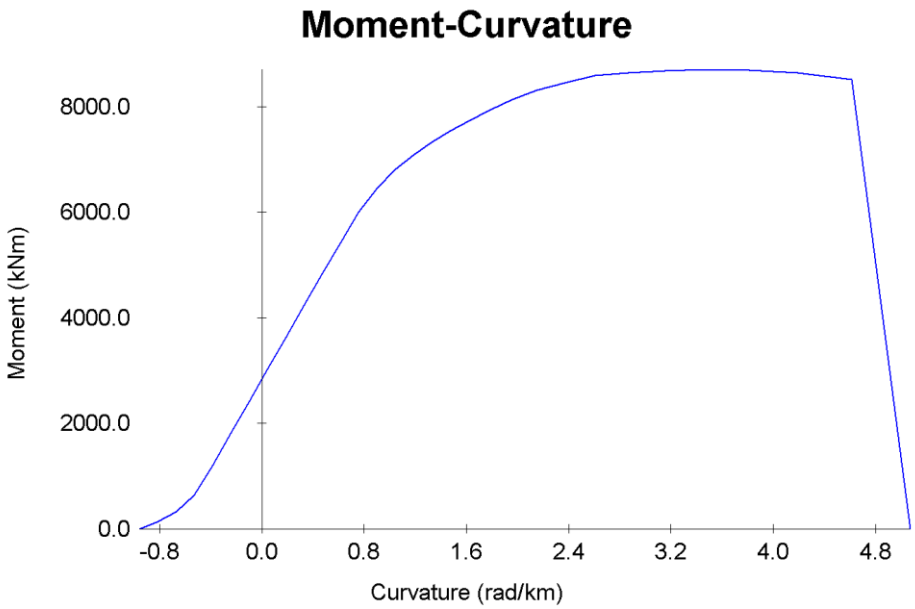

Figure 51 - Curvature-Moment curve, Response 2000

Figure 48 shows the input and primary output of the pre-stressed beam section response calculation sheet. The main input parameters are the concrete types used (two types in case of a composite section), section geometry by coordinates, total amount of tensile and compressed mild reinforcement with the corresponding cover depth, amount of pre-stressing tendons, initial force and location, as well as type (bonded/un-bonded), material design strength ,required moment capacity and given axial force. The main output is a summary of the given quantities, a diagram of the equivalent section, a summary of forces acting in the section at peak moment, the strains in the concrete corresponding to it, with their respective lever arms in relation to the section's center of gravity. It also shows a diagram of the forces acting in the section, where the red curve is the compressive force

distribution (not to be confused with the somewhat similar compressive stress distribution), the light and dark squares are the forces from the mild and stressing steel respectively, and the red square is the force from mild compression reinforcement. There is no mild steel present in the given example. The sheet also outputs the expected type of failure, center of gravity, location of the natural axis in relation to the compressive fiber, and the approximated crack capacity. The sheet calculates other quantities and displays additional output such as a moment-curvature graph and crack width estimation.

Figure 49 shows the Response 2000 output for the analysis of the same section. The 9 graph display (starting from top left and moving right and downwards) shows:

- The cross-section, where tensile-yielding steel marked in red, compressive-yielding steel in green (not shown in this example) the tensile area in light grey and the compressive area in dark grey.
- The longitudinal strain distribution, with negative values for compressive strains
- Additional strains accounted for such as shrinkage and thermal added to the total load (not applicable in this example)
- A crack diagram showing the width, depth and directionality of the cracks
- Stress in the longitudinal reinforcement at each ordinate
- Stress in the longitudinal reinforcement at the cracked ordinate, which include additional effects related to shear at the crack.
- Concrete stress distribution
- Internal forces diagram
- External forces diagram

While the Response calculation shows a higher ultimate capacity, the two calculation results correlate well.

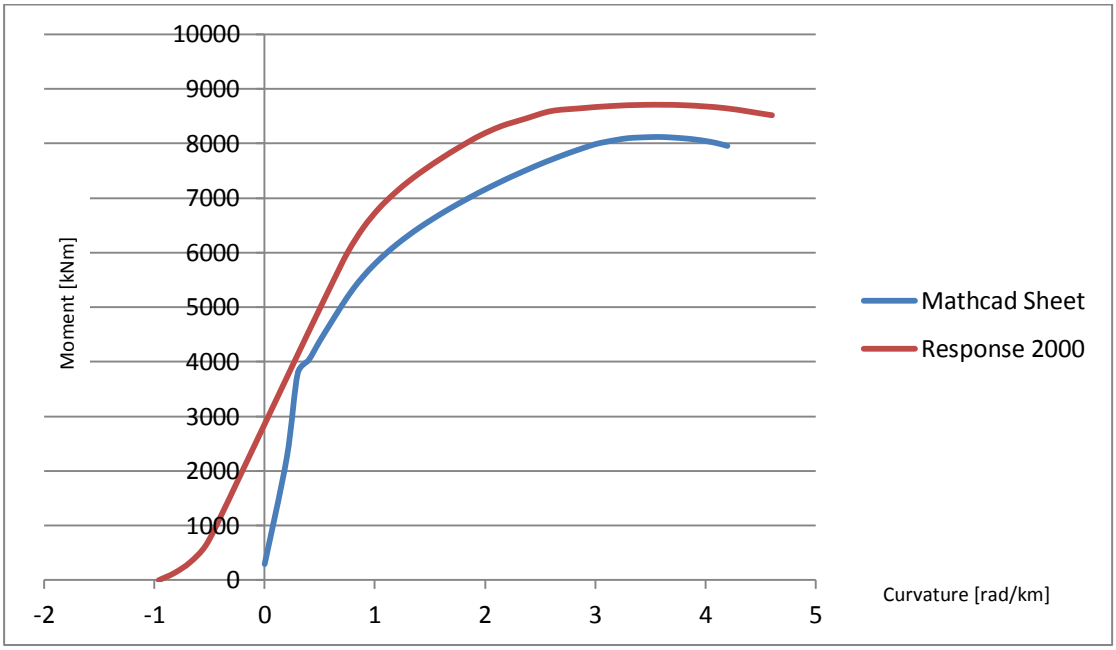

Figure 52 - Curvature-Moment Curve, Comparison

The differences between the curves are attributed to small discrepancies between the two methods in material strength curves, and Response considering tensile stresses in the concrete.

In this Compression controlled section example, the Mathcad sheet gives a more conservative result.

Grillage validation

A comparison between a Discrete Kichhoff Mindlin quadrilateral shell element model of a ceiling and a grillage model had been carried out.

The measurements of the ceiling are the same as in the experimental models, i.e. 16 x12 meters. Element length for the grillage model is 1m for internal elements and 0.5m for near-boundary elements. The internal DKMQ elements are 1x1 meters, and the near boundary elements are 0.5x1 meter for the edges and 0.5x0.5 meter for the corners. Note that despite it may look otherwise doe to overlapping in the rendering of the elements in the grillage result output, the two models have the same number of nodes.

Both models were loaded with self-weight only.

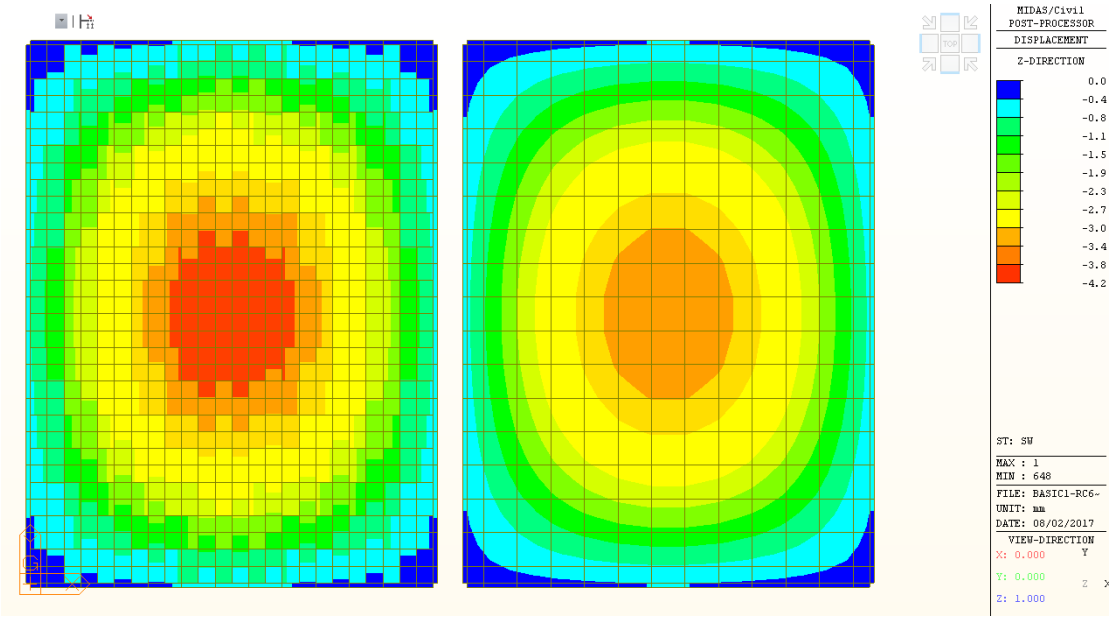

Figure 53 -Model Comparison, vertical deflection. Grillage vs. Shell. The Grillage Model is on the Right, Shell Model on the Left.

The Grillage model vertical displacement resultant is 10% larger than the one obtained from the shell element model. This is due to decreased overall stiffness, resulting from the removal of torsion in the grillage model.

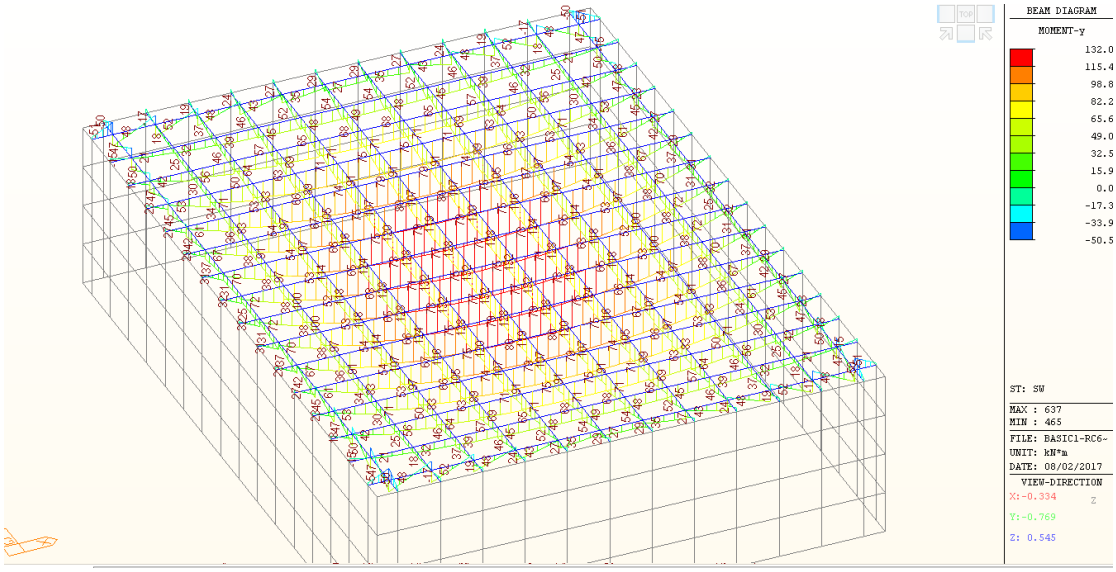

Figure 54 – Bending Moments, Grillage Model

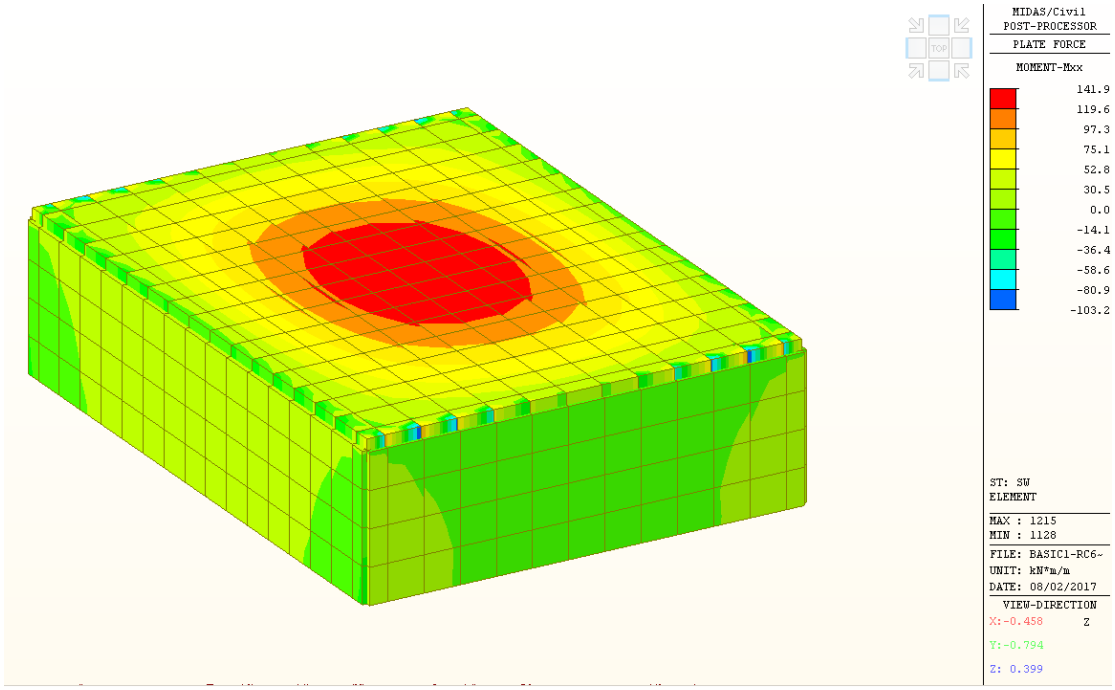

Figure 55 – Bending Moments in the Short Span Direction, Shell Element Model

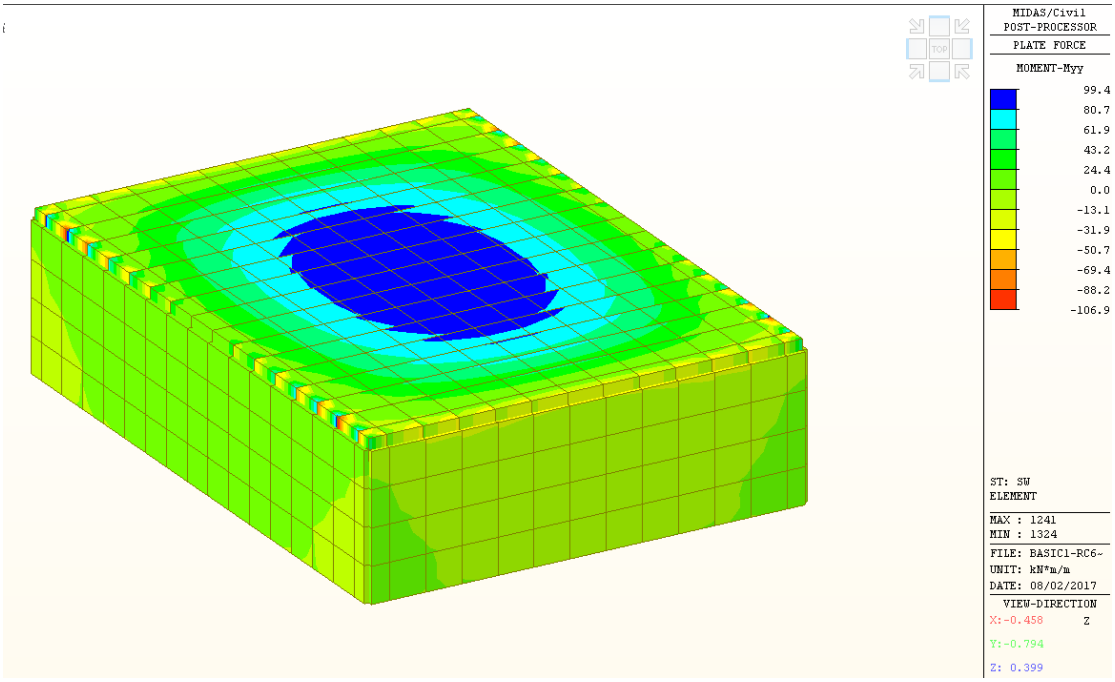

Figure 56 - Bending Moments in the long Span Direction, Shell Element Model

The grillage model show 132 and 80 kNm of moment in the short and long directions respectively.

The shell model show 142 and 99 kNm of moment in the short and long directions respectively.

This shows the results obtained from the grillage models to be slightly less conservative, due to better distribution of the moments expressed in higher resultants away from the center of the span.

5. Blast Load Analysis Results

The analysis carried out for each system included several stages:

- Basic period calculation- using eigenvalue analysis to determine the type of loading
- Section response analysis -to obtain moment-curvature data for inelastic hinge modeling
- Time history analysis under blast loading – to examine the structural behavior of each system.

RC slab results

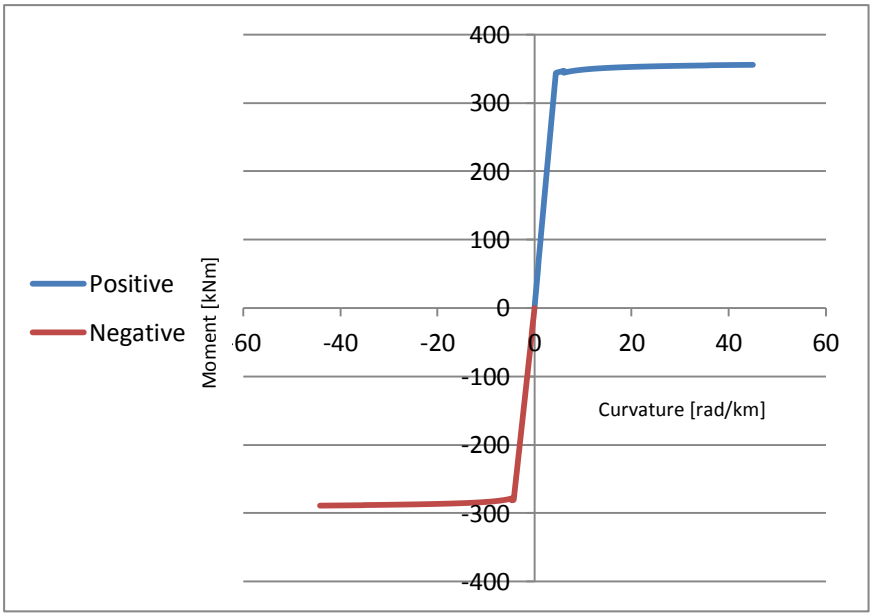

Figure 57 - RC slab, bending moment capacity [kNm]

Bending moment capacity for the slab is 355kNm, yielding at 343 kNm.

The section is calculated to crack at 194.4 kNm.

Negative moment capacity is 289kNm.

Curvature at ultimate is 42.4 rad/km

The tensile strength of the concrete is neglected from the calculation sheet, and so the cracking point was entered into the skeleton curve directly.

The idealized skeleton curve is therefore tri-linear, having un-cracked, cracked and post-yield phases.

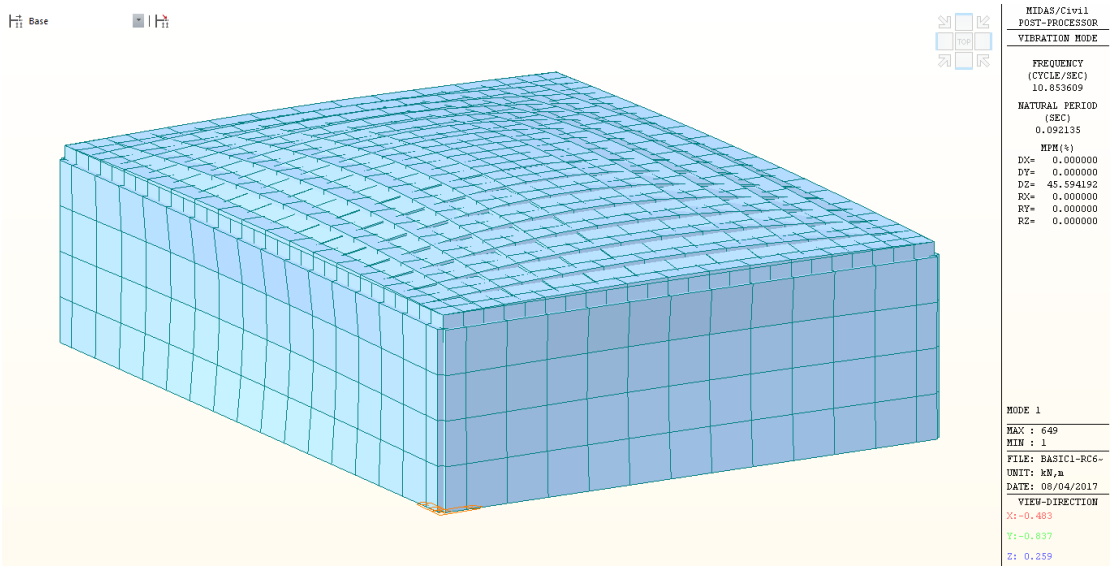

Figure 58 - RC Slab eigenvalue analysis. Natural period is 0.092 sec

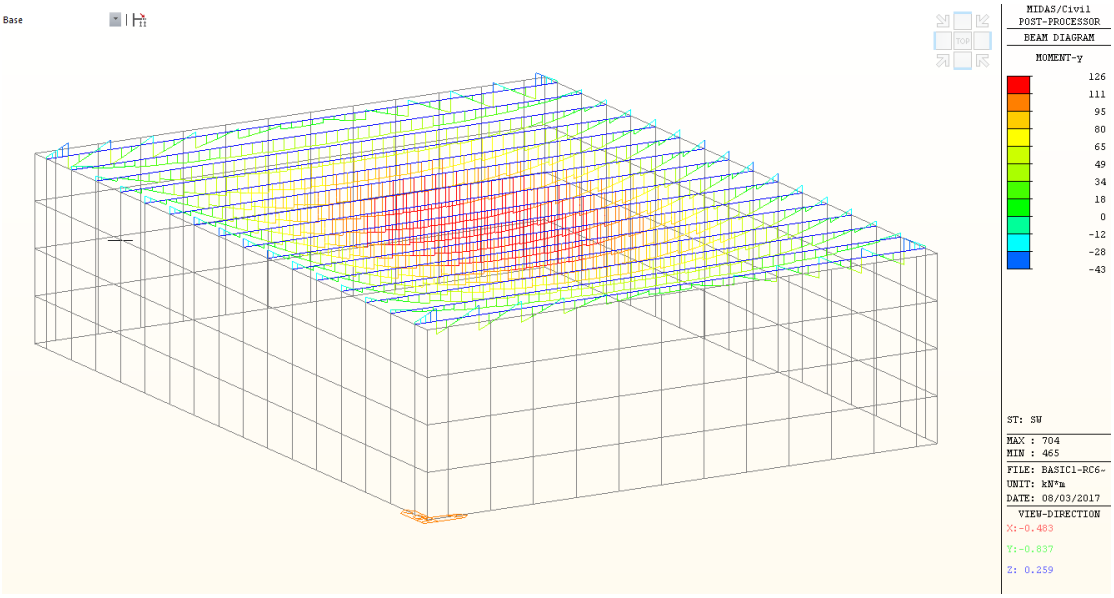

Figure 59 – RC slab, Moment distribution at rest, short span direction [kNm]

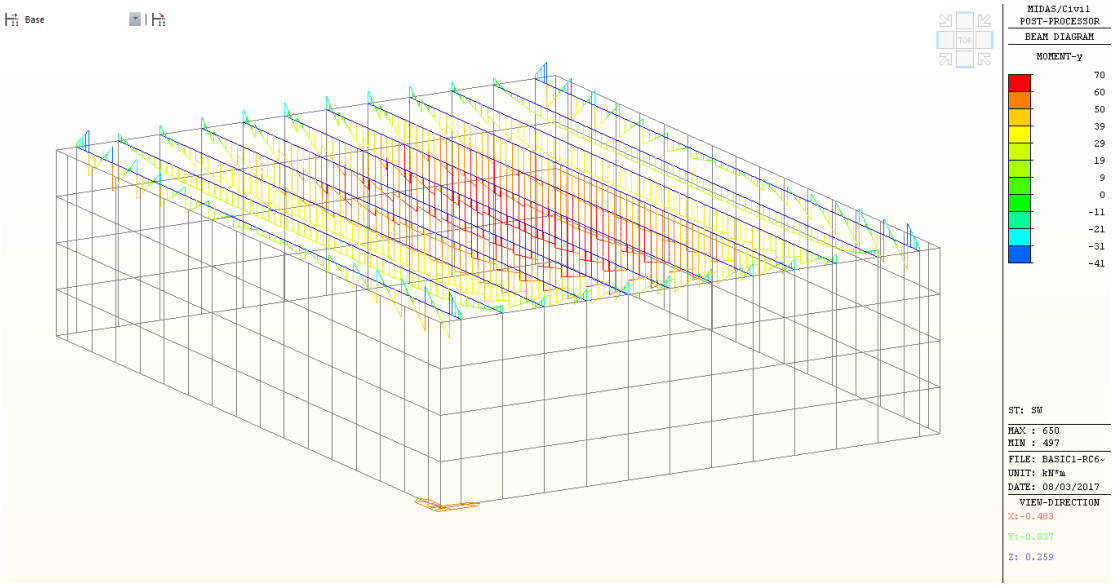

Figure 60 - RC slab, Moment distribution at rest, long span direction [kNm]

According to section analysis, the moment result at rest shows no cracking at any direction.

Case 1.1 – RC slab under 81mm mortar blast

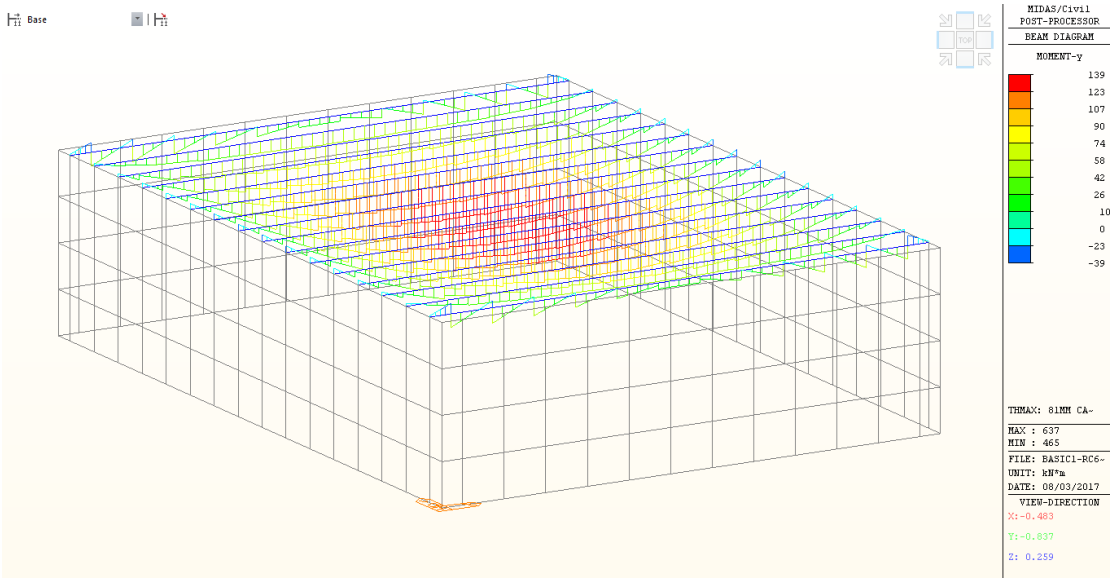

Figure 61 – Maximum positive moment envelope, 81mm mortar, short span direction [kNm]

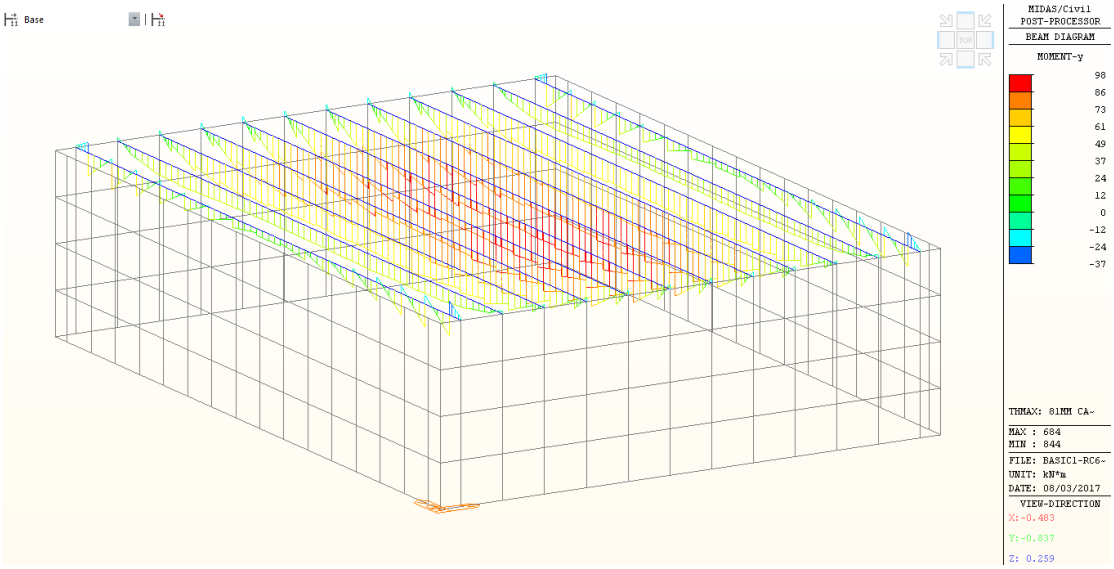

Figure 62 - Maximum positive moment envelope, 81mm mortar, long span direction [kNm]

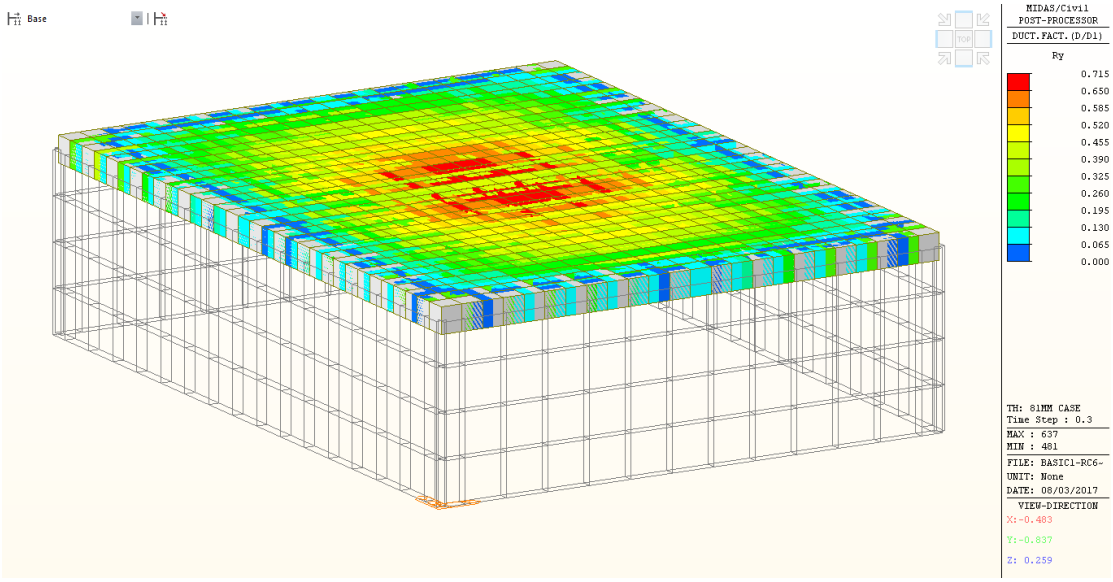

Figure 63 – D1 Ductility factors, 81mm mortar

The Time-History results show that the structure sustains no flexural damage from the blast.

The D1 ductility ratio is the ratio between the resultant curvature and the curvature calculated for the cracking of the section. Results under 1 indicate no cracking. The maximum resultant for this case is 0.715.

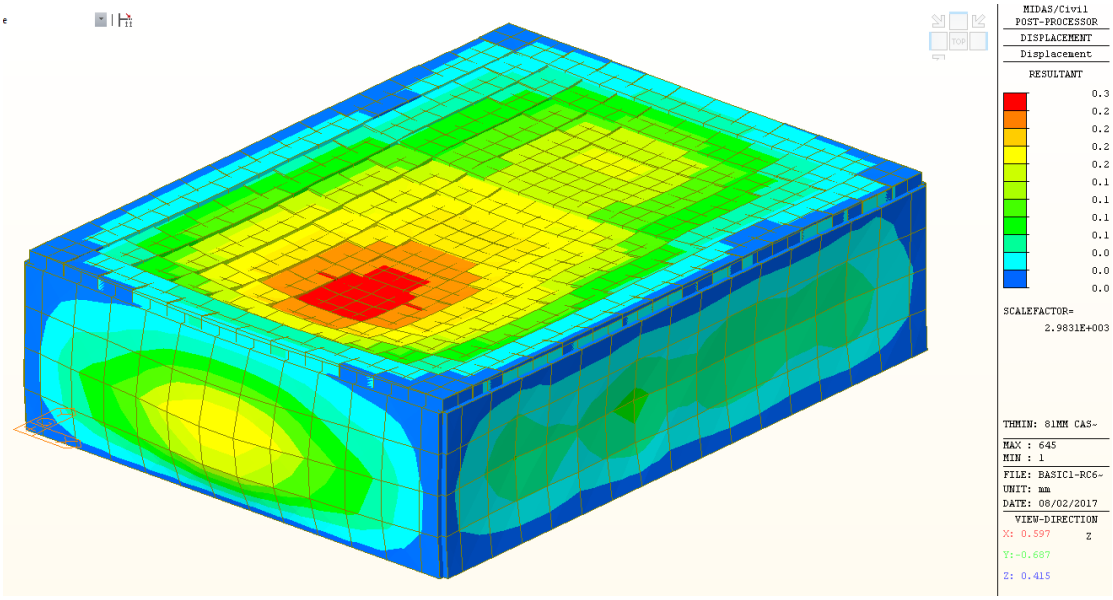

Figure 64 – RC slab, 81mm Mortar, Maximum Deflection [mm]

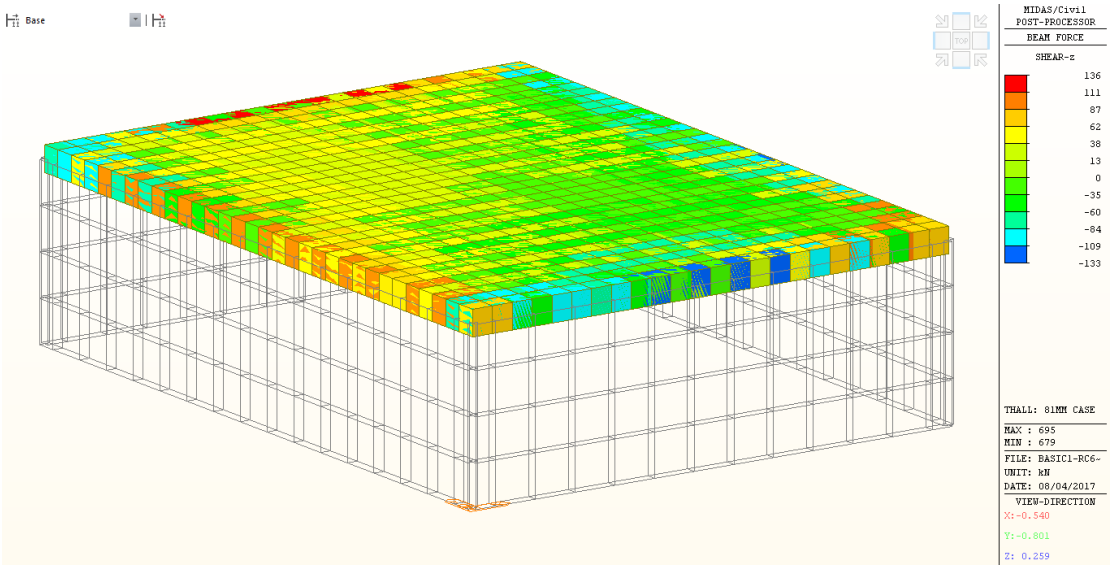

Figure 65- RC slab, 81mm Mortar, Shear force envelope [kN]

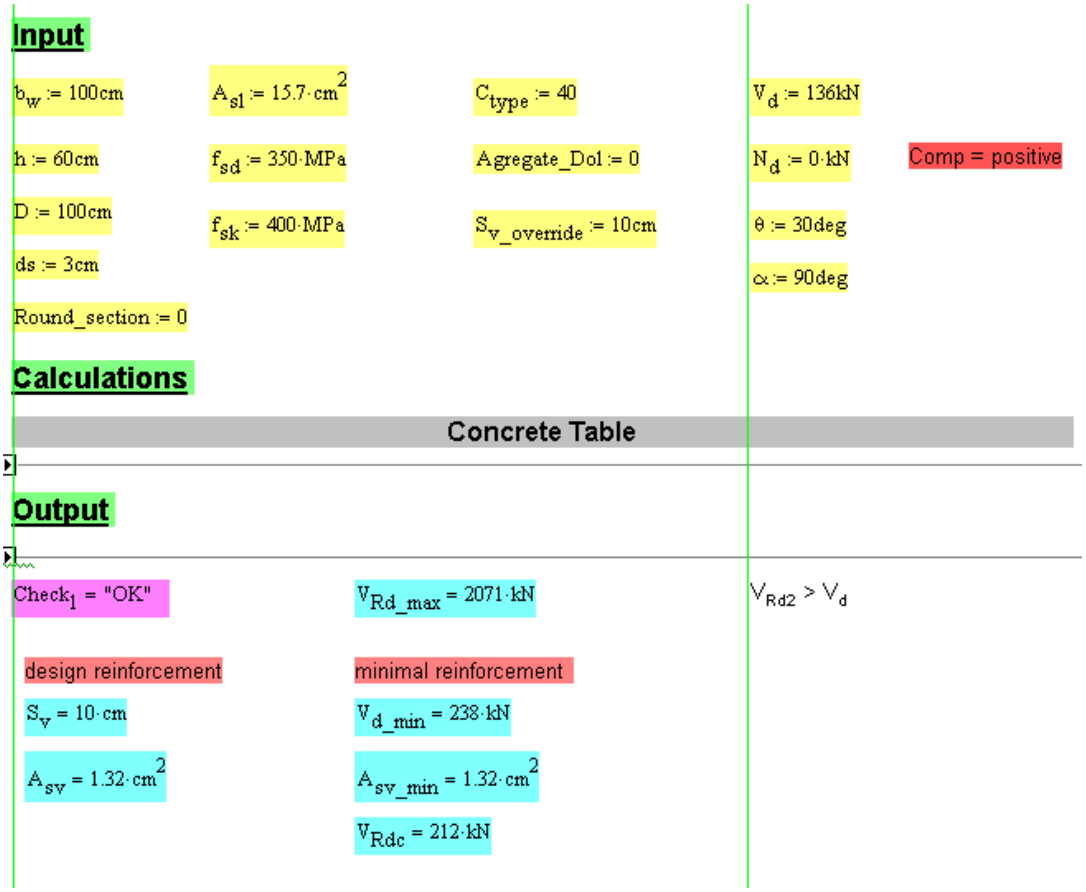

Figure 66 -RC slab, Shear capacity analysis for 81mm mortar case

The shear force resultant shows that the shear forces are small enough to be resisted by the slab, even when unreinforced with any shear reinforcement.

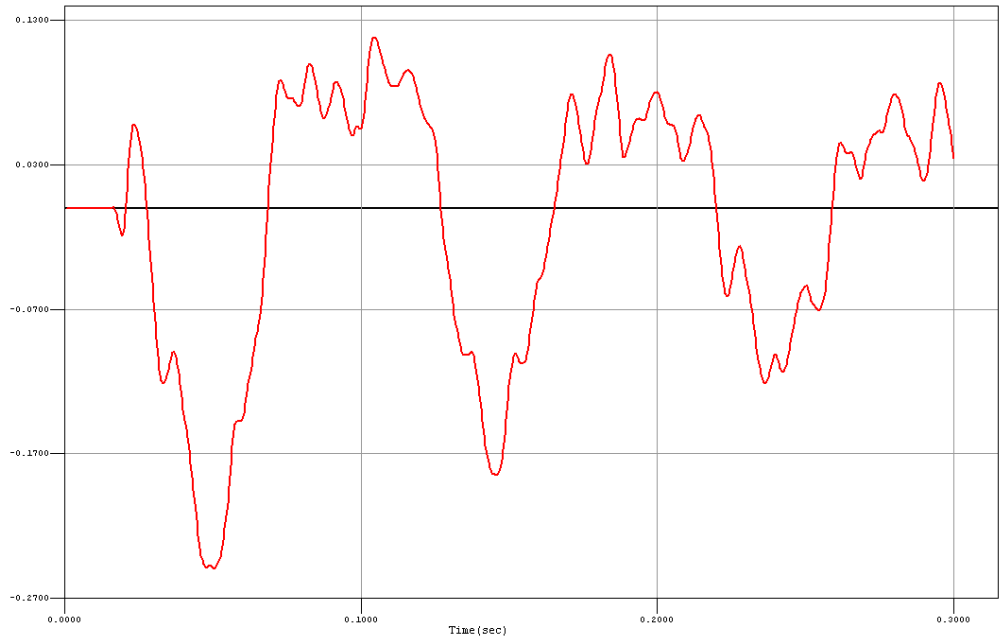

Figure 67 - Time-History vertical deflection at mid-span. The cycle lasts 0.0965 sec, indicating a slight increase from elastic natural period

The analysis results show good results for the case of the RC slab under the 81mm mortar air-blast scenario.

All data indicates having no damage done to the structure.

Case 1.2 – RC slab under 122mm rocket blast

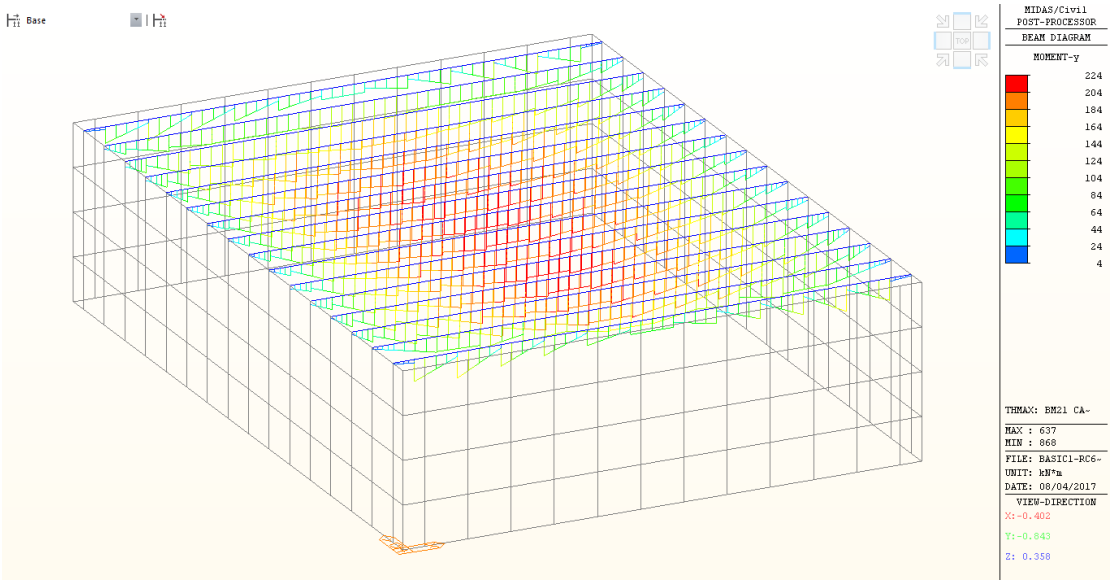

Figure 68 - Maximum positive moment envelope, 122mm rocket, short span direction [kNm]

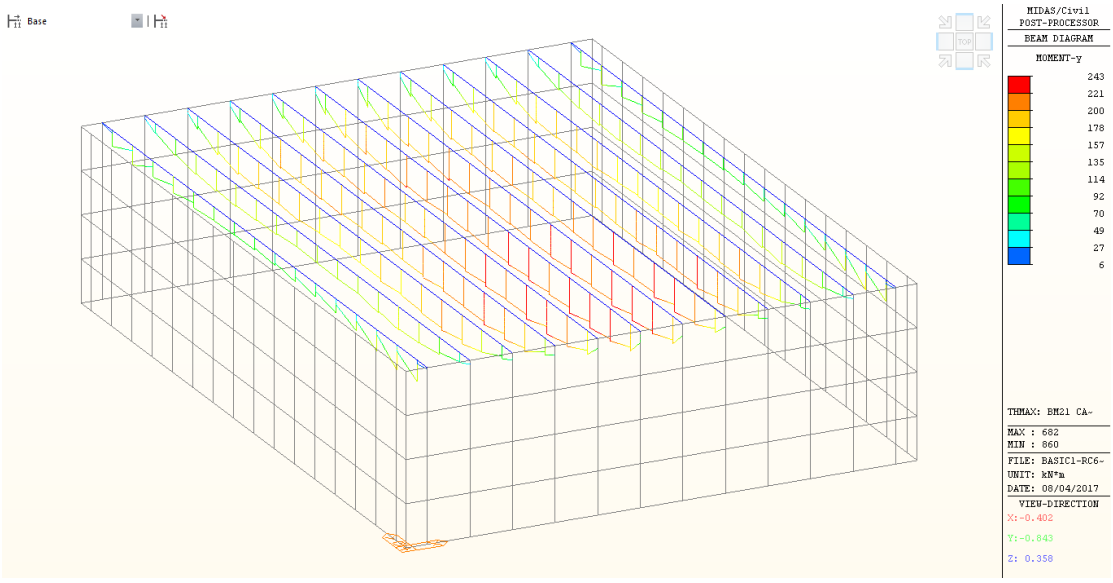

Figure 69 - Maximum positive moment envelope, 122mm rocket, long span direction [kNm]

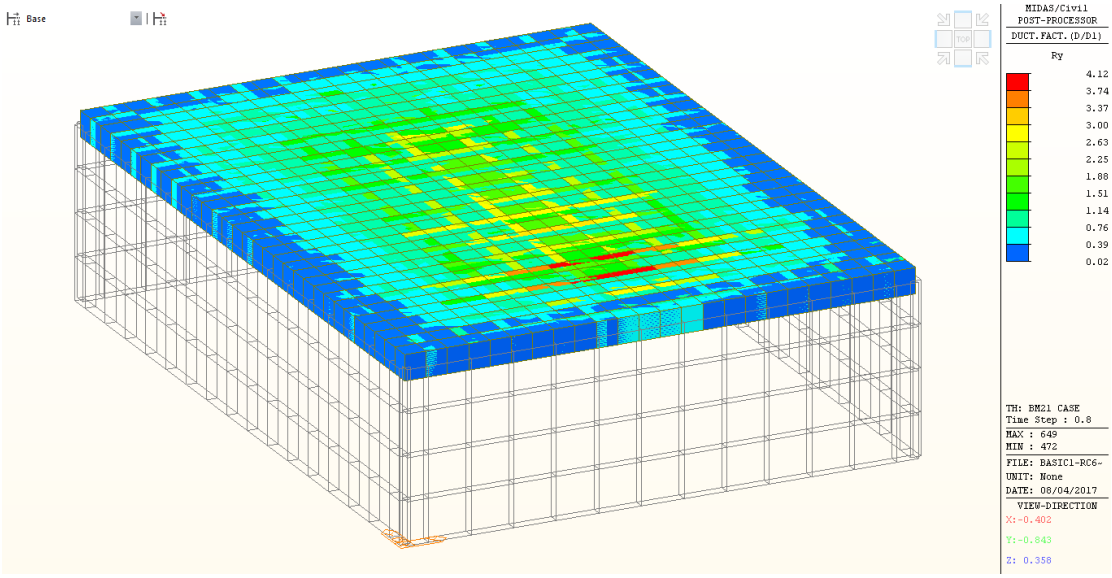

Figure 70 - D1 Ductility factors, 122mm rocket

The Time-History results show that the structure sustains some flexural cracking as a result of the blast, as also shown in the yield status output:

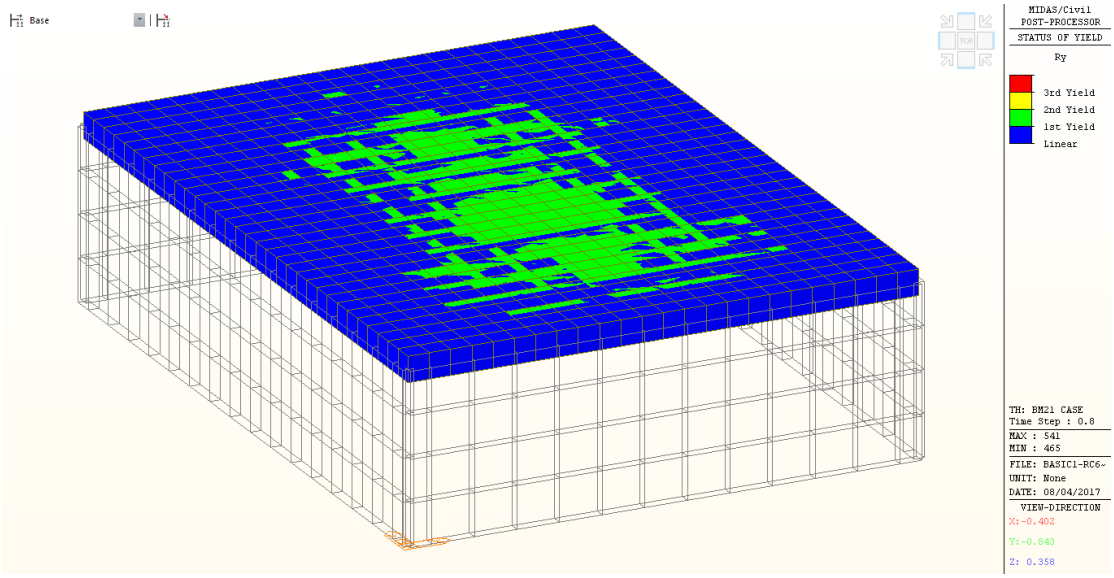

Figure 71 – Yield status output, 122mm rocket. Internally cracked regions are marked in green.

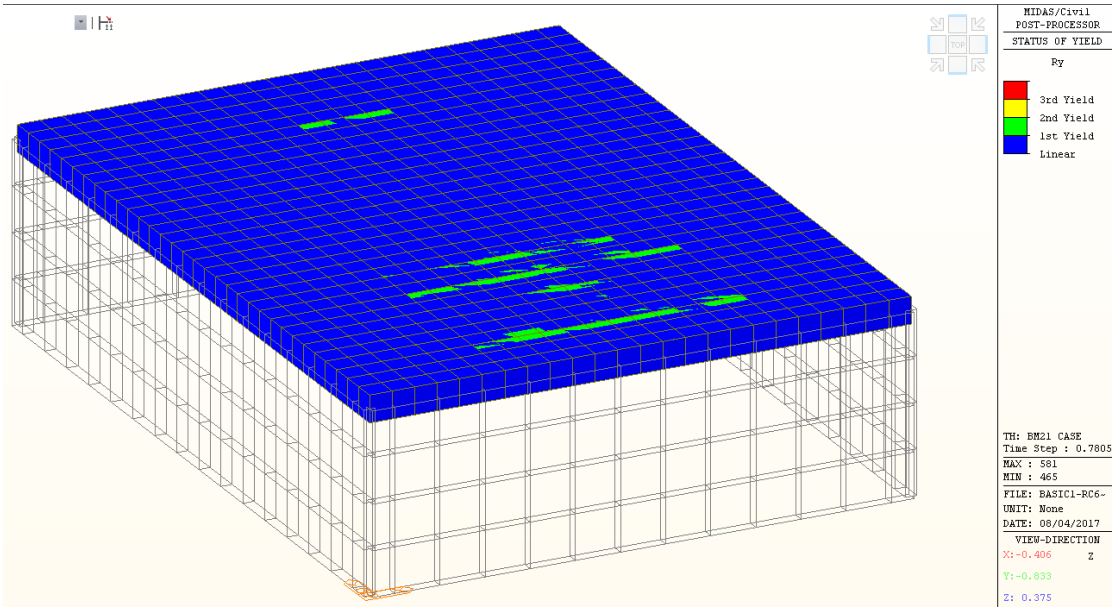

Figure72 - Yield status output, 122mm rocket. Externally cracked regions are marked in green.

Interestingly, the most severe damage is caused at the end that is away from the blast location.

The maximum crack width is estimated to be 0.072mm.

Similar cracks were also predicted to be formed at the exterior of the slab.

None of the sections yielded.

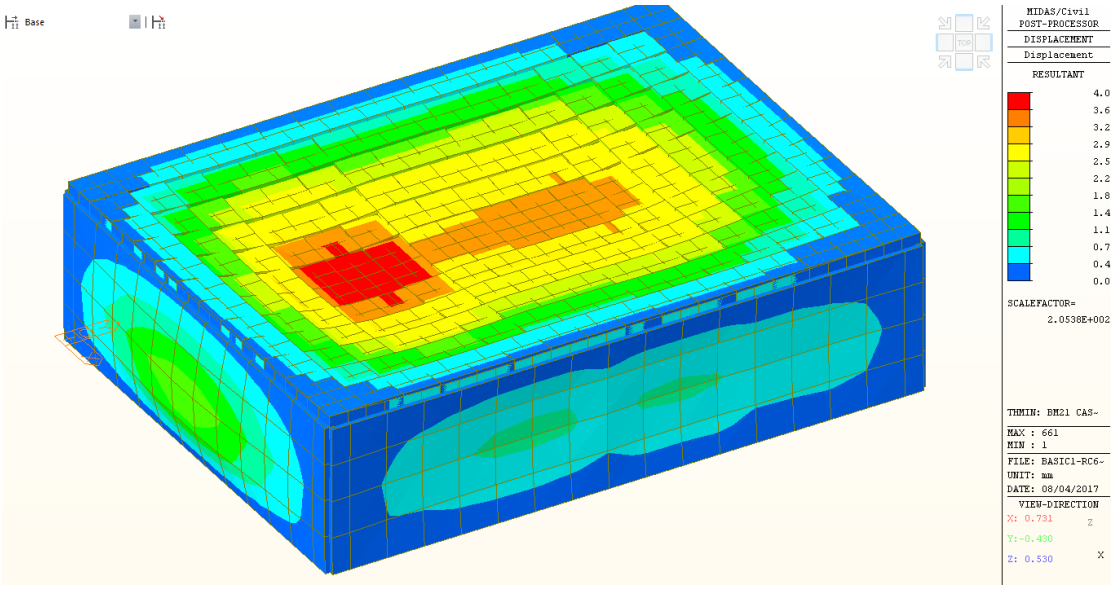

Figure 73- RC slab, 122mm rocket, Maximum Deflection [mm]

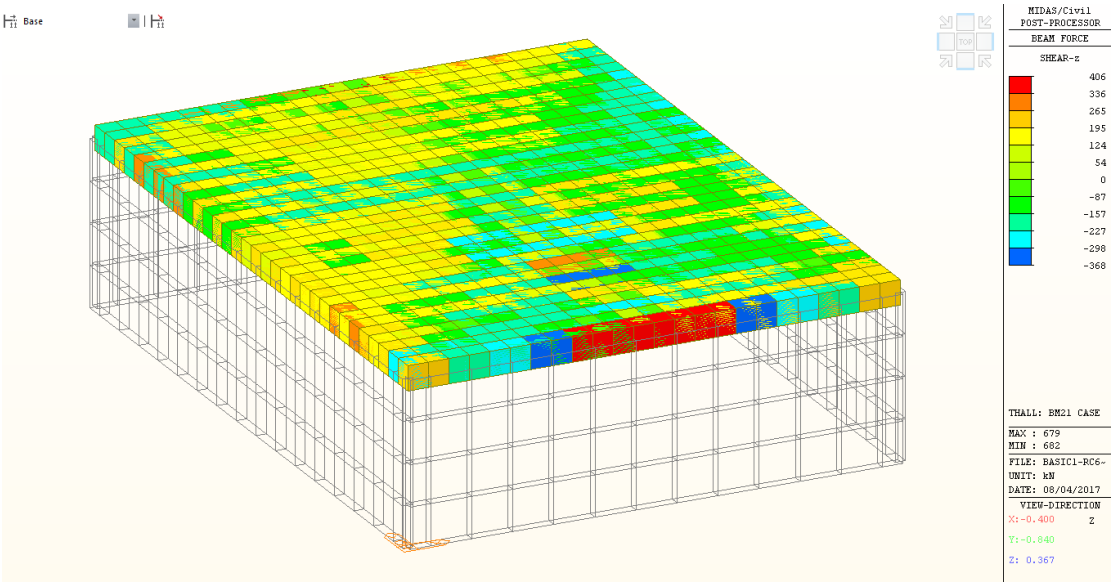

Figure 74- RC slab, 122mm rocket, Shear force envelope [kN]

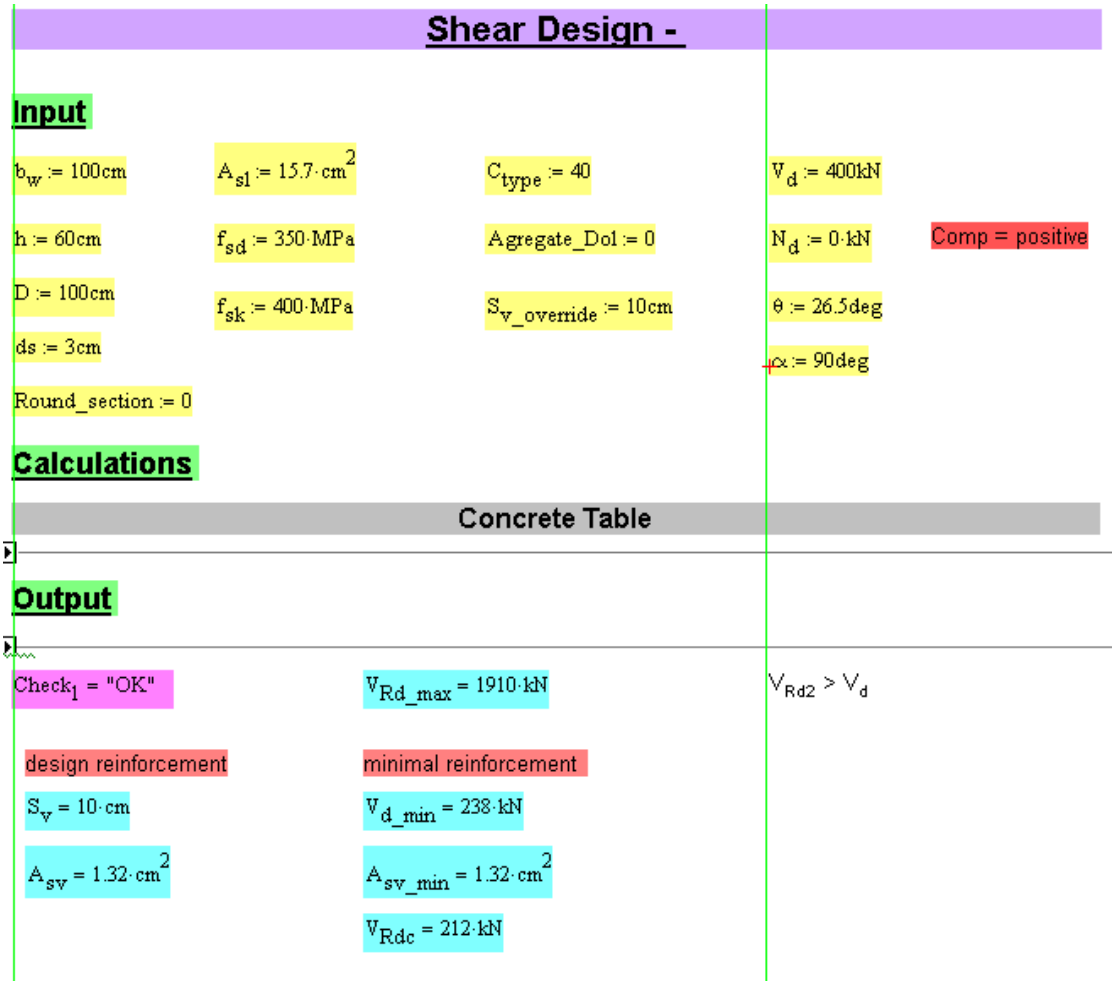

Figure 75 - RC slab, Shear capacity analysis for the 122mm rocket case

The shear force resultant shows that some stirrups are necessary to resist the blast load.

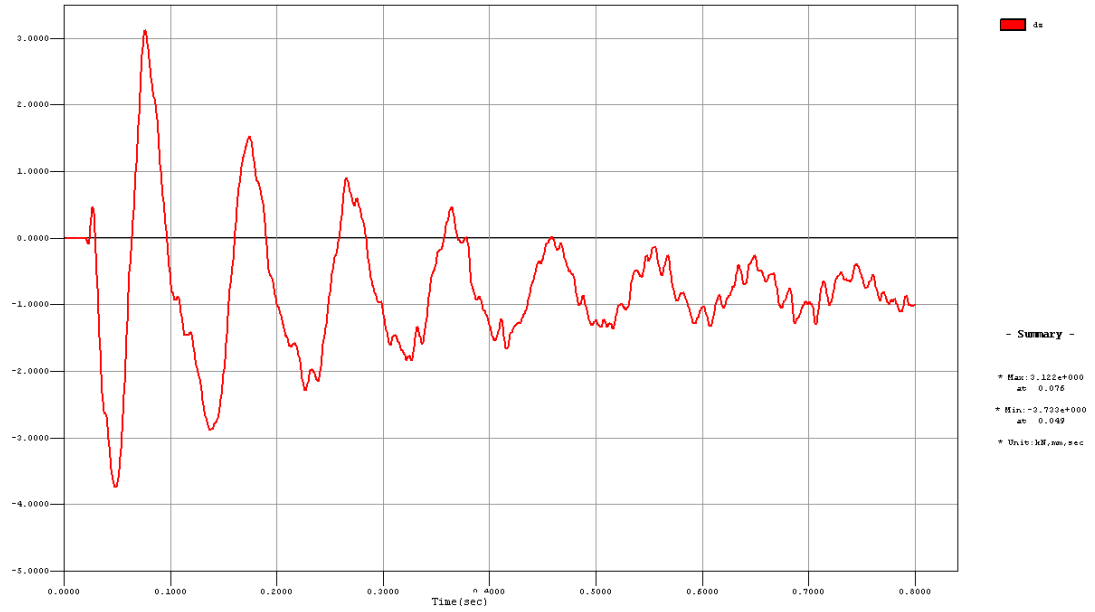

Figure 76 - Time-History vertical deflection at mid-span. The cycle lasts 0.0958 sec, indicating a slight increase from elastic natural period

The analysis results show good results for the case of the RC slab under the 122mm rocket air-blast scenario.

Data indicates having mild damage done to the structure, with very small cracks, that may not even require repairs

Case 1.3 – RC slab under 250kg GP bomb blast

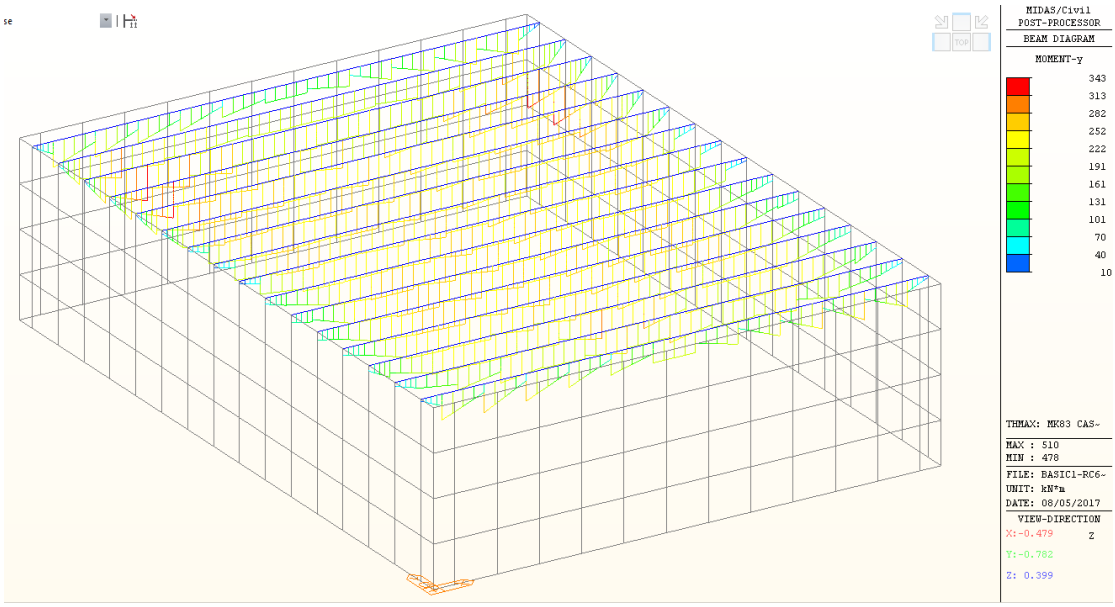

Figure 77 - Maximum positive moment envelope, 250kg GP bomb, short span direction [kNm]

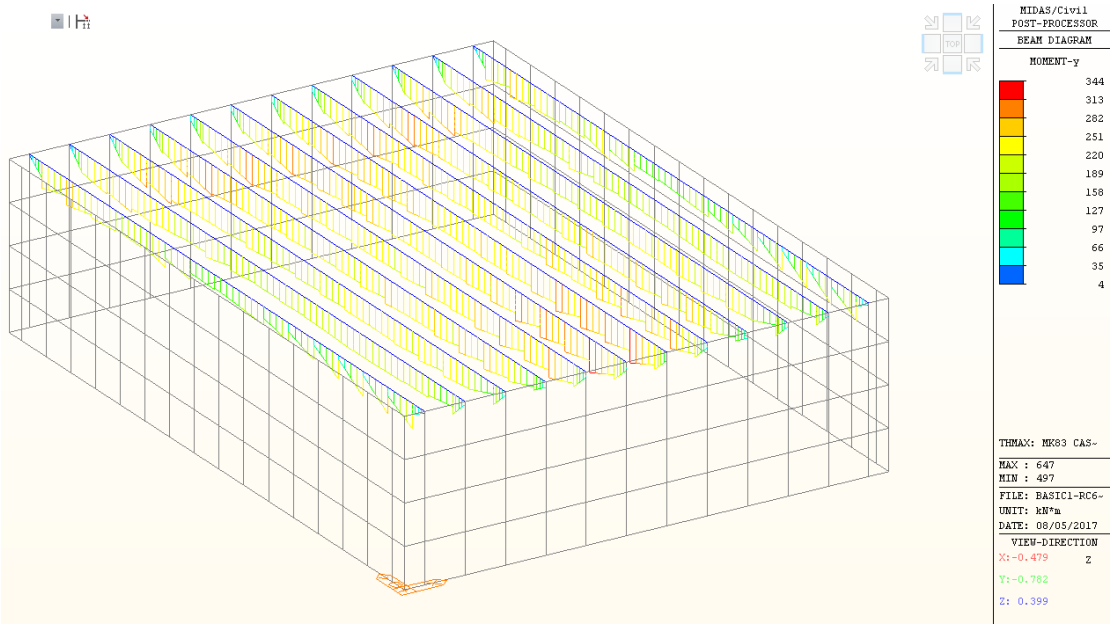

Figure 78 - Maximum positive moment envelope, 250kg GP bomb, long span direction [kNm]

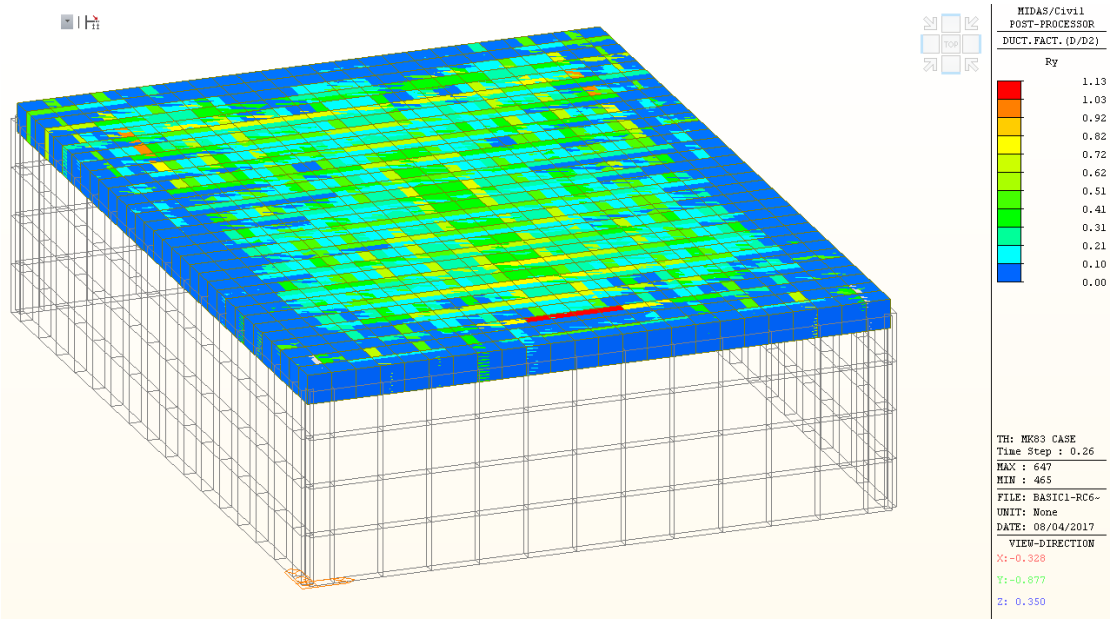

Figure 79 - Figure 80 – D2 Ductility factors, 250kg GP bomb

The Time-History results show that the structure was damaged from the blast, yet it is estimated that no flexural failure occurred.

The D2 ductility ratio is the ratio between the resultant curvature and the curvature calculated for the yielding of the section. Results over 1 indicate yielding. The maximum resultant for this case is 1.13, showing some sections flexed a little bit beyond the yielding point.

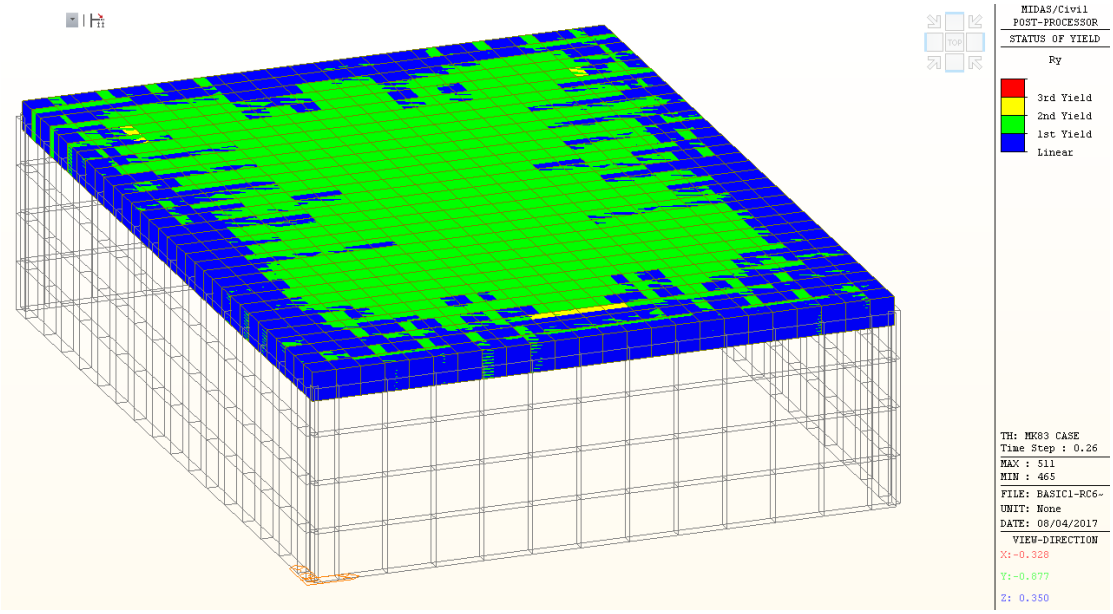

Figure 81 - Yield status output, 250kg GP bomb. Internally cracked regions are marked in green, yielding sections are in yellow.

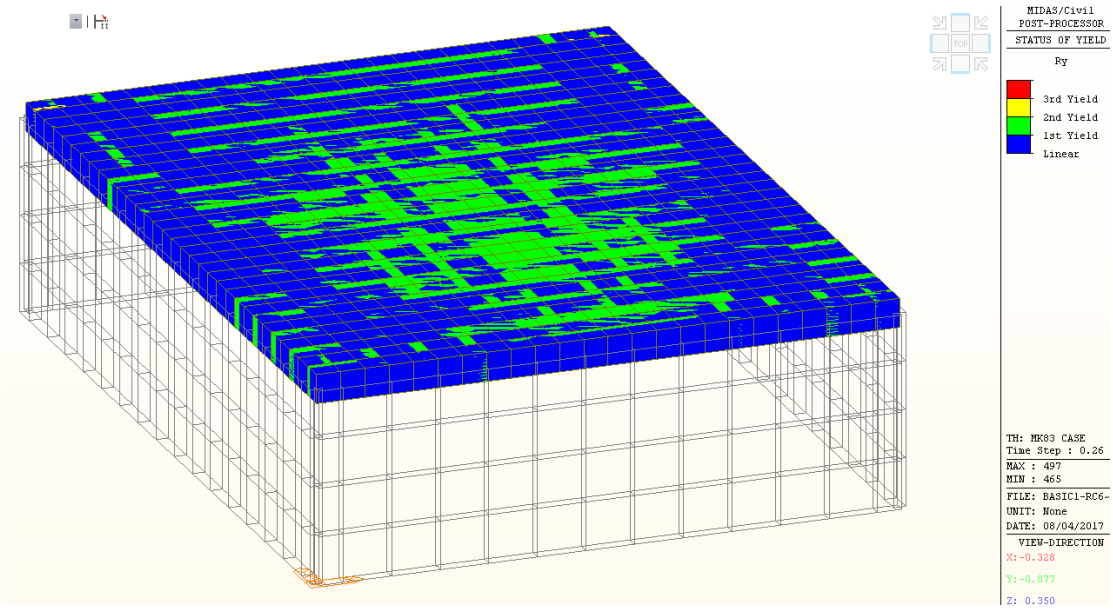

Figure 82 - Yield status output, 250kg GP bomb. Externally cracked regions are marked in green, yielding sections are in yellow.

Almost the entire interior of the slab cracks as a result of the blast. The exterior of the slab also cracks, yet the cracks are not as ubiquitous.

However, the cracks themselves are not very severe. The maximum curvature value was 4.2 rad/km, which correlated to surprisingly small cracks, about 0.1mm in width.

It seems that even the extreme case does not cause irreparable damage to the slab, barring cases of shear failure.

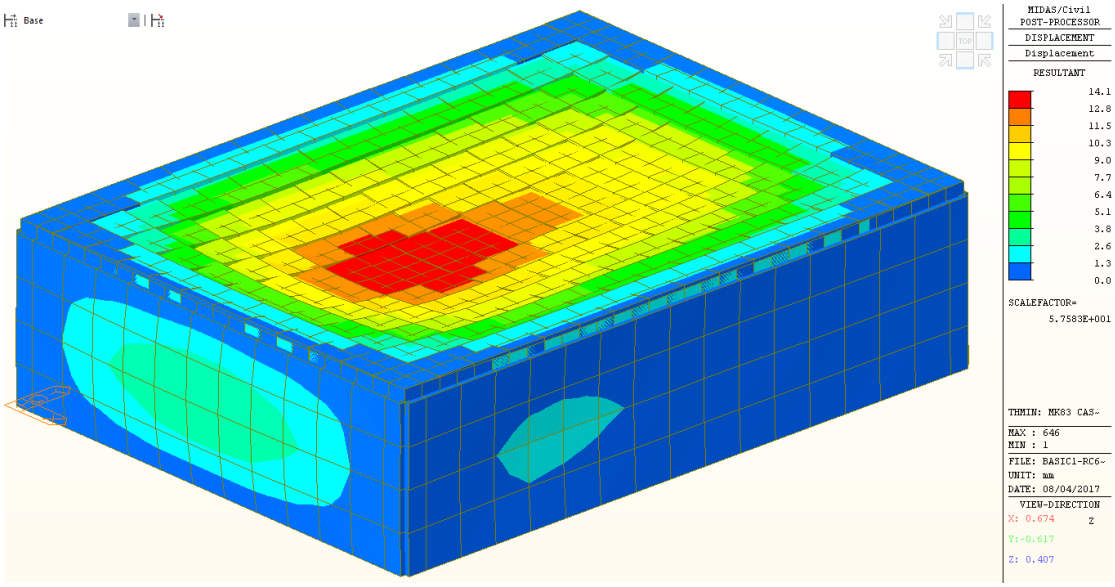

Figure 83 - RC slab, 250kg GP bomb, Maximum Deflection [mm]

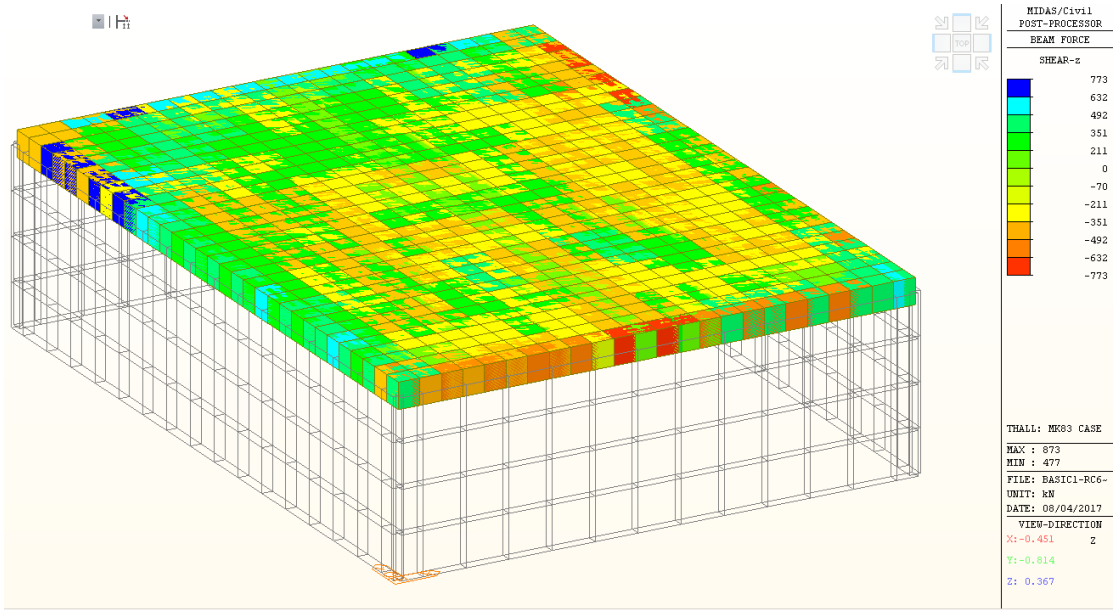

Figure 84 - RC slab, 250kg GP bomb, Shear force envelope [kN]

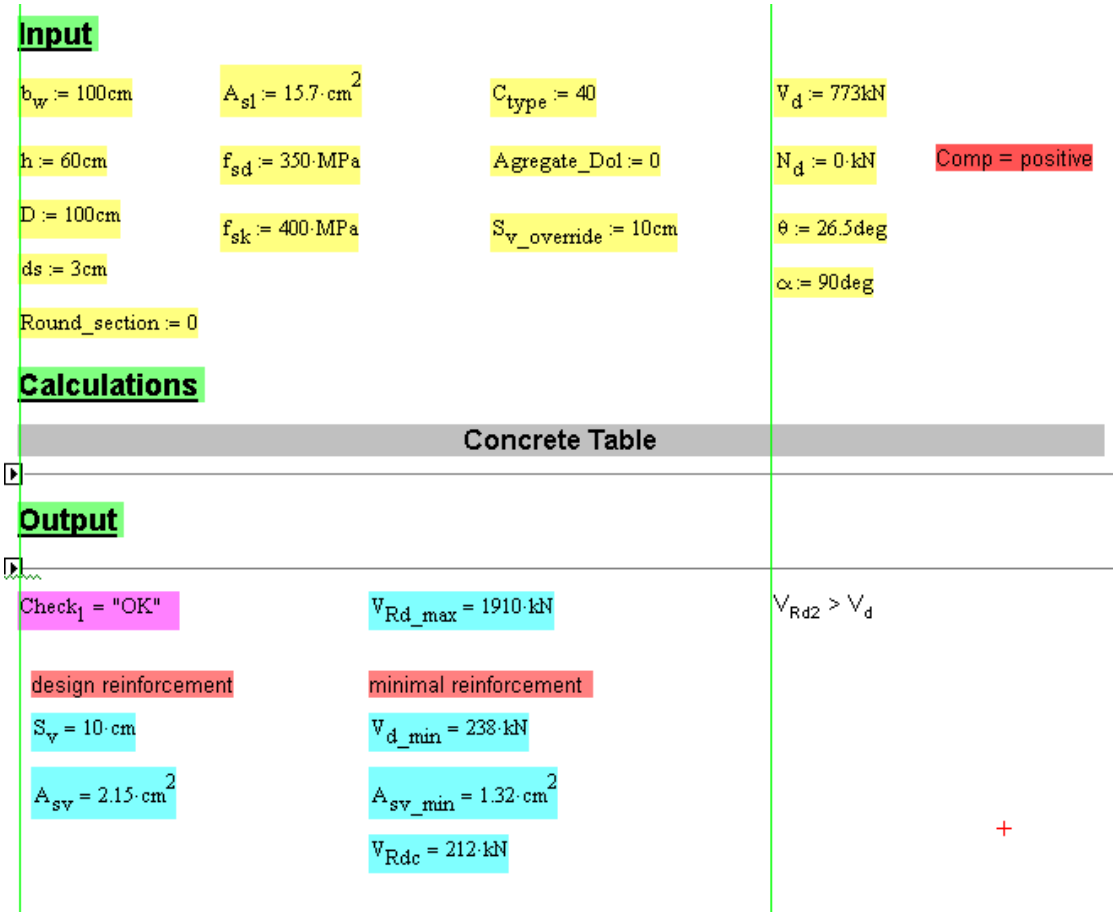

Figure 85 - RC slab, Shear capacity analysis for the 250kg GP bomb case

The shear values indicate that with a reasonable amount of shear reinforcement, the slab could successfully resist the loads imposed.

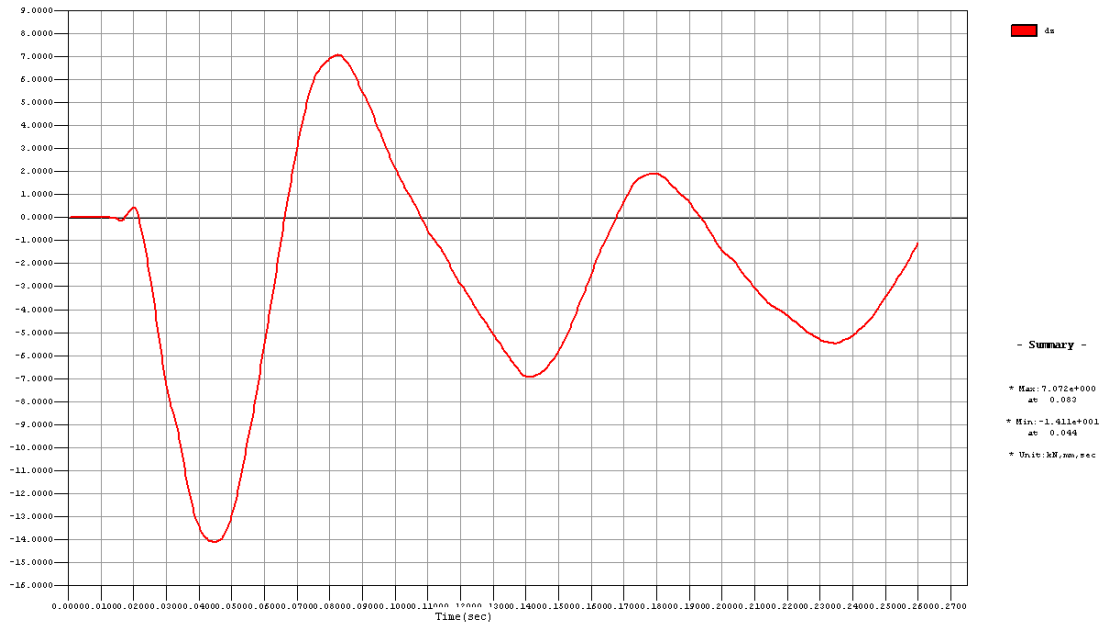

Figure 86 - Time-History vertical deflection at mid-span. The cycle lasts 0.0965 sec, indicating a slight increase from elastic natural period

The analysis surprisingly predicts no significant increase in permanent deformation, from the calculated 3.2 mm at rest, to a projected 5mm.

The structure is damaged, but is not at all beyond serviceability, provided that proper shear reinforcement is placed correctly throughout the slab. It is not only predicted to remain within serviceability, but is likely being able to protect against falling debris.

Prefabricated Hollow Core Slab Results

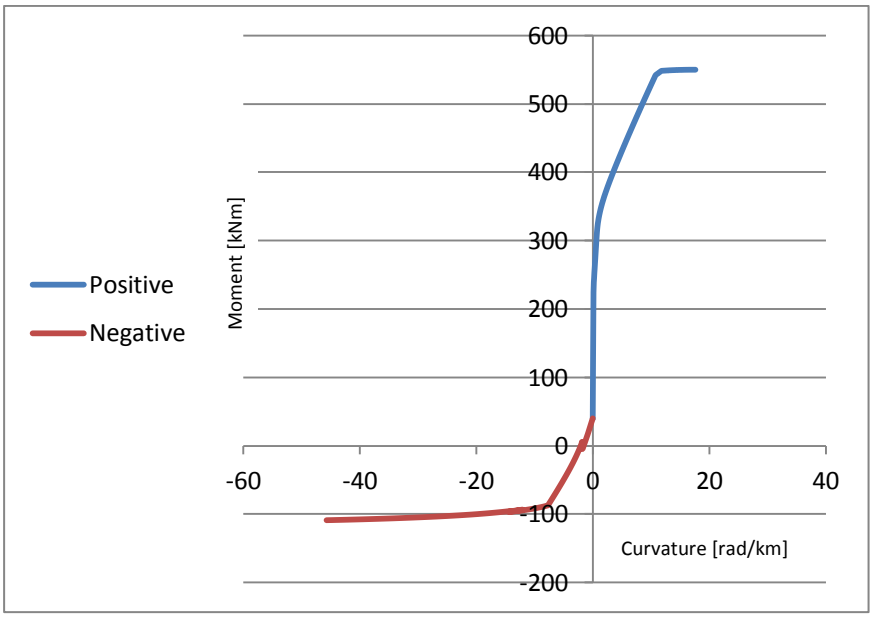

Figure 87 – Prefabricated Slab, bending moment capacity [kNm]

Bending moment capacity for each element is 556.6 kNm

Negative moment capacity is 111.2 kNm.

The section is calculated to crack at 377.1 kNm at the bottom, or whenever the external moment becomes negative at the top.

Curvature at ultimate is 17.6 rad/km positive, and 80.2 rad/km negative.

It is easy to tell from the shape of the curve, that the positive phase is of greater ultimate capacity than the negative phase, yet it is less ductile.

The section's capacity is enough to satisfy the requirement stated in TM-5-1300 chapter 5 for the minimal ductility for application of dynamic increase factors ($\mu \geq 10$, where μ is the ratio between the section's ultimate curvature and its maximum elastic curvature). This is true despite considering having defined ultimate failure strain for the tendons to be ~1%, when in fact EN10138 requires a minimal elongation of 3.5%.

The reason for this is the EN1992.1.1.2004 limitation of 1% strain, supposedly to avoid de-bonding situations.

The section's ductility can be tuned by modifying the initial tensioning force in the strands, at the expense of crack resistance and therefore serviceability. This may also be countered by the controlled further addition of tendons to the section, increasing capacity overall.

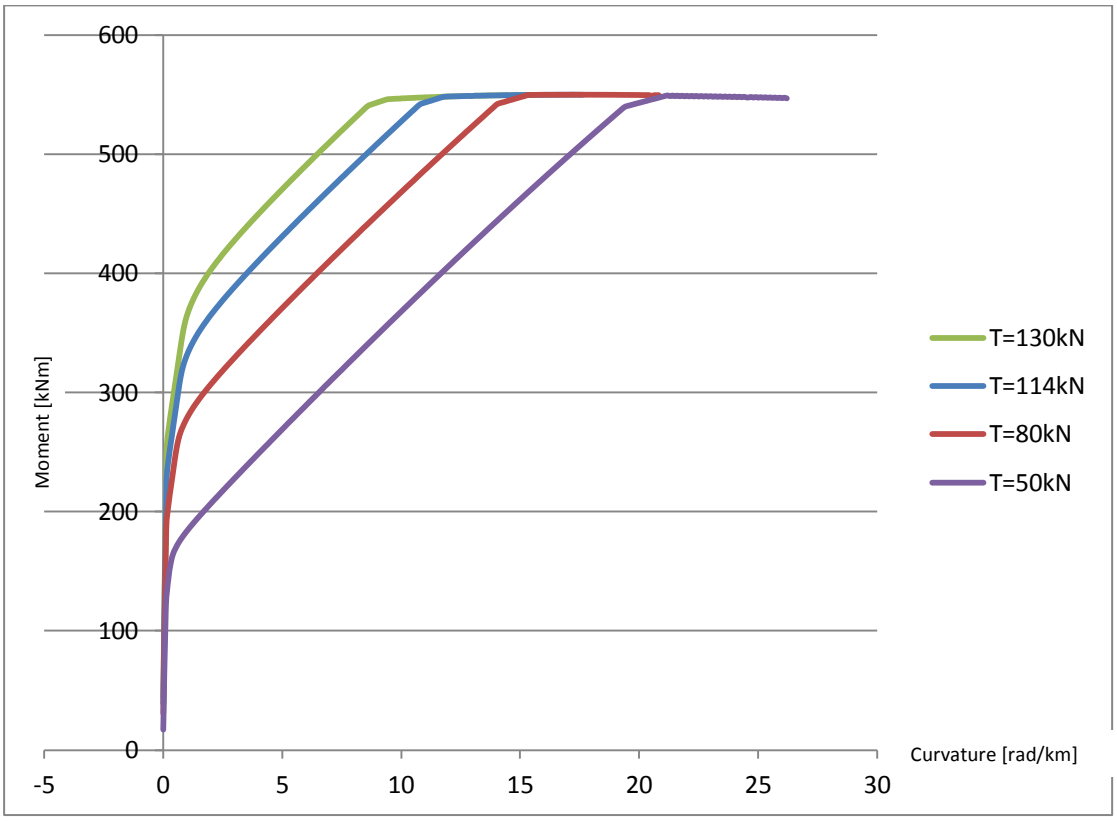

Figure 88 -Curvature moment curves for a hollow core slab element, using different initial tensioning force per strand.

It can be seen in figure 87 that the higher the tensioning force, the lesser the ultimate curvature, yet the higher the cracking moment.

The initial force does not affect almost at all the section's ultimate capacity.

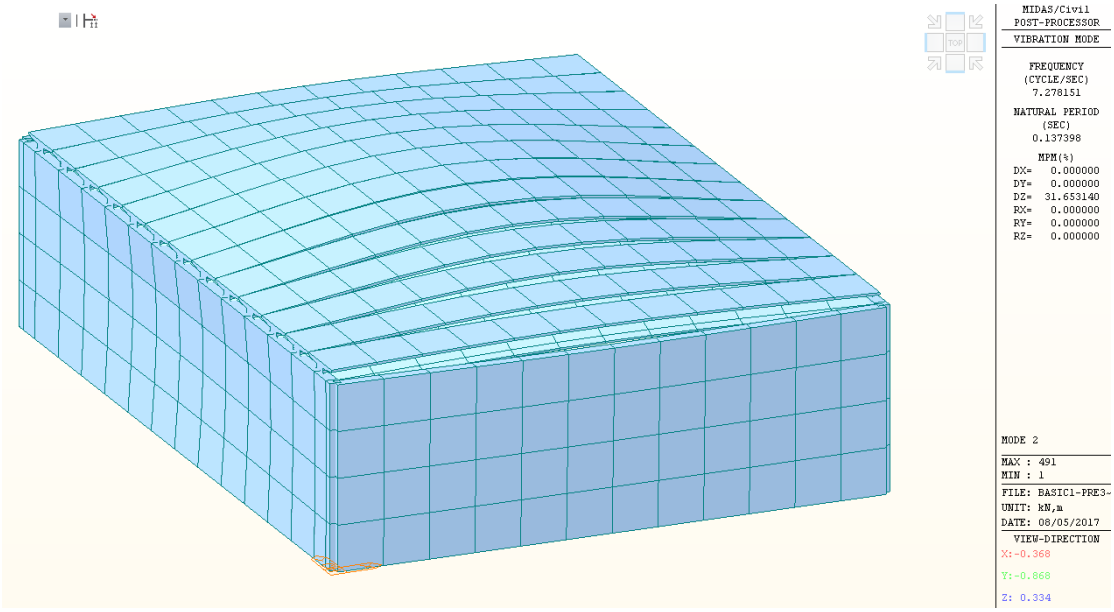

Figure 89 - Pre-tensioned elements, eigenvalue analysis. Natural period is 0.137 sec

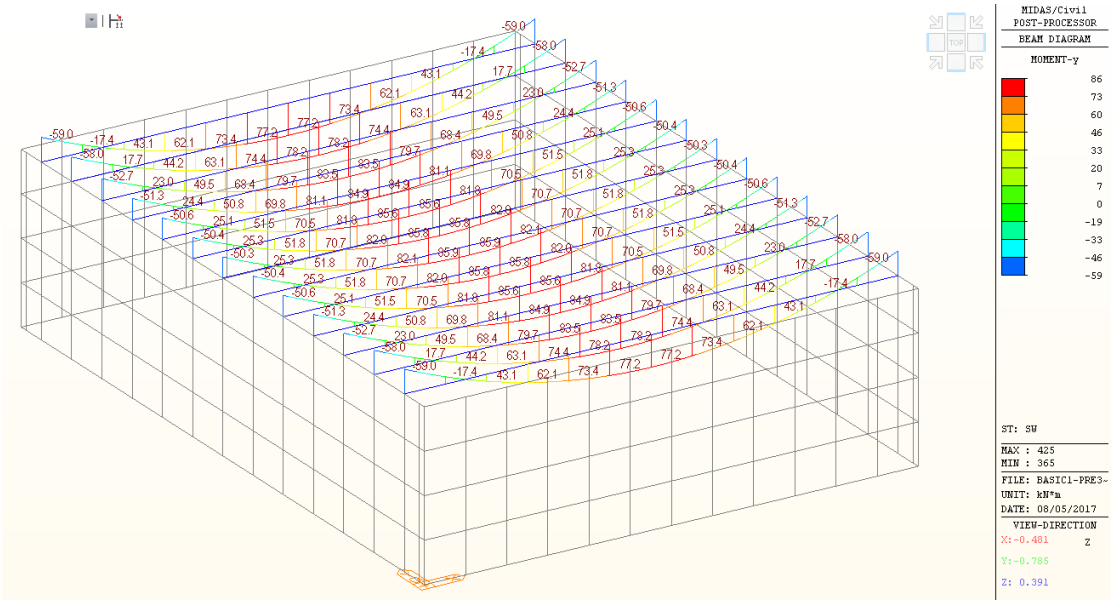

Figure 90 – Pre-tensioned elements, External Moment distribution at rest [kNm]

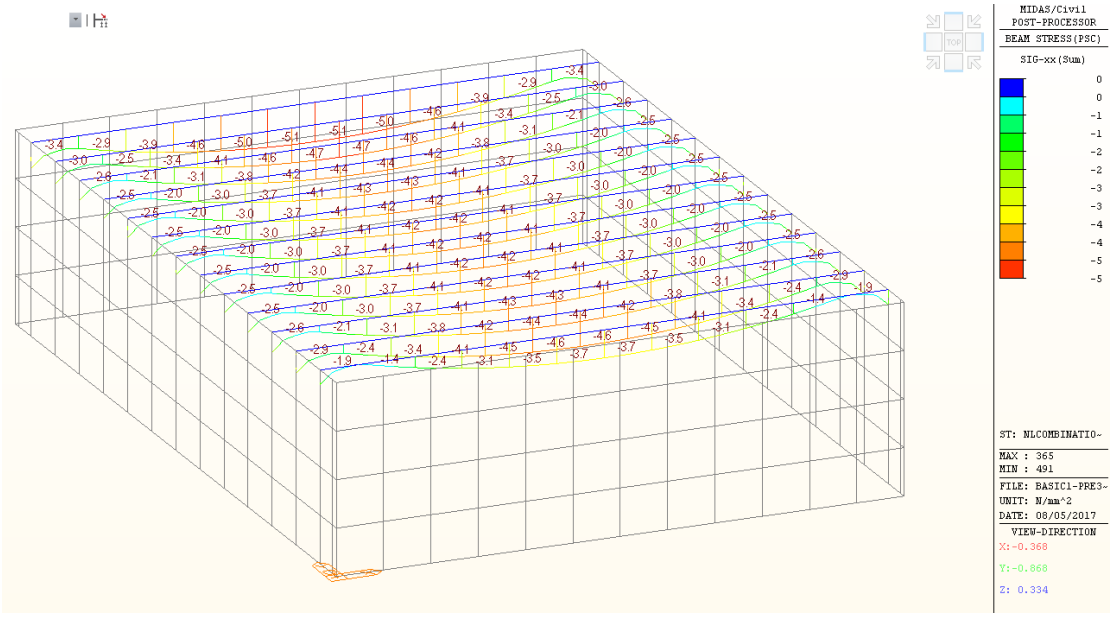

Figure 91 - Pre-tensioned elements, top fiber stresses at rest [MPa]

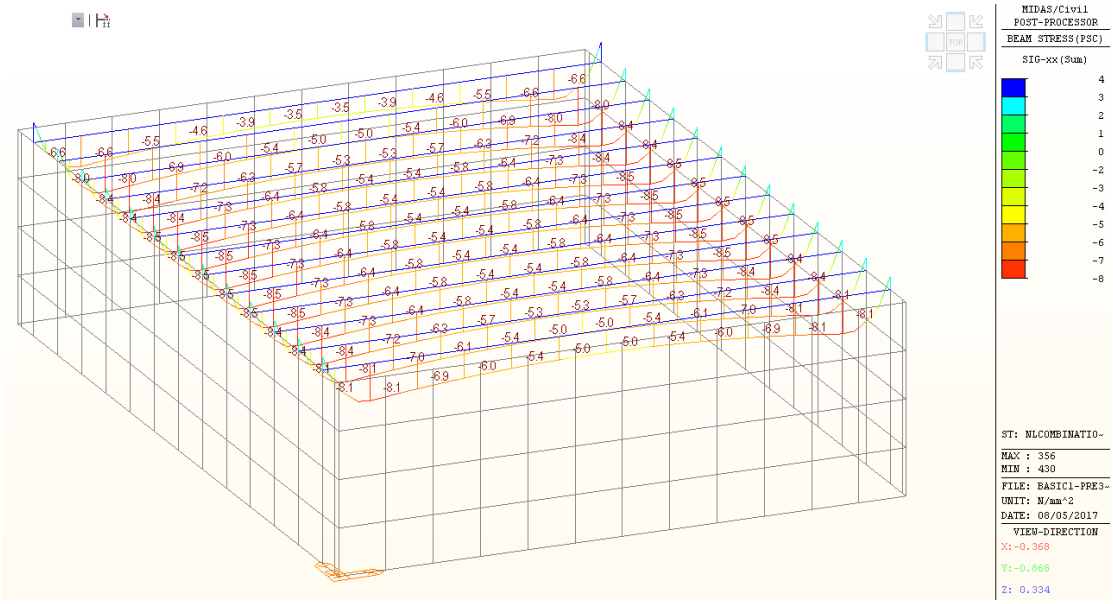

Figure 92- Pre-tensioned elements, bottom fiber stresses at rest [MPa]

The results show that the structure is designed to sustain loads well beyond its self-weight and is not tensioned to the point of damaging its serviceability.

Case 2.1 – Pre-tensioned elements under 81mm mortar blast

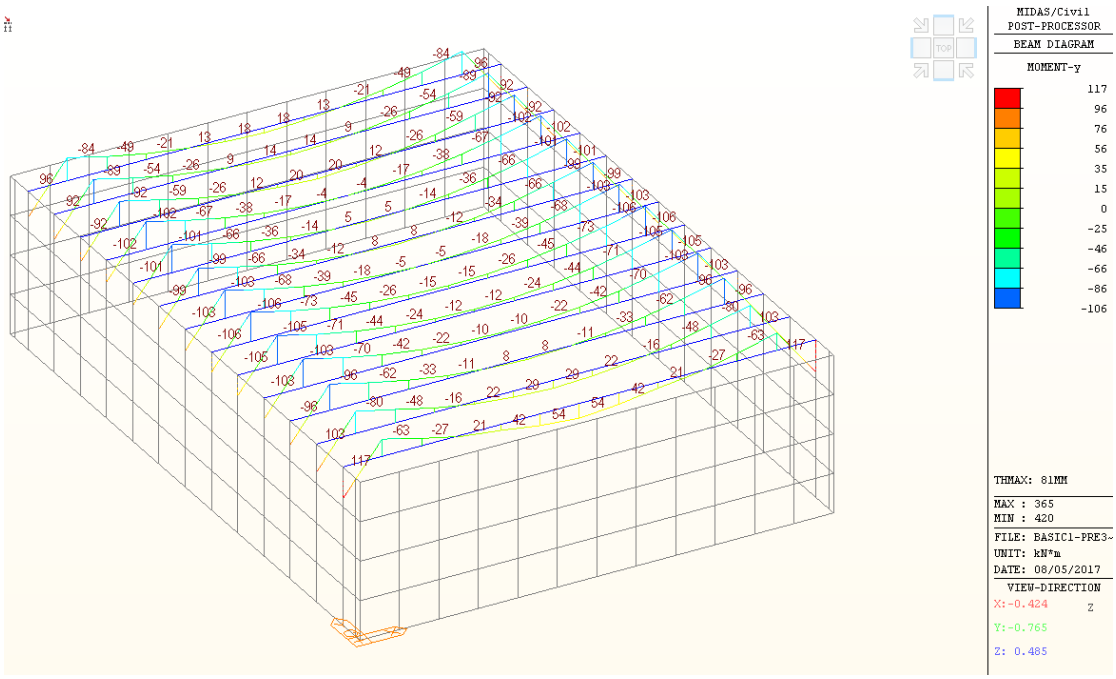

Figure 93 - Maximum positive moment envelope, 81mm mortar [kNm]

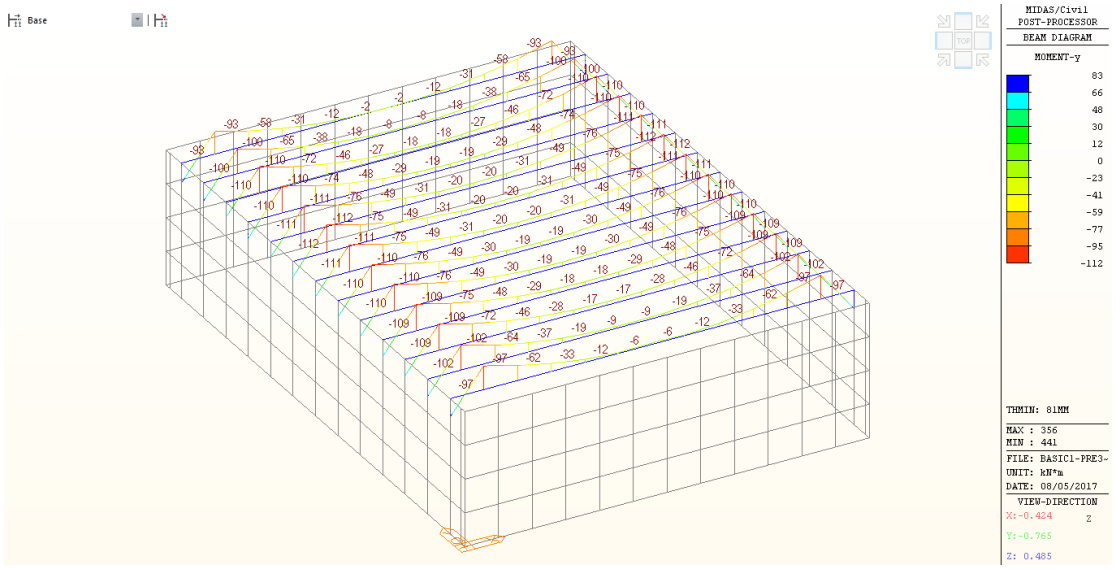

Figure 94 - Minimum positive moment envelope, 81mm mortar [kNm]

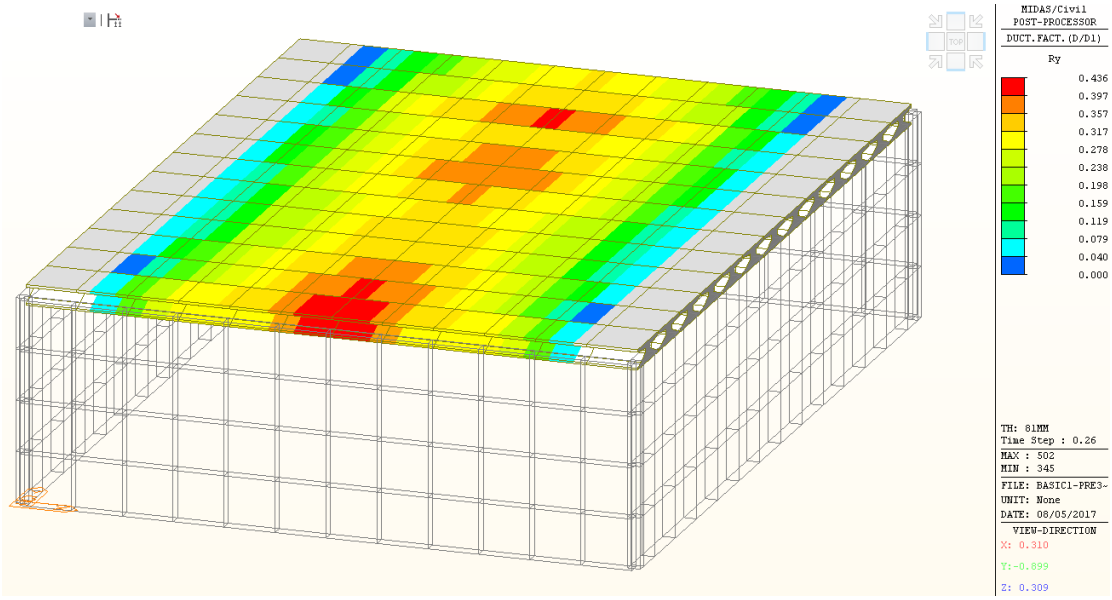

Figure 95 - D1 Ductility factors, 81mm mortar

The time history results indicate that the bottom (inner) side of the elements remains un-cracked.

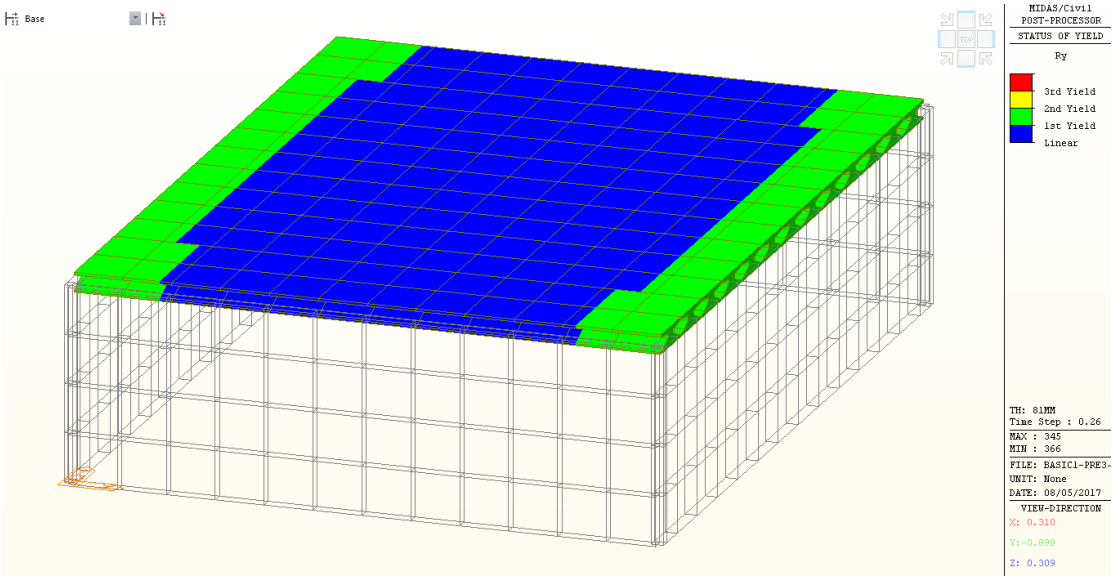

Figure 96 - Yield status output, 81mm mortar. Externally cracked regions are marked in green

The external face of the elements is marked as cracked, yet it is not due to the blast but to a design error of not including end releases.

The results show minor flexural damage to the pre-stressed elements.

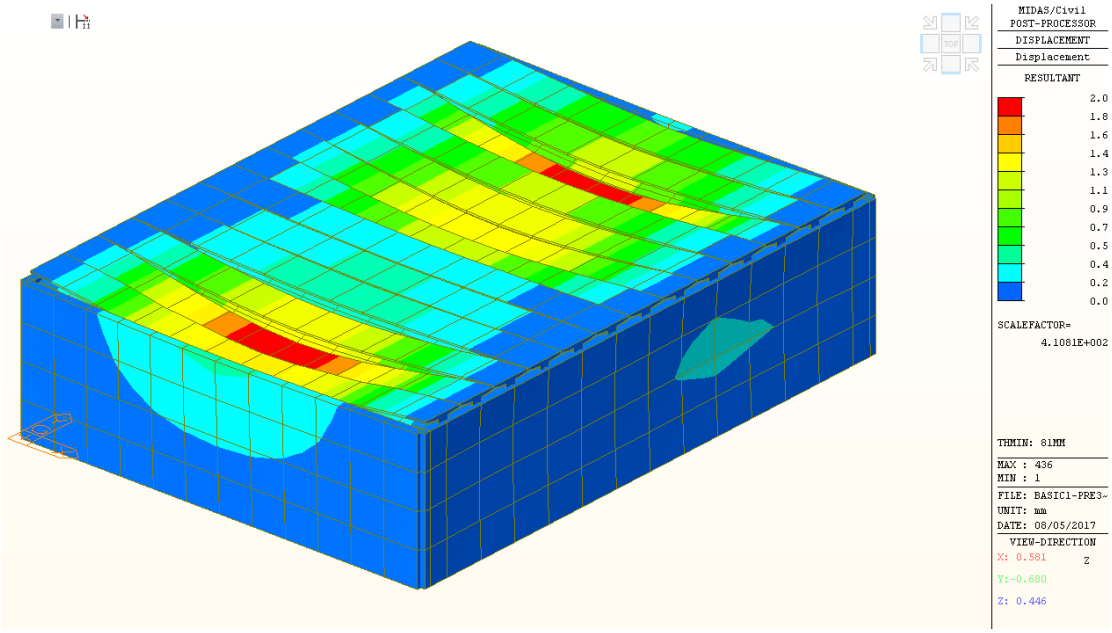

Figure 97 - Pre-tensioned elements, 81mm Mortar, Maximum Deflection [mm]

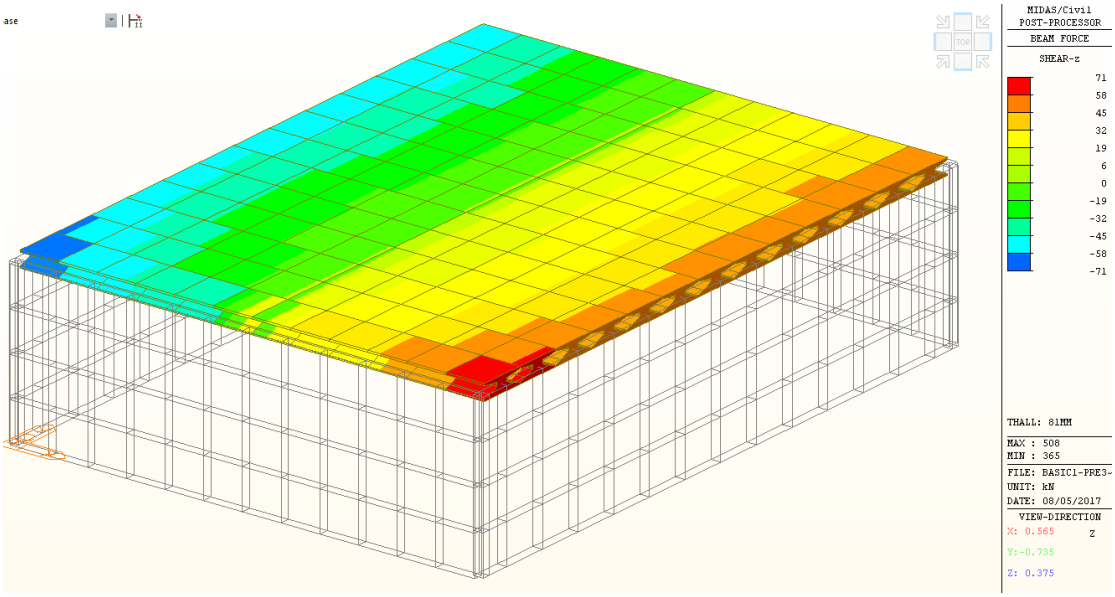

Figure 98 – Pre-tensioned elements, 81mm mortar, Shear force envelope [kN]

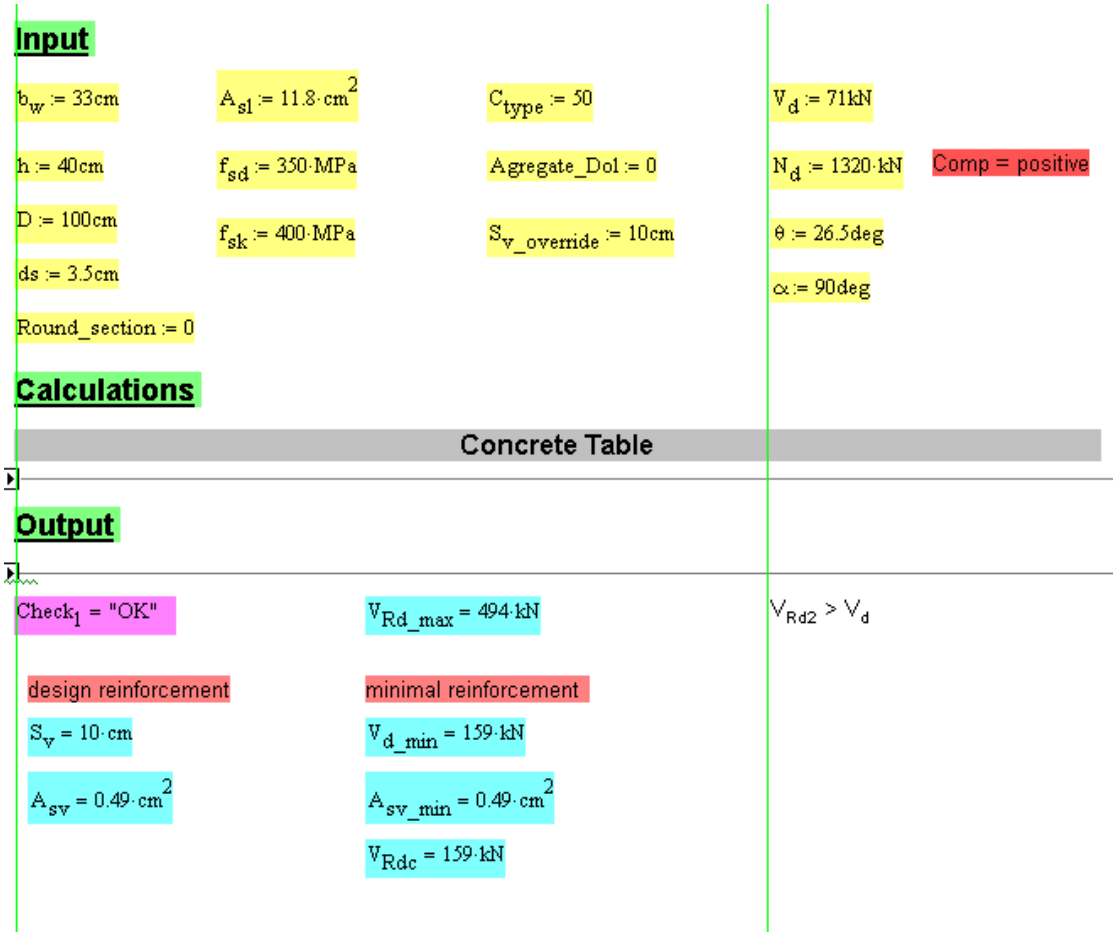

Figure 99 - Pre-tensioned elements, Shear capacity analysis for 81mm mortar case

The shear resultants are well within the sections shear capacity even without any added reinforcement.

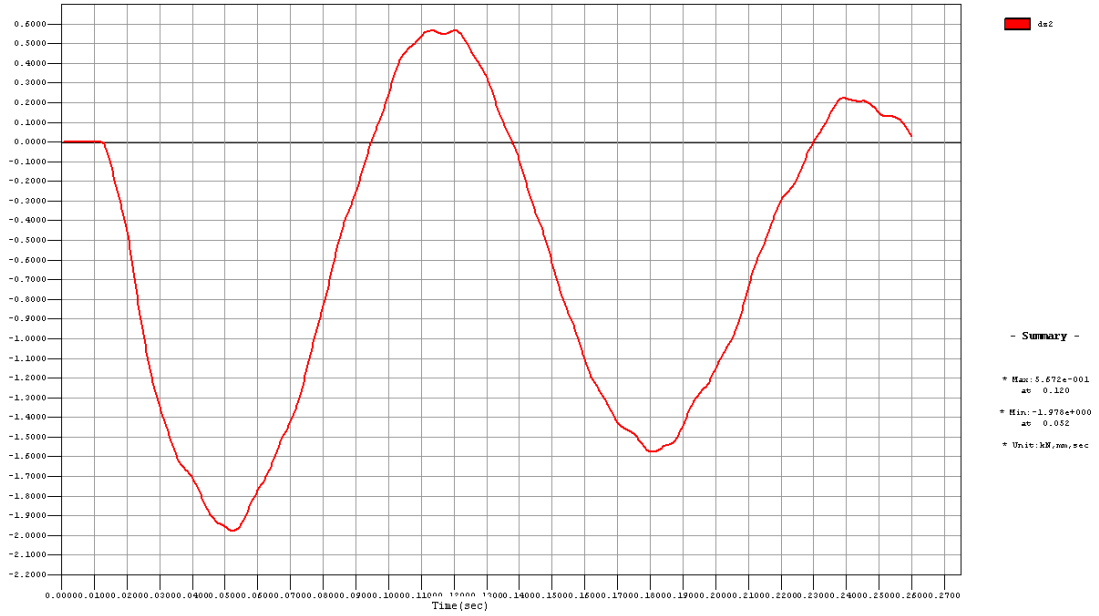

Figure 100 - Time-History vertical deflection at mid-span. The cycle lasts 0.13 sec, indicating no loss in stiffness compared to the eignvalue analysis result

The analysis results show that the pre-stressed element system is able to successfully resist the blast load without needing any repairs.

Case 2.2 – Pre-tensioned elements under 122mm rocket blast

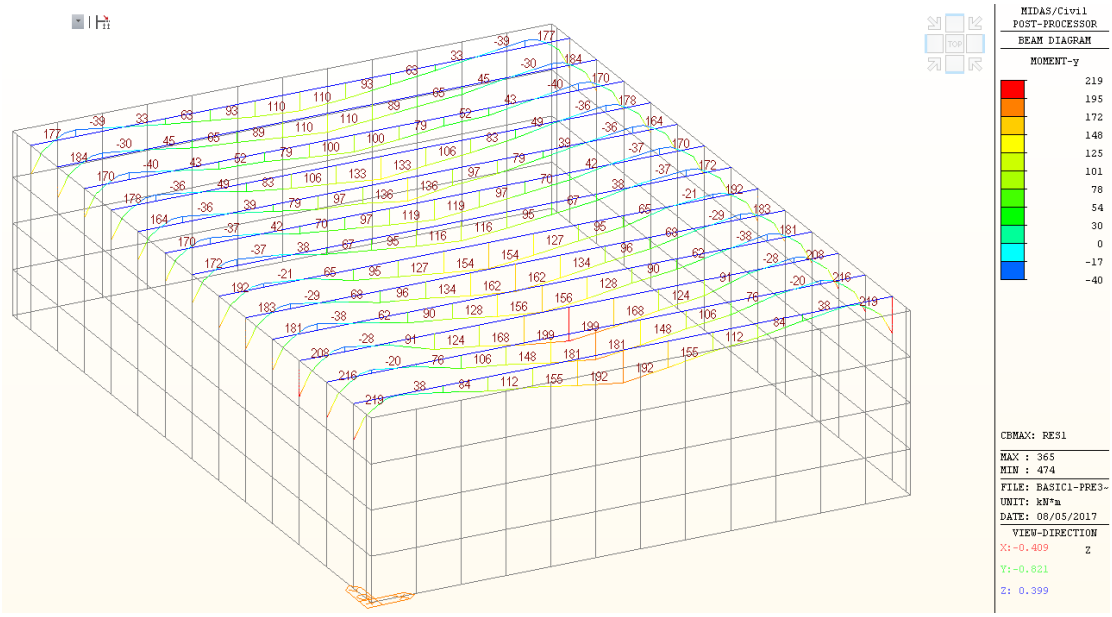

Figure 101 - Maximum positive moment envelope, 122mm rocket [kNm]

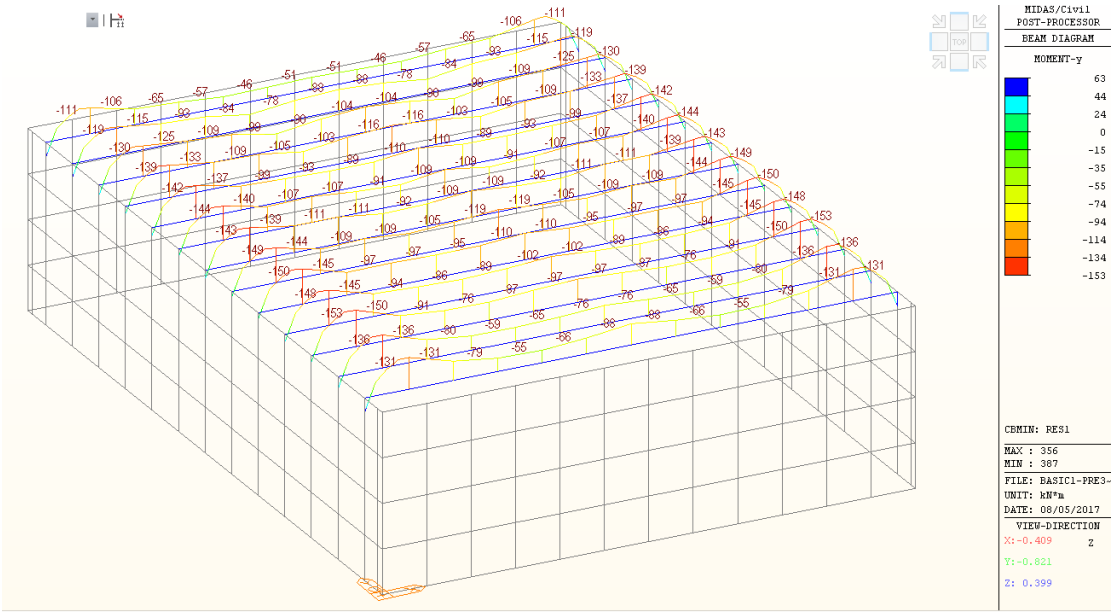

Figure 102 - Maximum negative moment envelope, 122mm rocket [kNm]

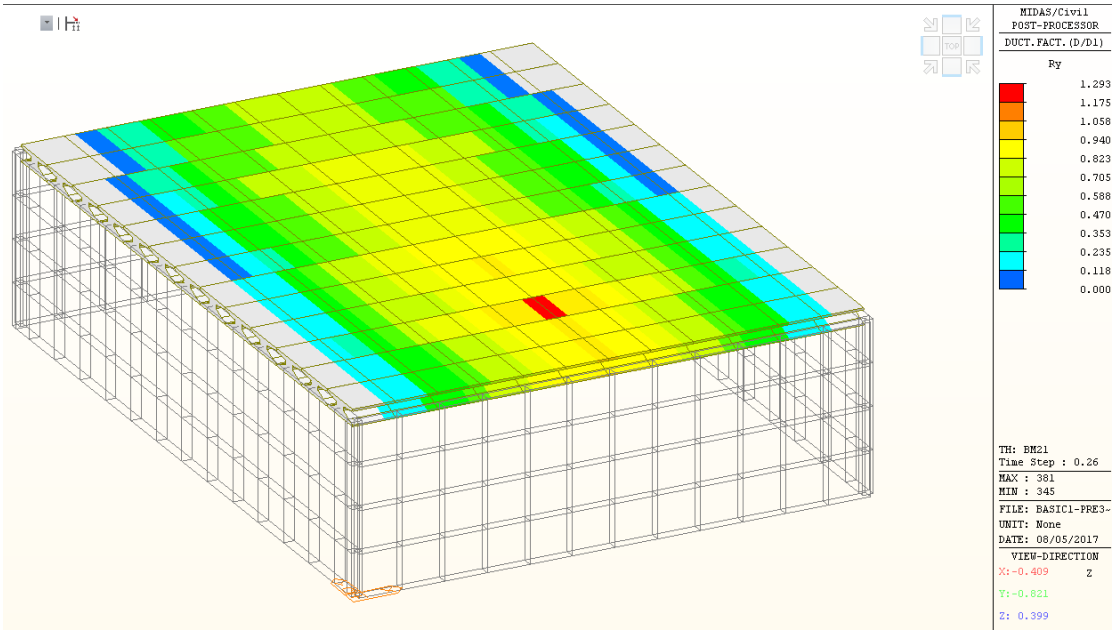

Figure 103 - D1 Ductility factors, 122mm rocket

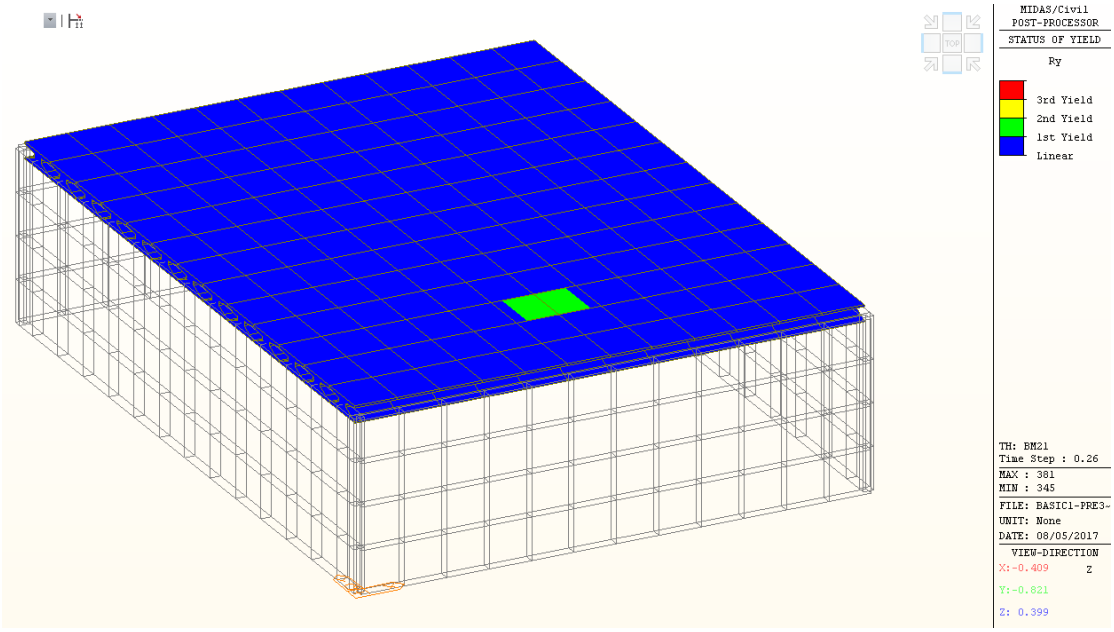

Figure 104 - Yield status output, 122mm rocket. Internally cracked regions are marked in green

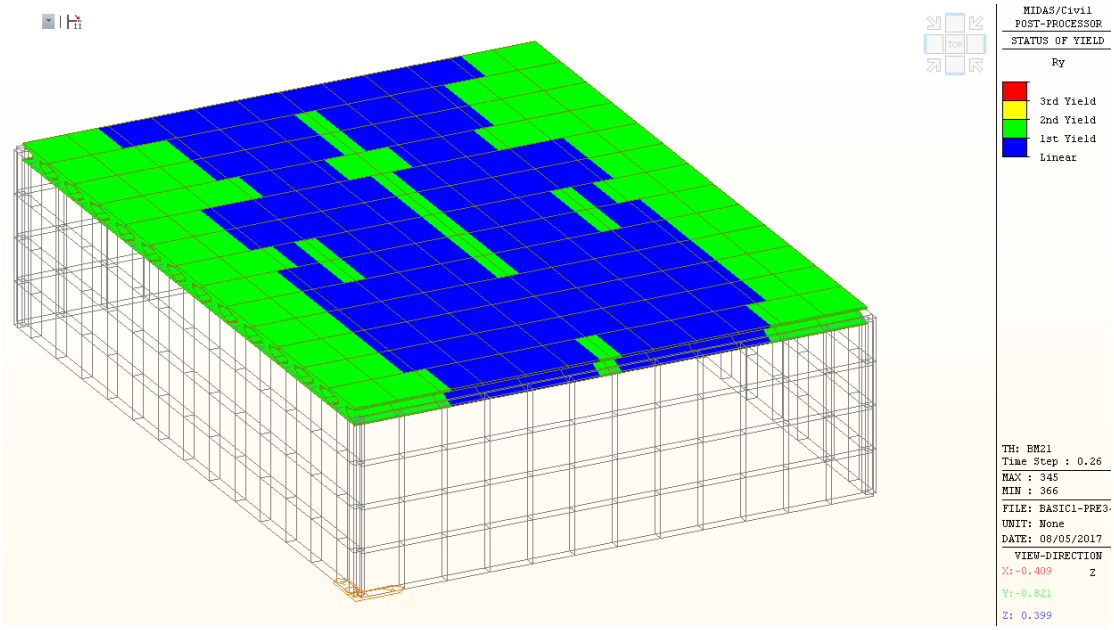

Figure 105 - Yield status output, 122mm rocket. Externally cracked regions are marked in green

Internal cracks are evaluated to be under 0.1mm in width, keeping the element in serviceability.

Maximum negative curvature is evaluated to be 3.6 rad/km. this correlate to Cracks in the external face of the elements that are under 0.1mm in width as well.

Overall, it is evident that the flexural damage due to the blast load is limited and will not even require repairs.

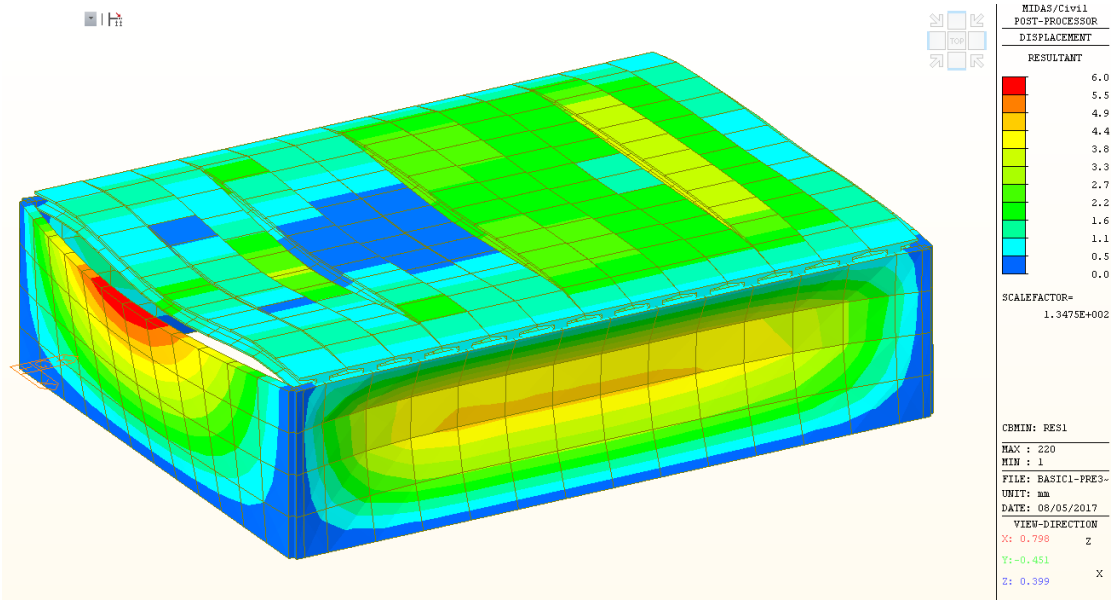

Figure 106 - Pre-tensioned elements, 122mm rocket, Maximum Deflection [mm]

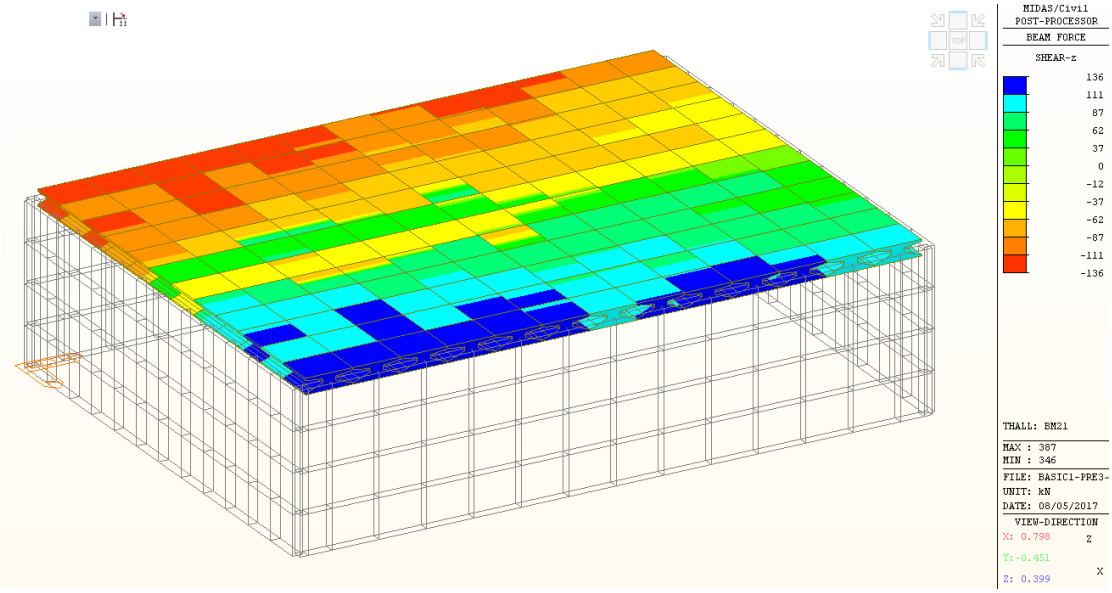

Figure 107 - Pre-tensioned elements, 122mm rocket, Shear force envelope [kN]

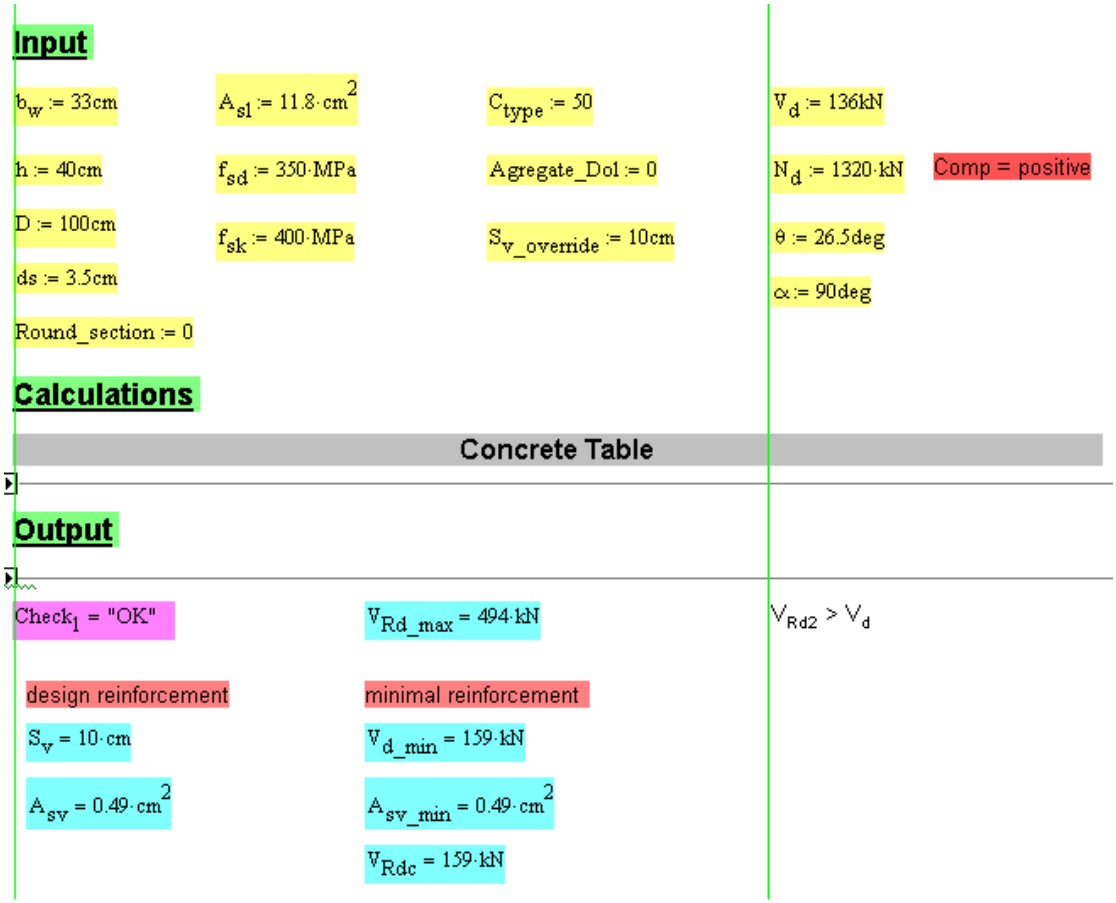

Figure 108 - Pre-tensioned elements, Shear capacity analysis for the 122mm rocket case

The results once again show that no reinforcement is required to withstand the shear forces.

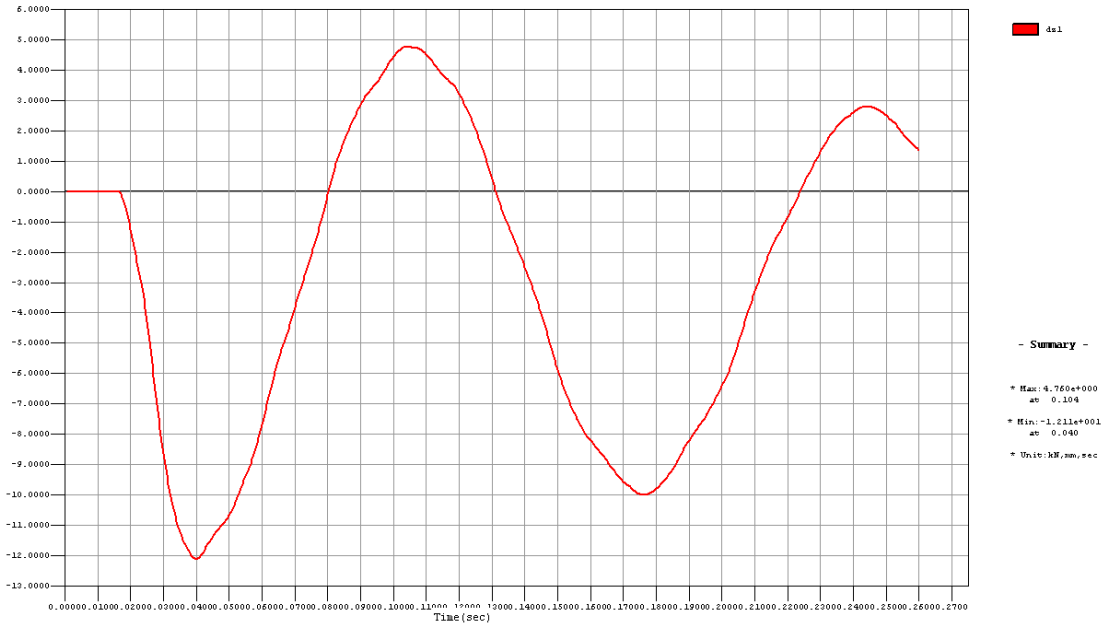

Figure 109 – Time history vertical deflection at mid span. The cycle lasts 0.137 sec, same as the natural period calculated using the Eigenvalue analysis.

The overall analysis of the result shows the elements successfully resisting the blast load without any damage requiring repair.

Case 2.3 – Pre-tensioned elements under 250kg GP bomb blast

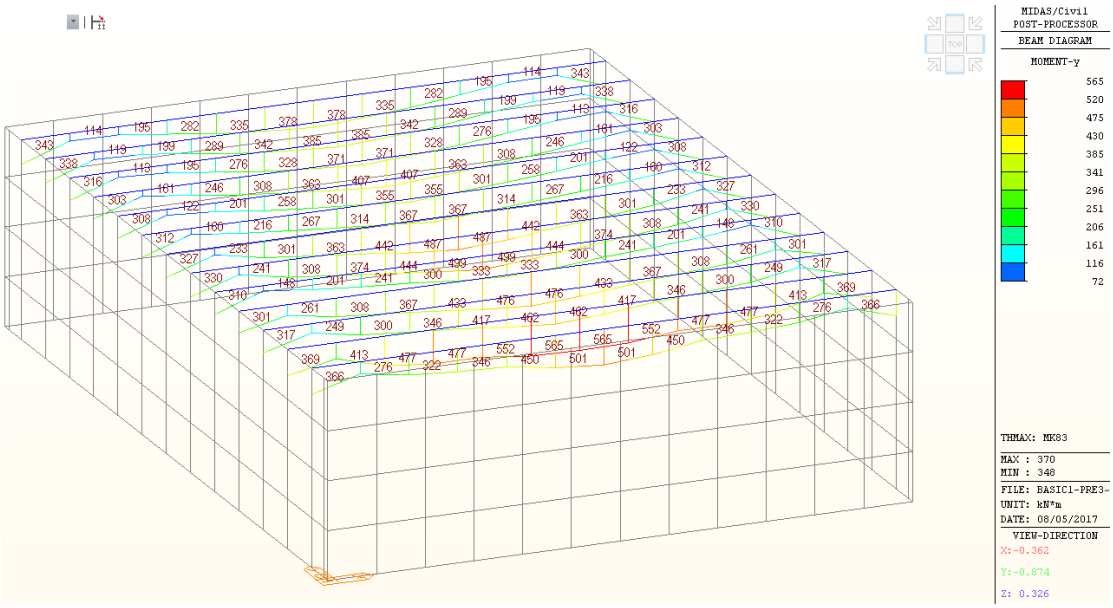

Figure 110- Maximum positive moment envelope, 250kg GP bomb [kNm]

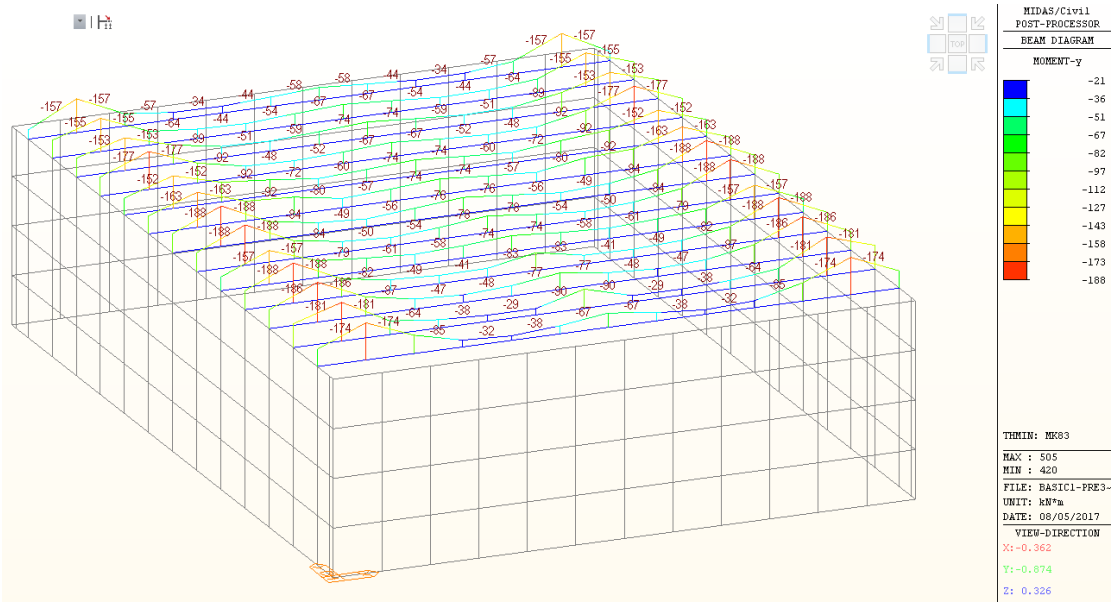

Figure 111- Maximum negative moment envelope, 250kg GP bomb [kNm]

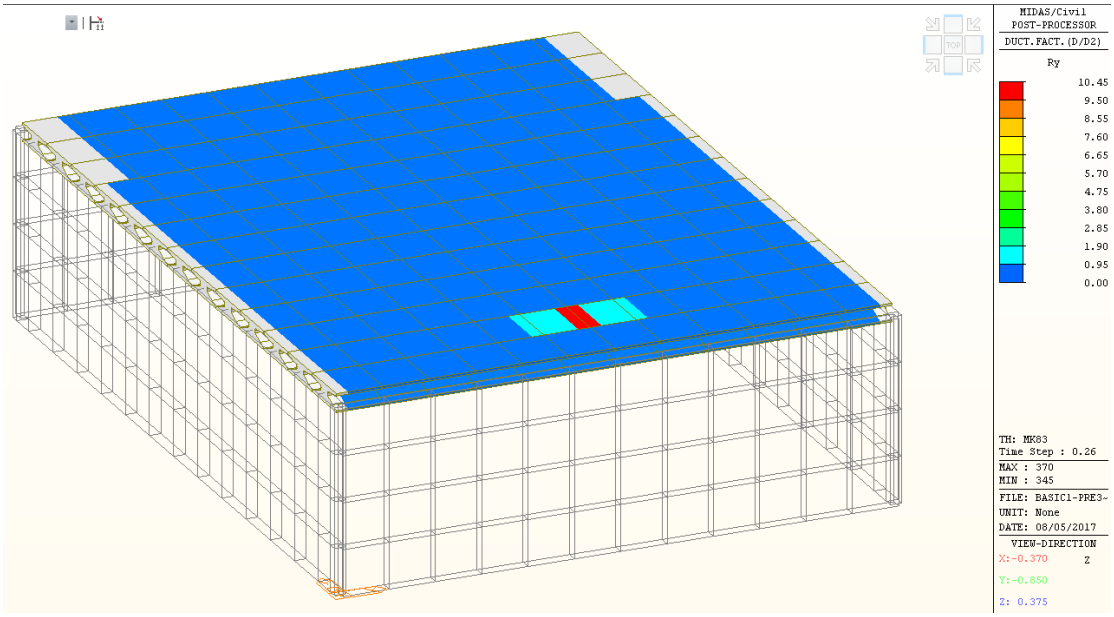

Figure 112 – D2 Ductility factors, 250kg GP bomb

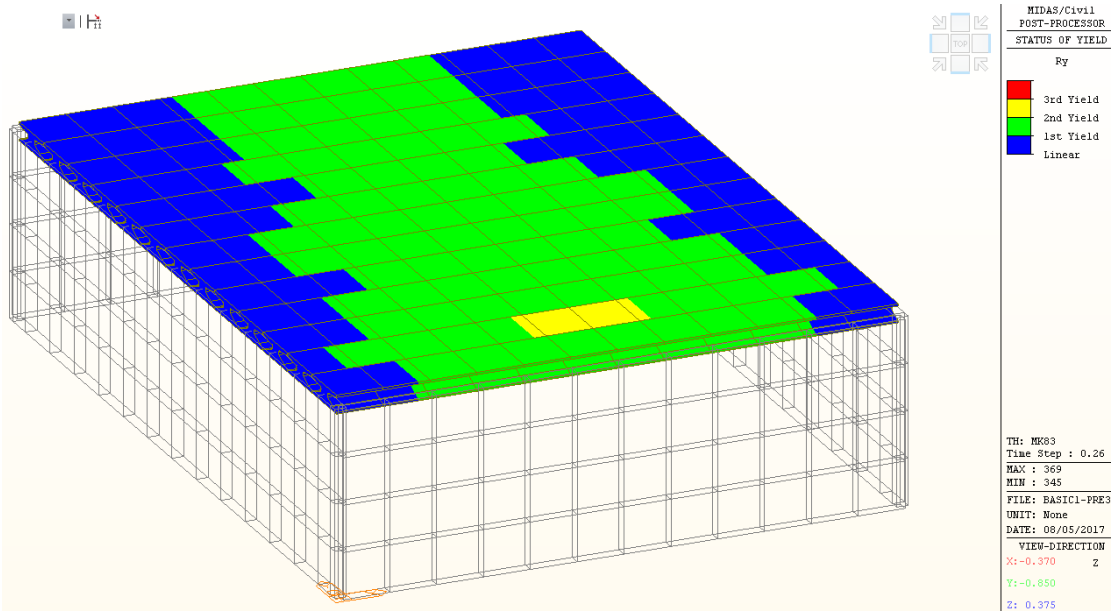

Figure 113 - Yield status output, 250kg GP bomb. Internally cracked regions are marked in green, yielding sections are in yellow

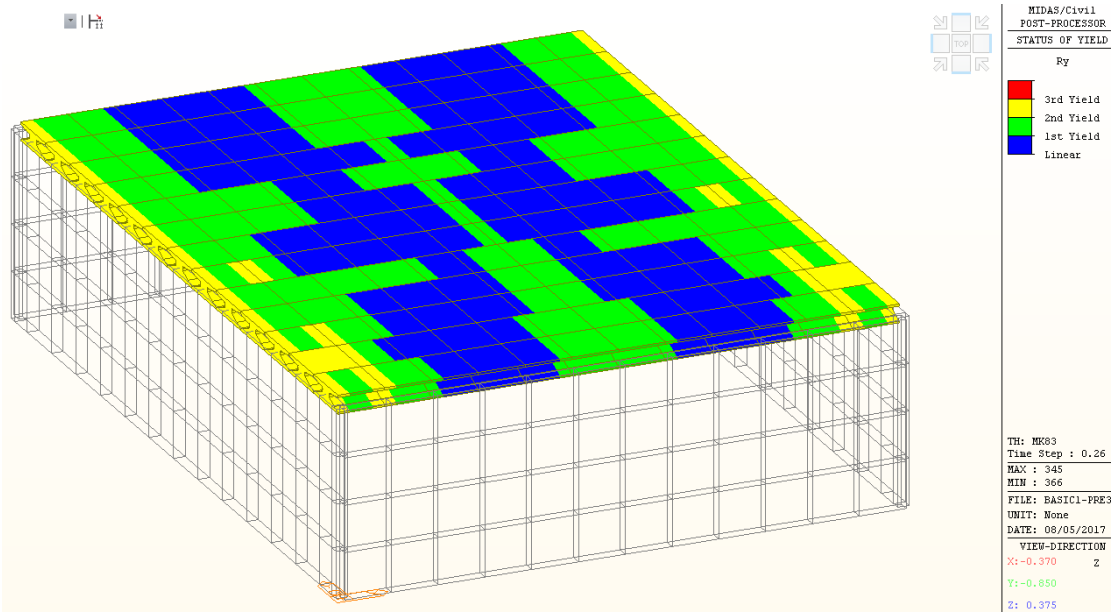

Figure 114 - Yield status output, 250kg GP bomb. Externally cracked regions are marked in green, yielding sections are in yellow

The results show several elements yielding and one element failing in flexure.

Cracked elements other than the failed one have the maximum positive curvature of 12.2 rad/km. This correlated to a crack width of 0.17mm, which is likely to be accompanied by some minor spalling.

The maximum negative curvature outside the failed element is 54.4 rad/km, which correlates to 0.96mm wide cracks.

Such large cracks are found in most elements.

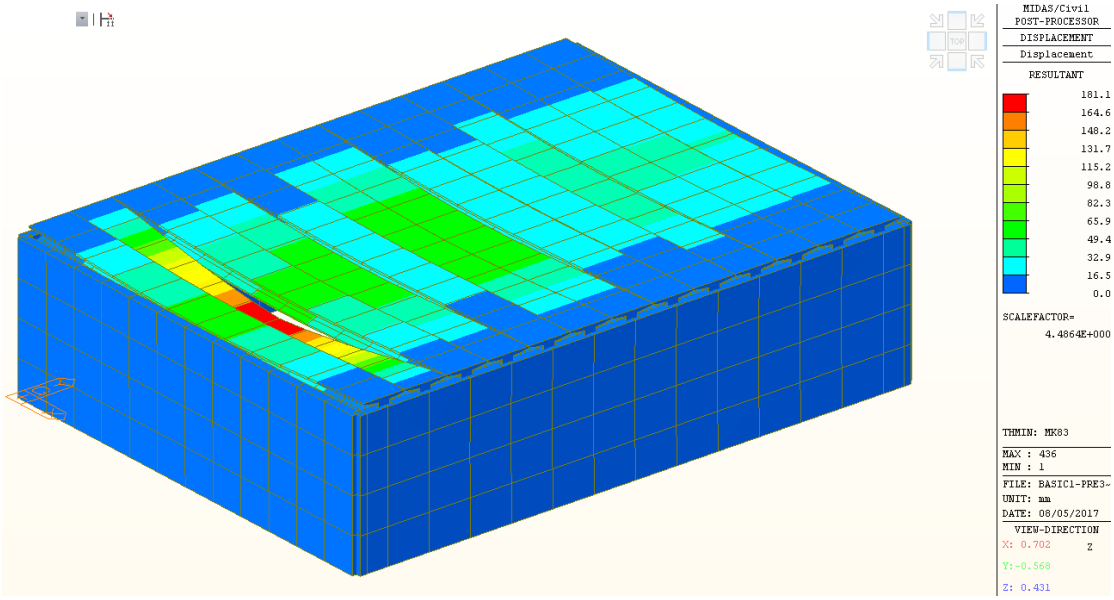

Figure 115 - Pre-tensioned elements, 250kg GP bomb, Maximum Deflection [mm]

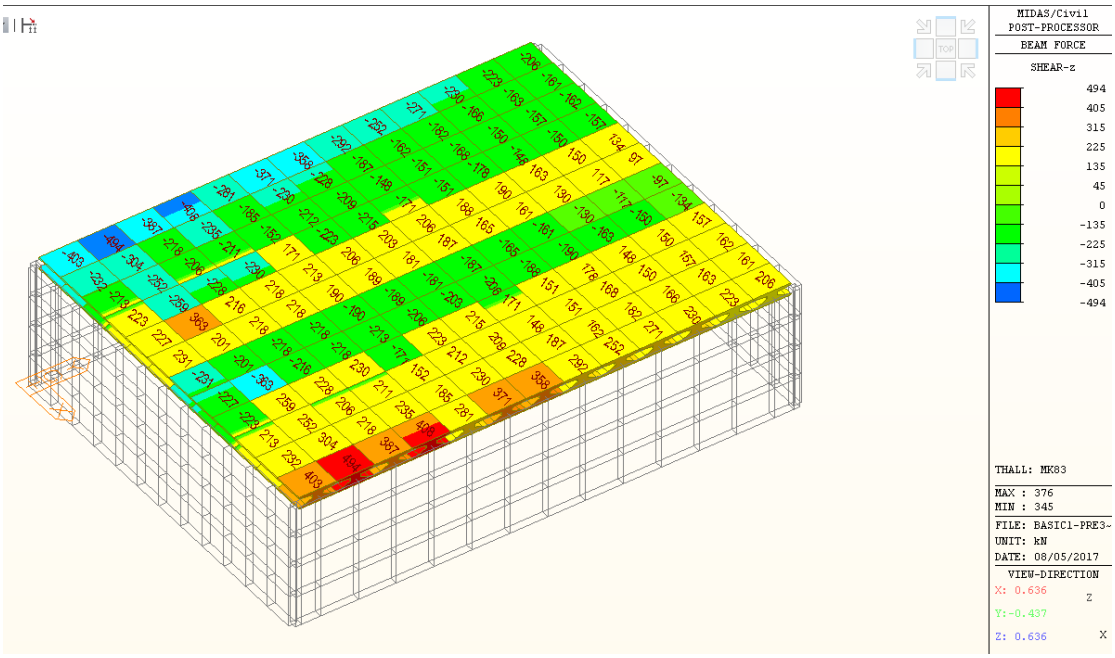

Figure 116 - Pre-tensioned elements, 250kg GP bomb, Shear force envelope [kN]

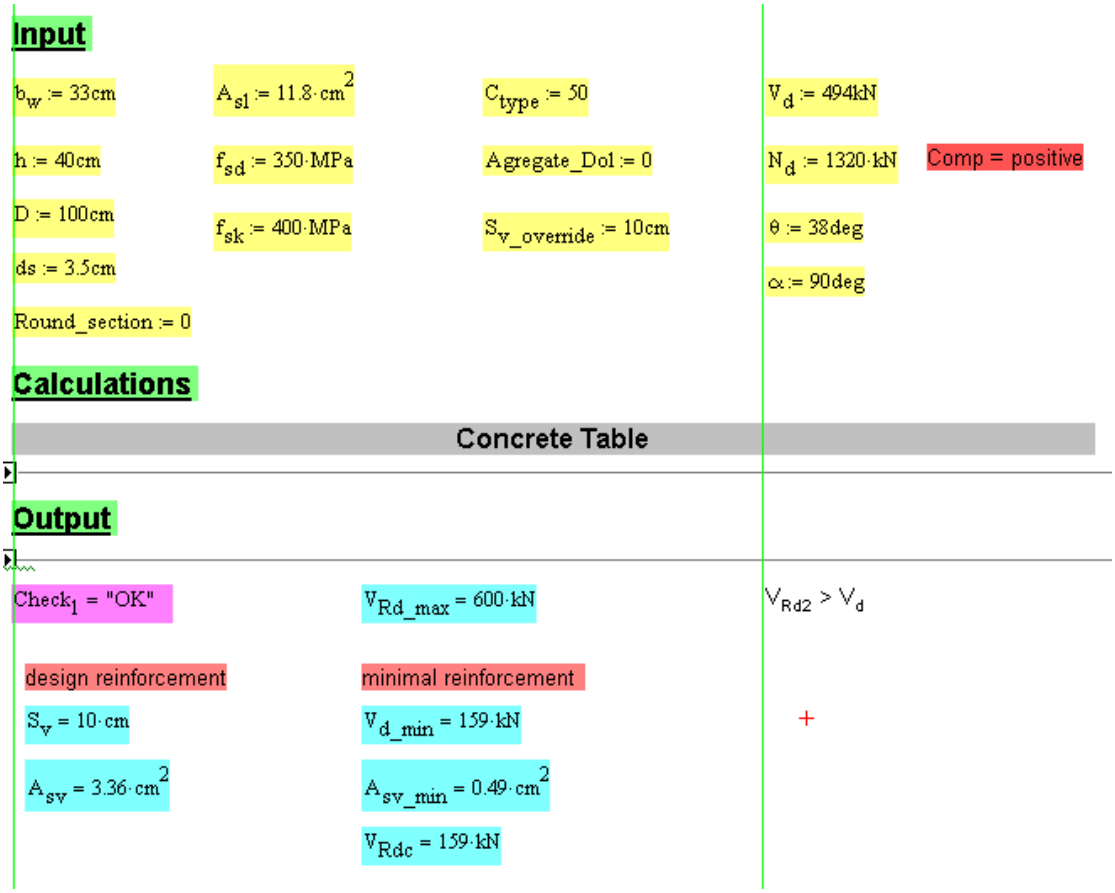

Figure 117 - Pre-tensioned elements, Shear capacity analysis for 81mm mortar case

The shear resultants show extremely high values that may only be resisted if the elements are reinforced properly. Values suggest possible failure in diagonal compression if the load is increased.

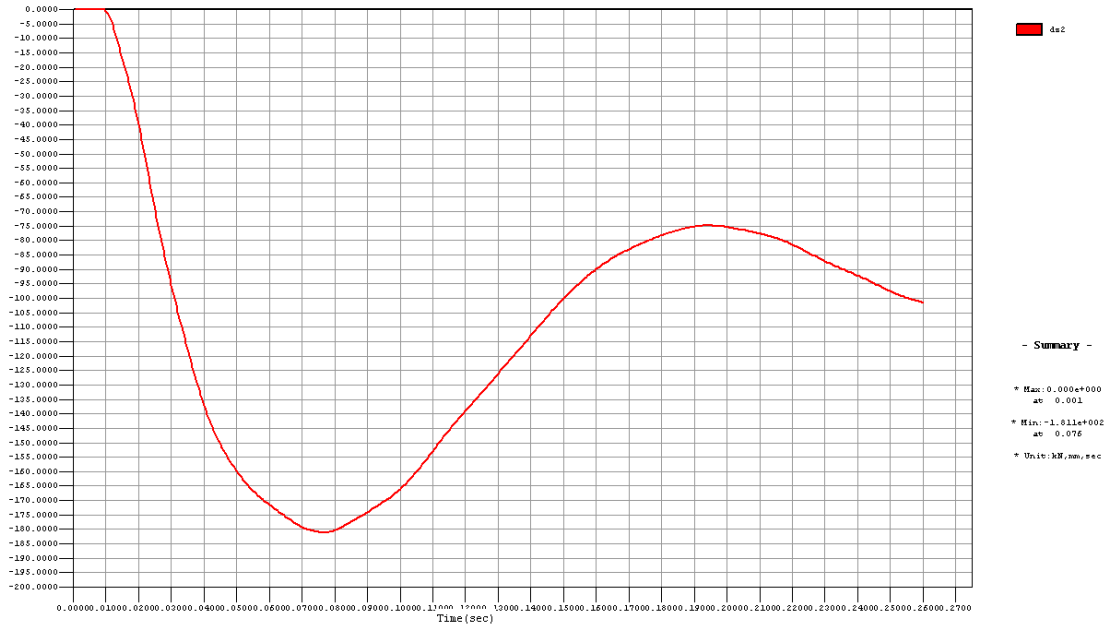

Figure 118 - Time-History vertical deflection at mid-span. Shows a post failure rebound that may not happen if actually tested.

The results show that the system does not fulfill the criterion for life-safety under the extreme case of a 250kg general purpose bomb air-blast.

Post Tensioned Un-bonded Strand Slab Results

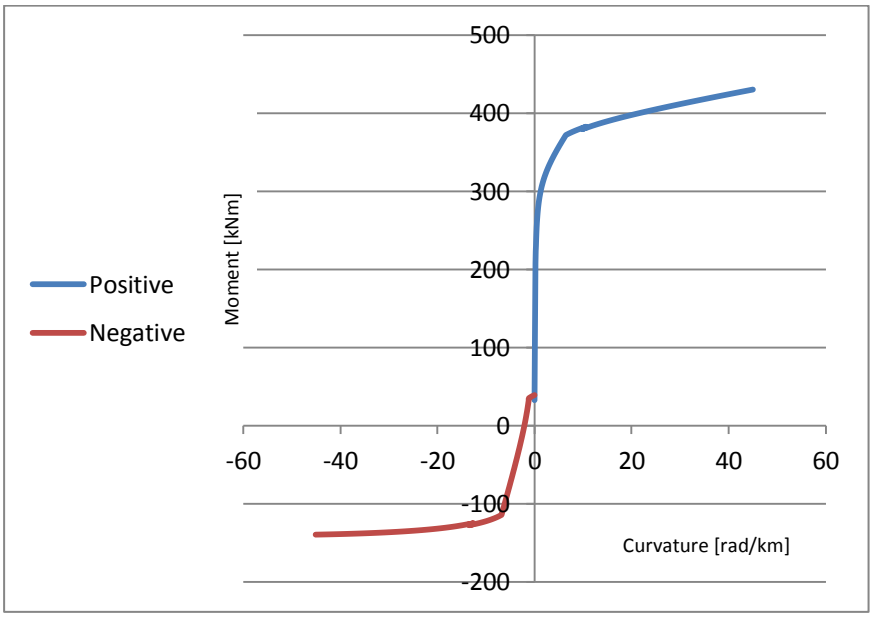

Figure 119 - - Post-tensioned Slab mid-span section, bending moment capacity [kNm]

Bending moment capacity for each element is 472 kNm.

Negative moment capacity is 140.2 kNm.

The section is calculated to crack at 337.3 kNm at the bottom, or whenever the external moment exceeds 14.4 kNm negative.

Curvature at ultimate is 84.5 rad/km positive, and 73.6 rad/km negative.

While ultimate capacity is not the best of the three examined structures, sectional ductility is extremely good.

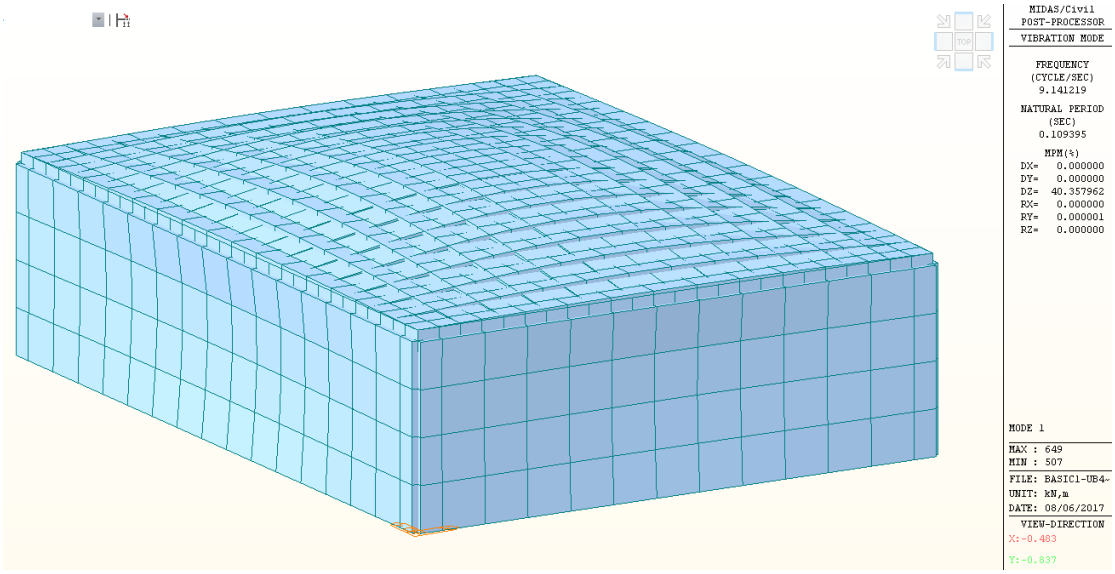

Figure 120 - Post-tensioned slab eigenvalue analysis. Natural period is 0.109 sec

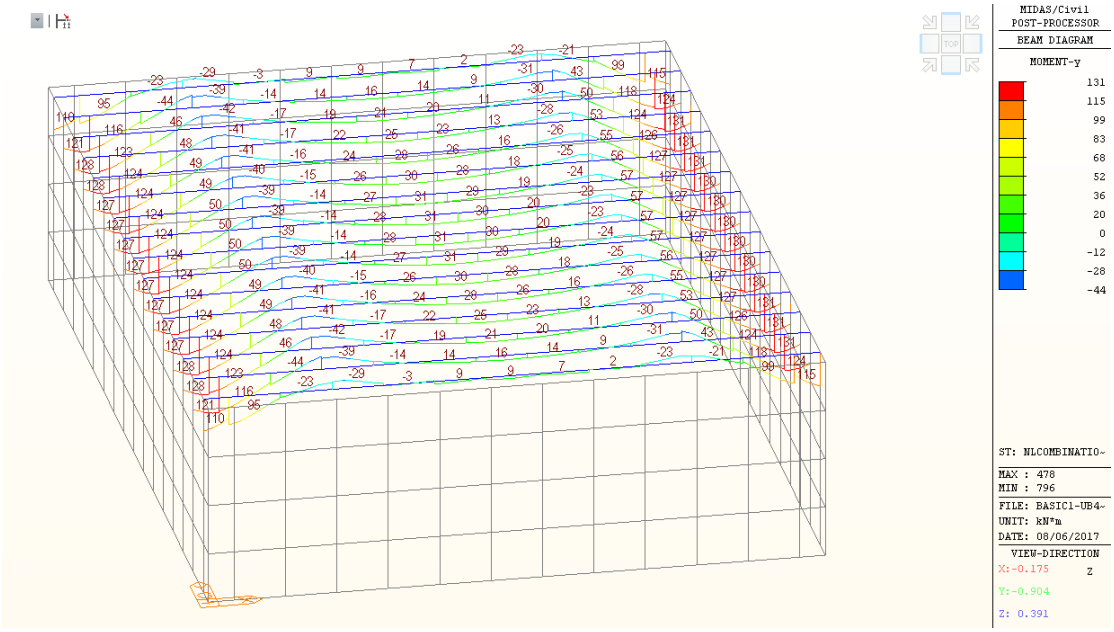

Figure 121 – Post-tensioned slab, Moment distribution at rest, short span direction [kNm]

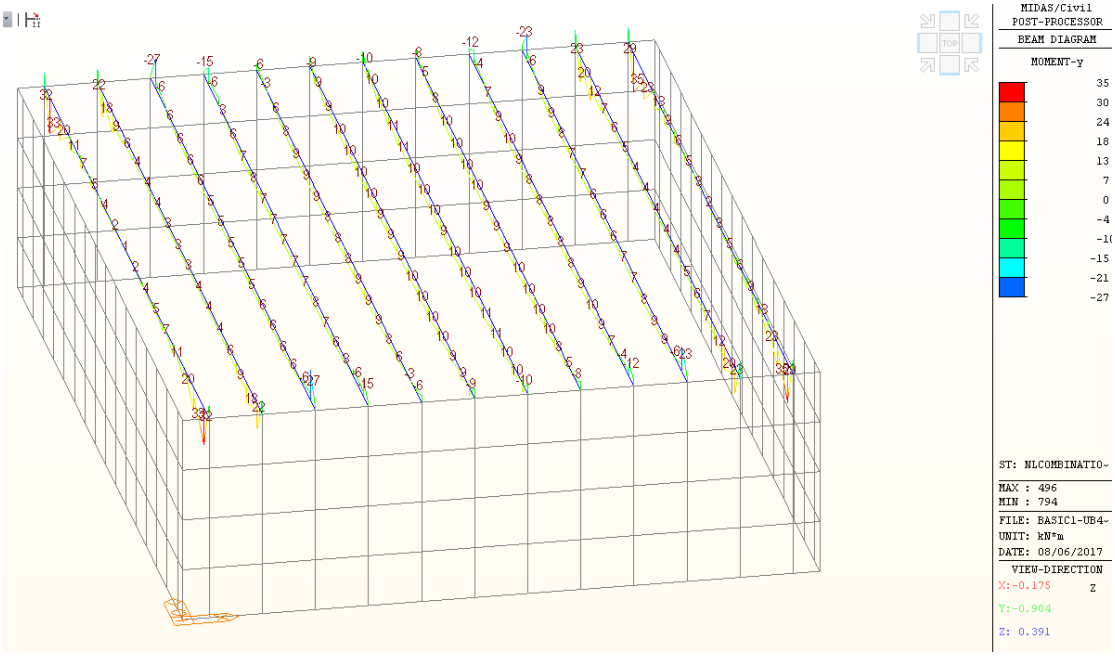

Figure 122 - Post-tensioned slab, Moment distribution at rest, long span direction [kNm]

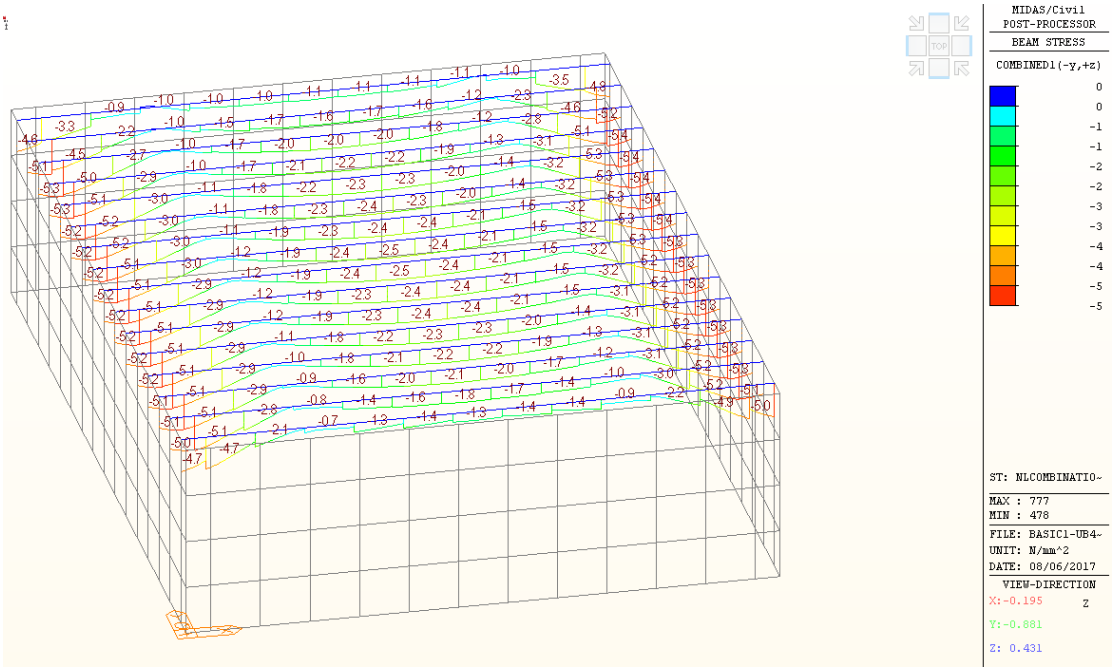

Figure 123 - Post-tensioned slab, top fiber stresses at rest [MPa]

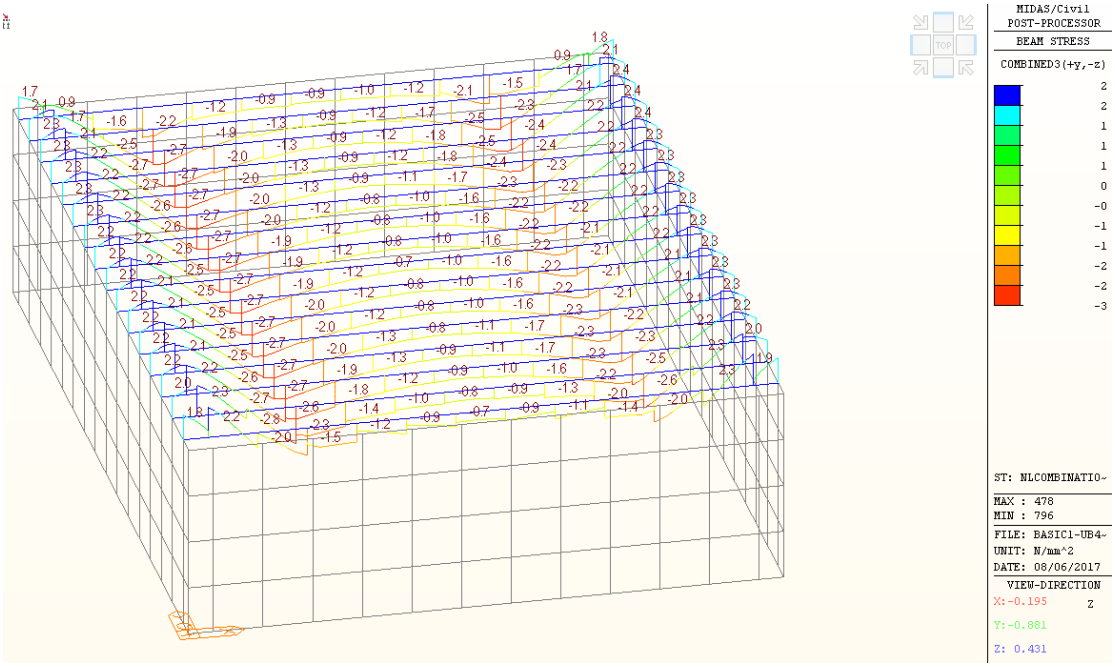

Figure 124 - Post-tensioned slab, bottom fiber stresses at rest [MPa]

The at-rest results show that the slab is under compression at the mid-span sections. The sections close to the support are pre-stressed so that the bottom fiber is under mild tension, opposing normative loads effects.

Case 3.1 – Post-tensioned slab under 81mm mortar blast

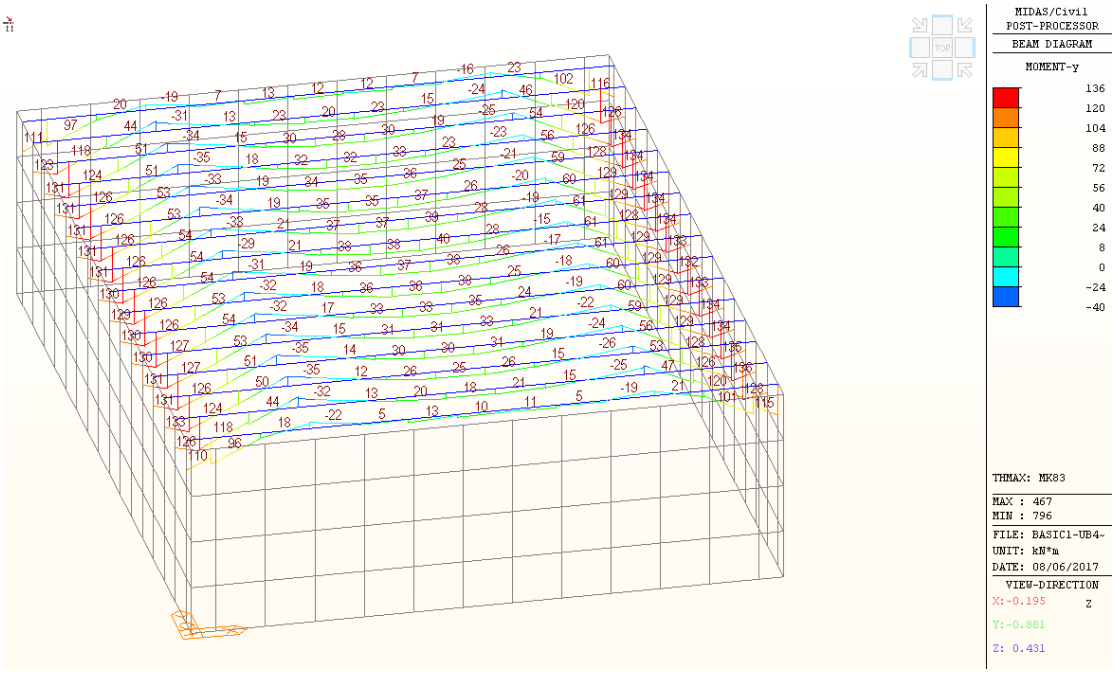

Figure 125– Maximum positive moment envelope, 81mm mortar, short span direction [kNm]

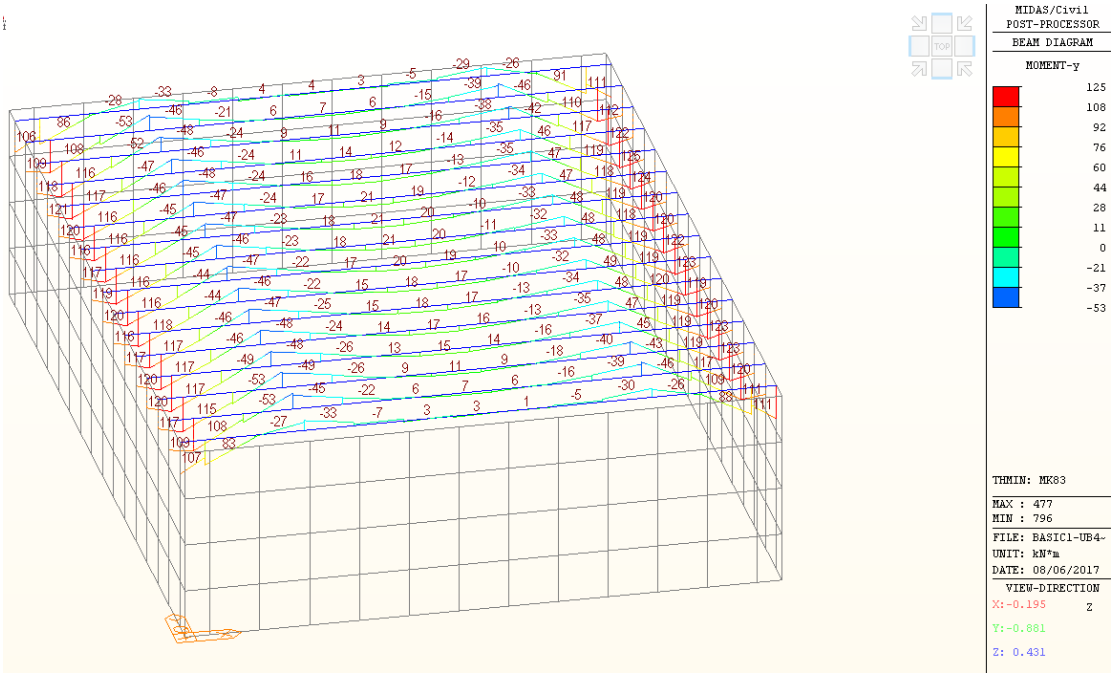

Figure 126 – Maximum negative moment envelope, 81mm mortar, short span direction [kNm]

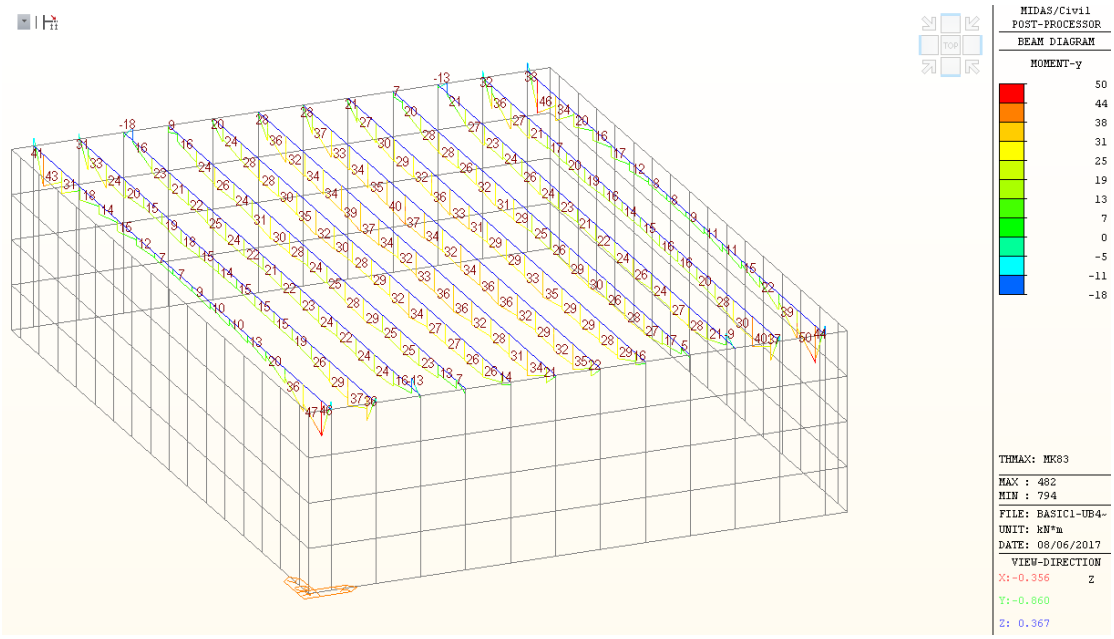

Figure 127 - Maximum positive moment envelope, 81mm mortar, long span direction [kNm]

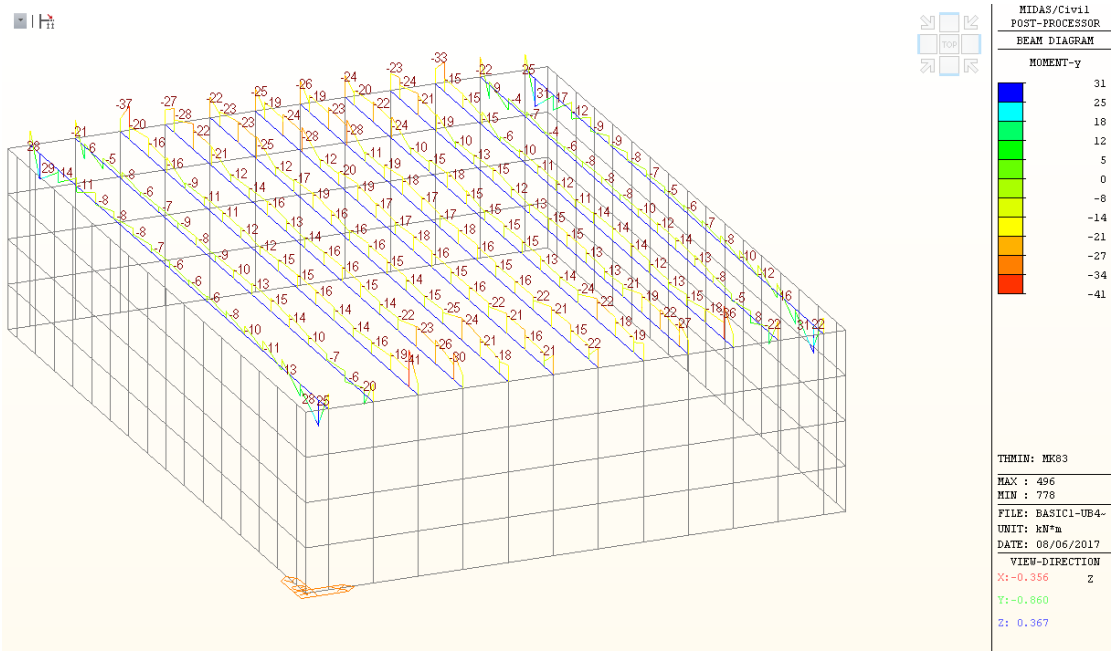

Figure 128 - Maximum negative moment envelope, 81mm mortar, long span direction [kNm]

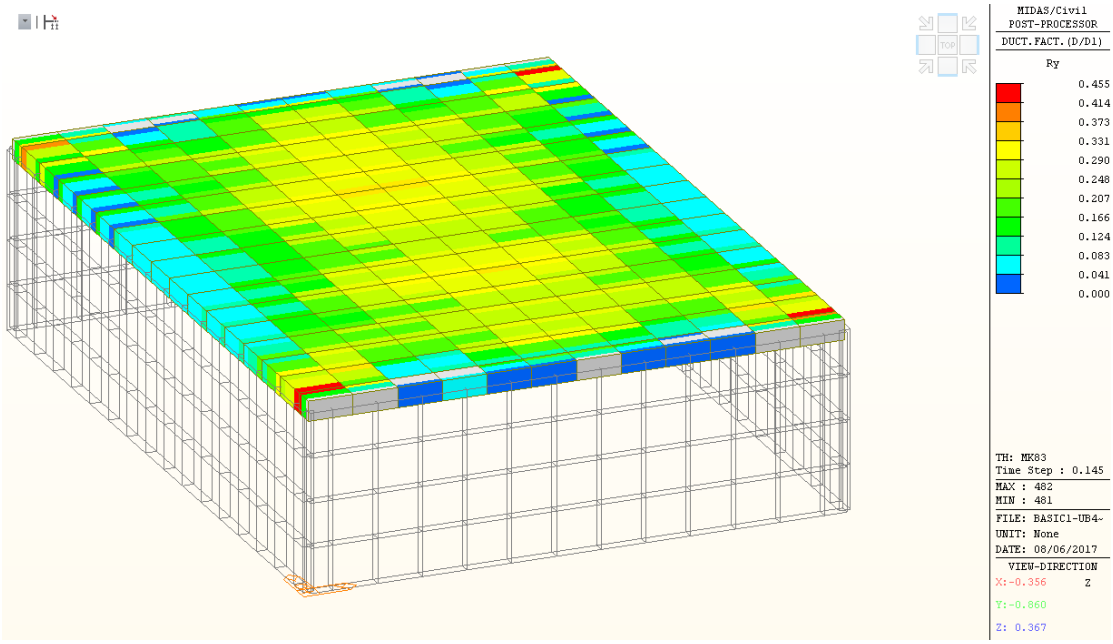

Figure 129 - D1 Ductility factors, 81mm mortar

Results show no damage from the blast load. The Analysis shows no cracks are shown to have developed.

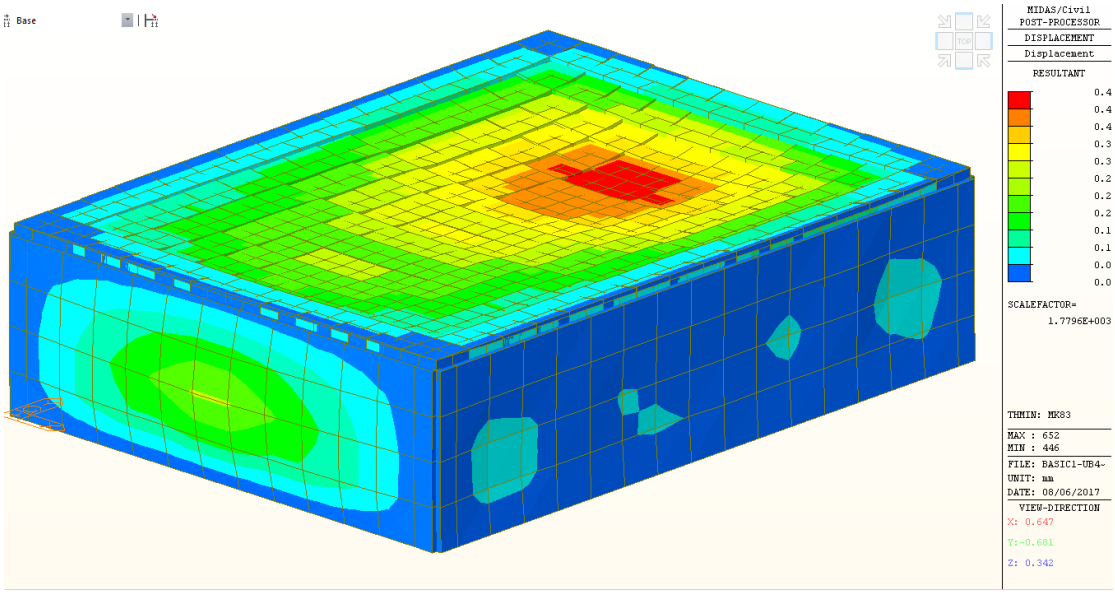

Figure 130 - Post-tensioned slab, 81mm Mortar, Maximum Deflection [mm]

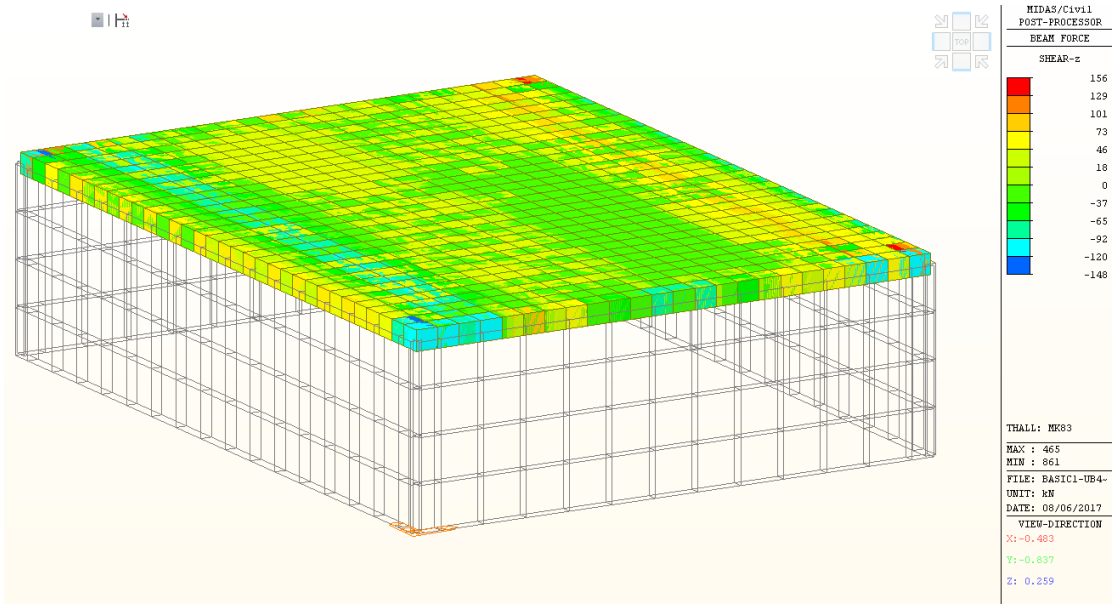

Figure 131 - Post-tensioned slab, 81mm mortar, Shear force envelope [kN]

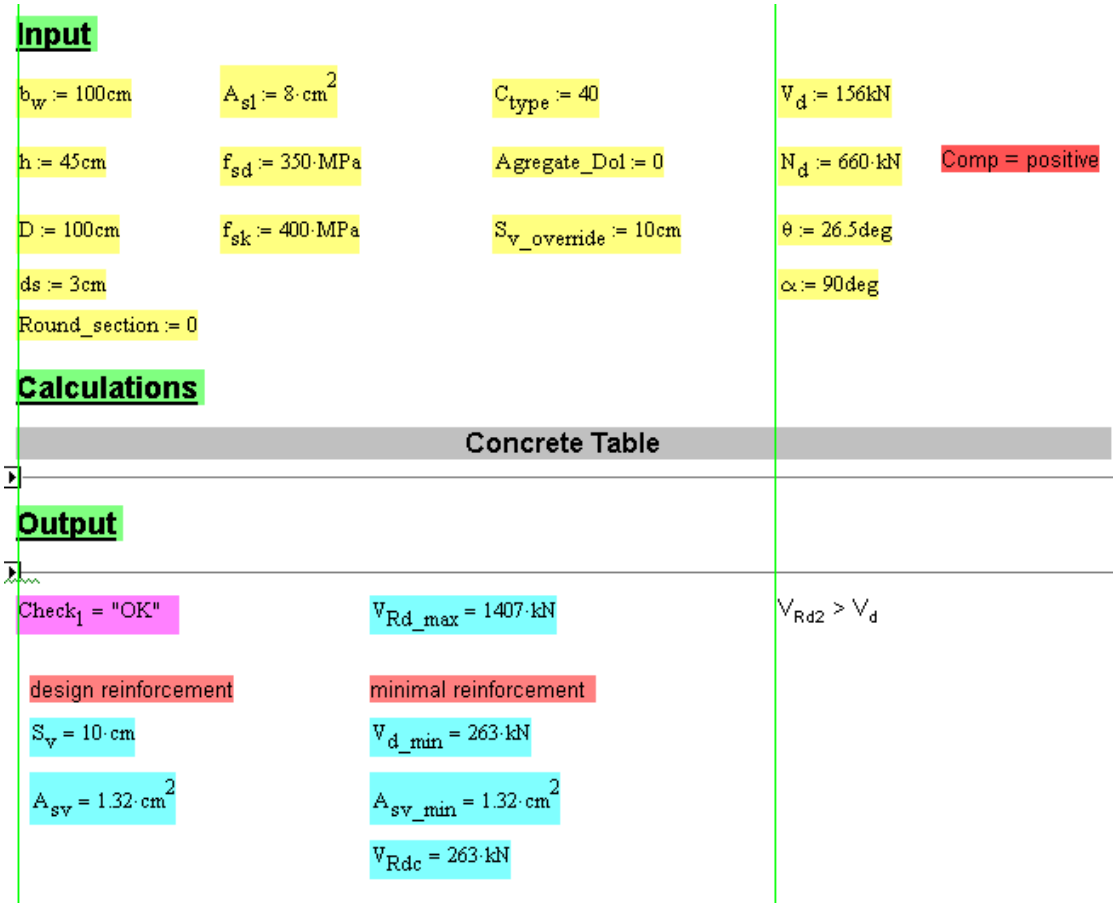

Figure 132 - Post-tensioned slab, Shear capacity analysis for the 81mm mortar case

The shear resultants indicate no need for reinforcements to resist the effects of the blast.

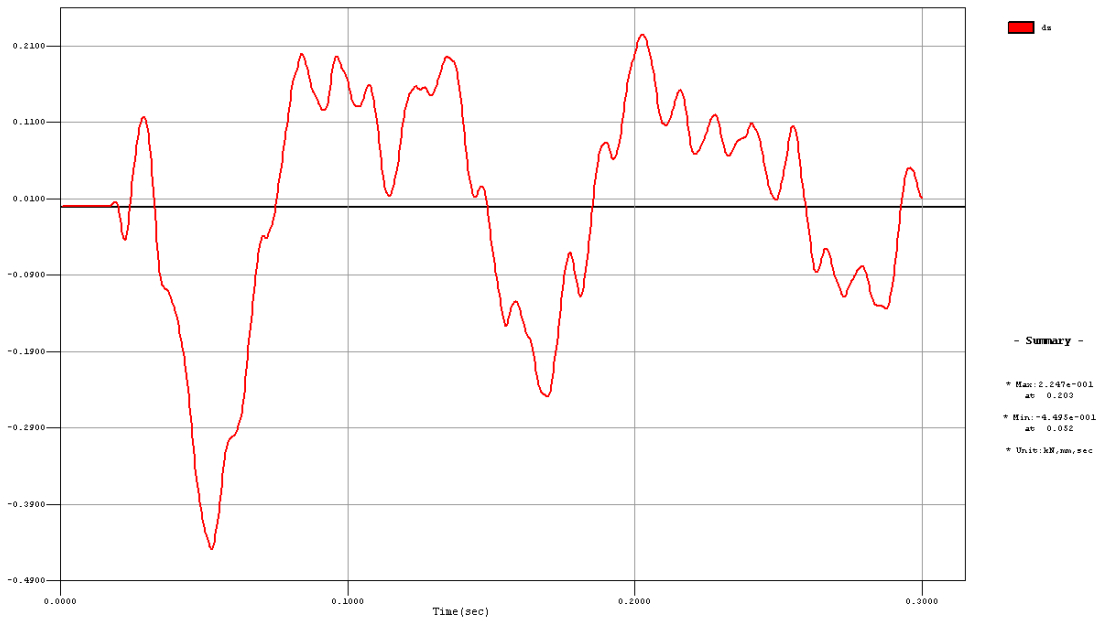

Figure 133 - Time history vertical deflection at mid span.

Results show that no damage was caused to the structure due to the blast load.

Case 3.2 – Post-tensioned slab under 122mm rocket blast

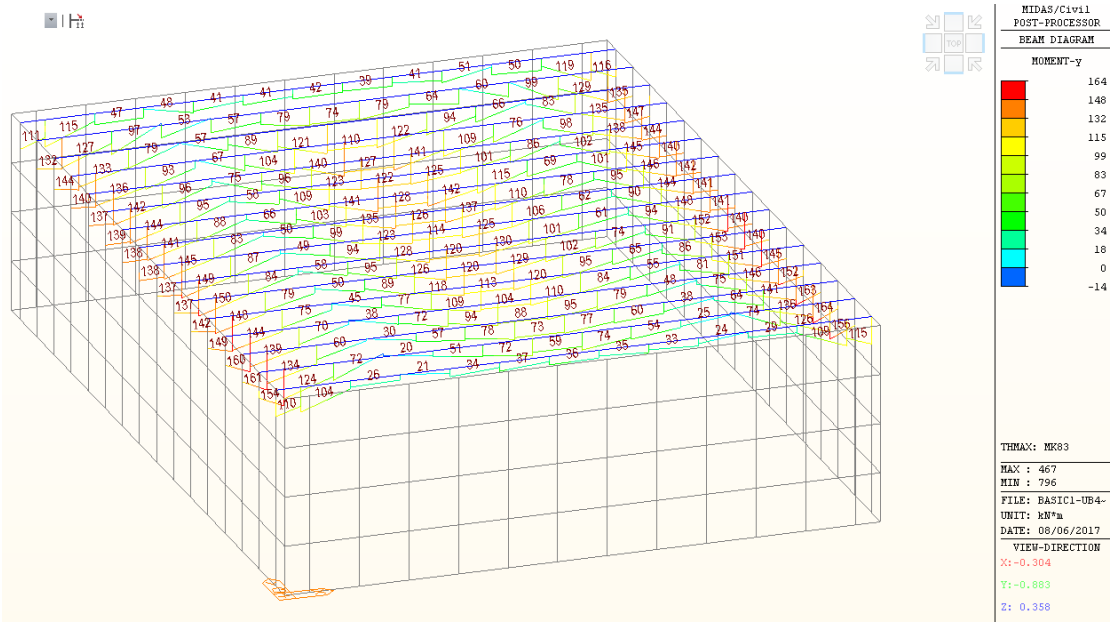

Figure 134 - Maximum positive moment envelope, 122mm rocket, short span direction [kNm]

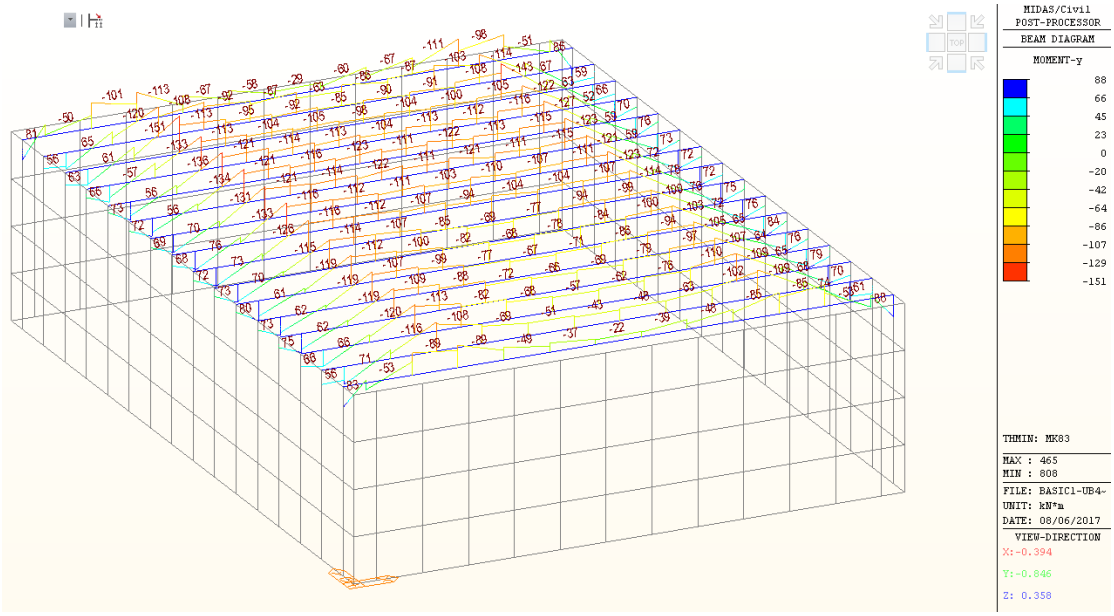

Figure 135 - Maximum negative moment envelope, 122mm rocket, short span direction [kNm]

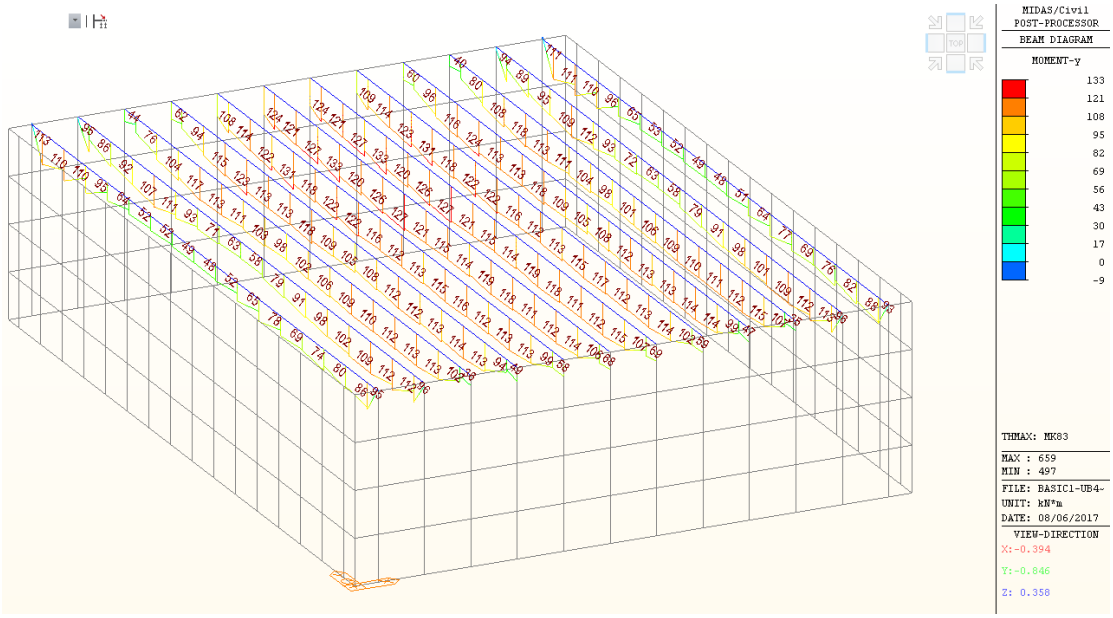

Figure 136 - Maximum positive moment envelope, 122mm rocket, long span direction [kNm]

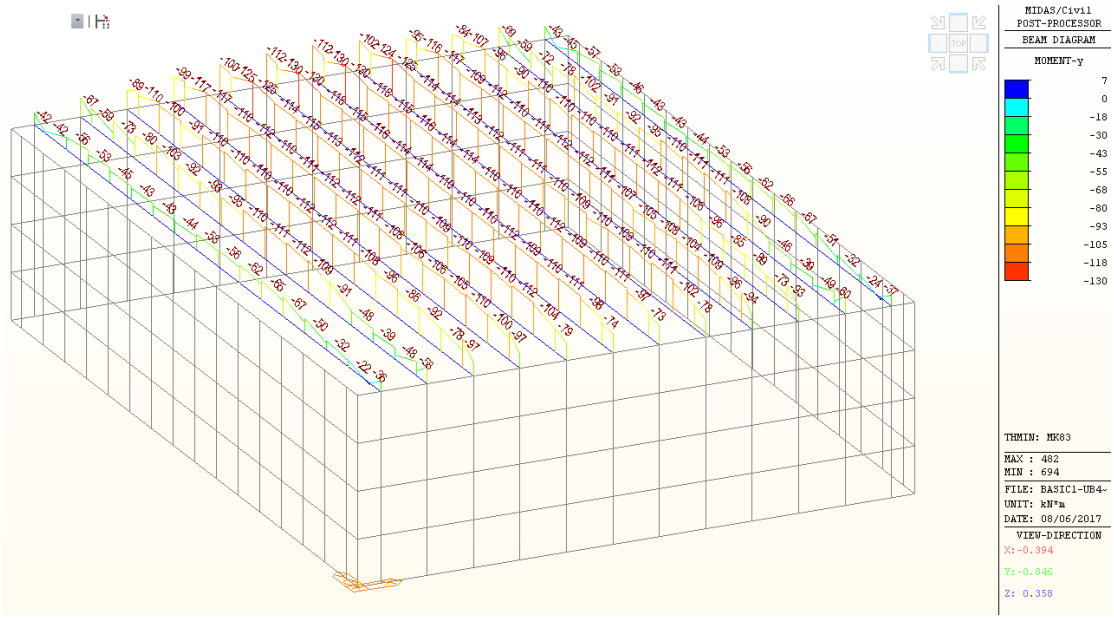

Figure 137 - Maximum negative moment envelope, 122mm rocket, long span direction [kNm]

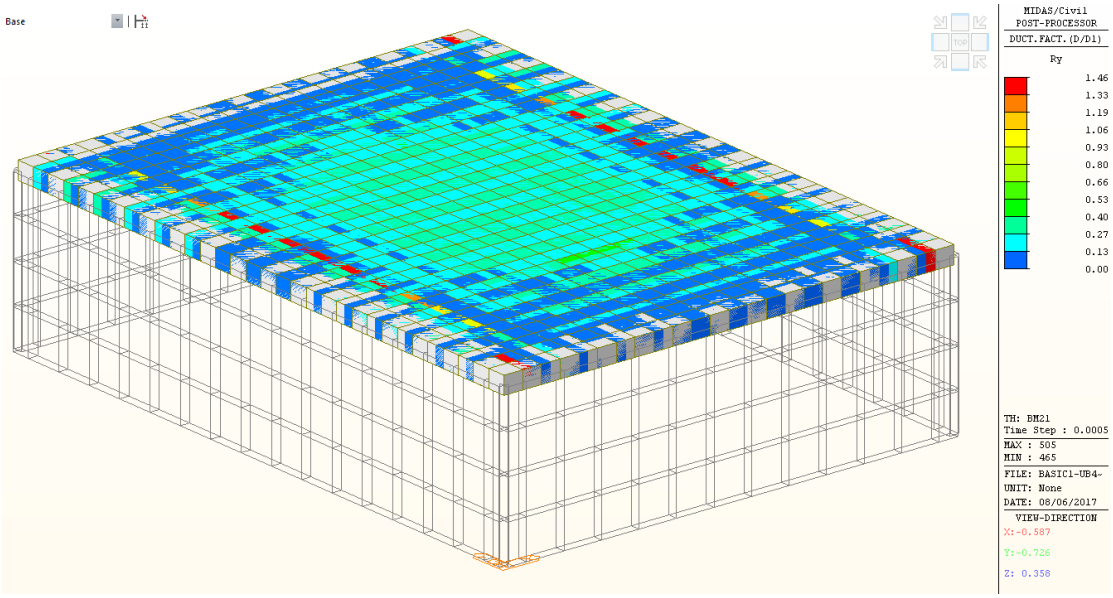

Figure 138 - D1 Ductility factors, 122mm rocket

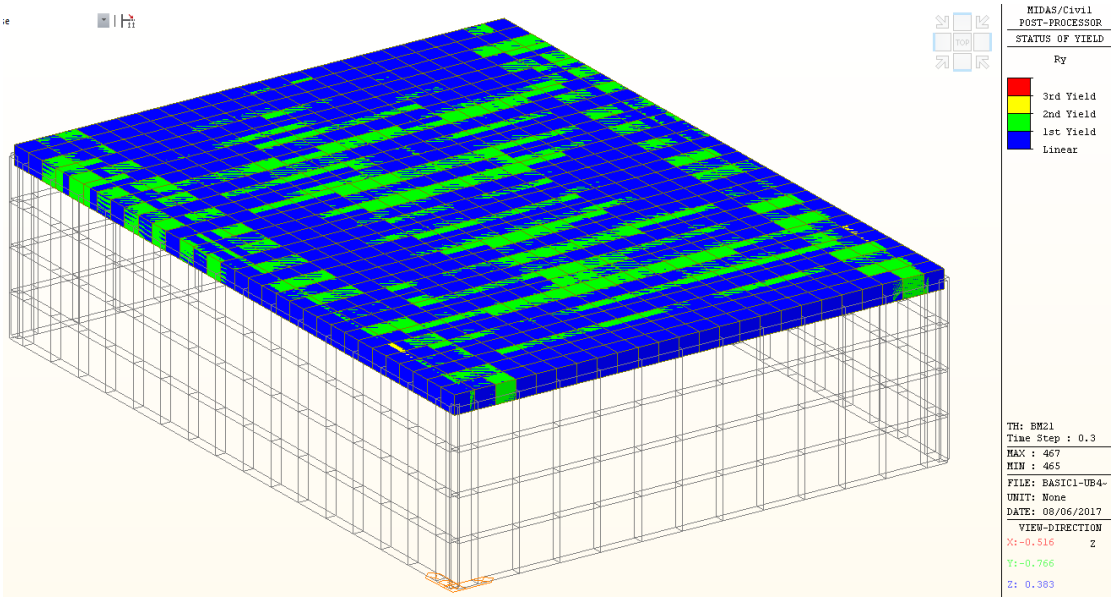

Figure 139 - Yield status output, 122mm rocket. Internally cracked regions are marked in green

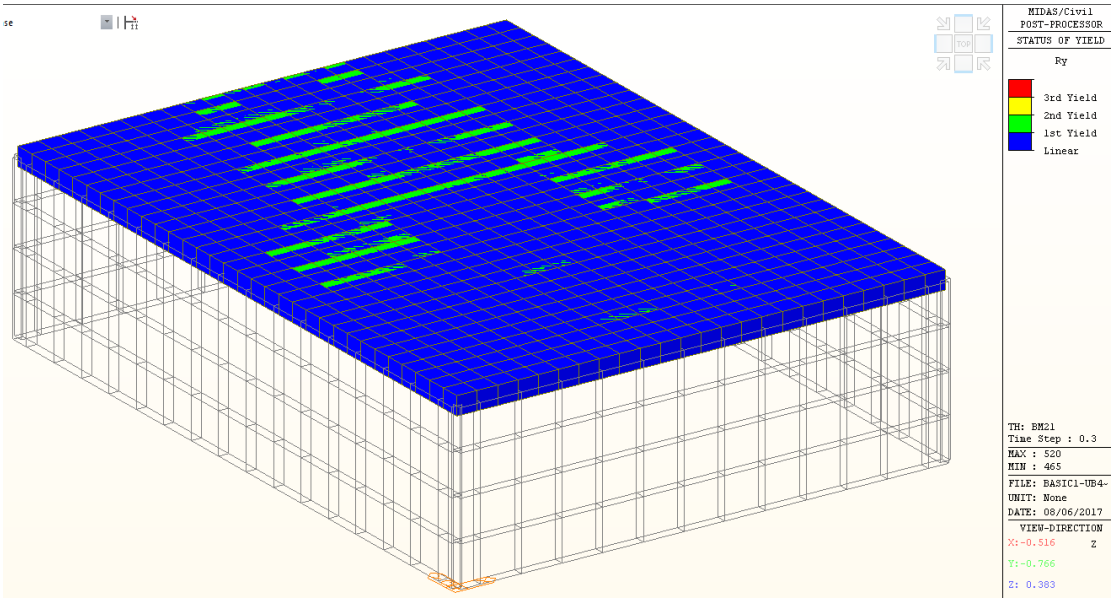

Figure 140 - Yield status output, 122mm rocket. Externally cracked regions are marked in green

The results show internal cracking in both directions and some external cracking in the short span direction (due to actions in the long span direction).

The maximum positive curvature is 3.4rad/km, which correlate to bottom fiber cracks that are ~0.05mm wide.

The maximum negative curvature is 4.3 rad/km, which correlate to top fiber cracks that are ~0.06mm wide.

All results show good flexure performance sustaining the blast load.

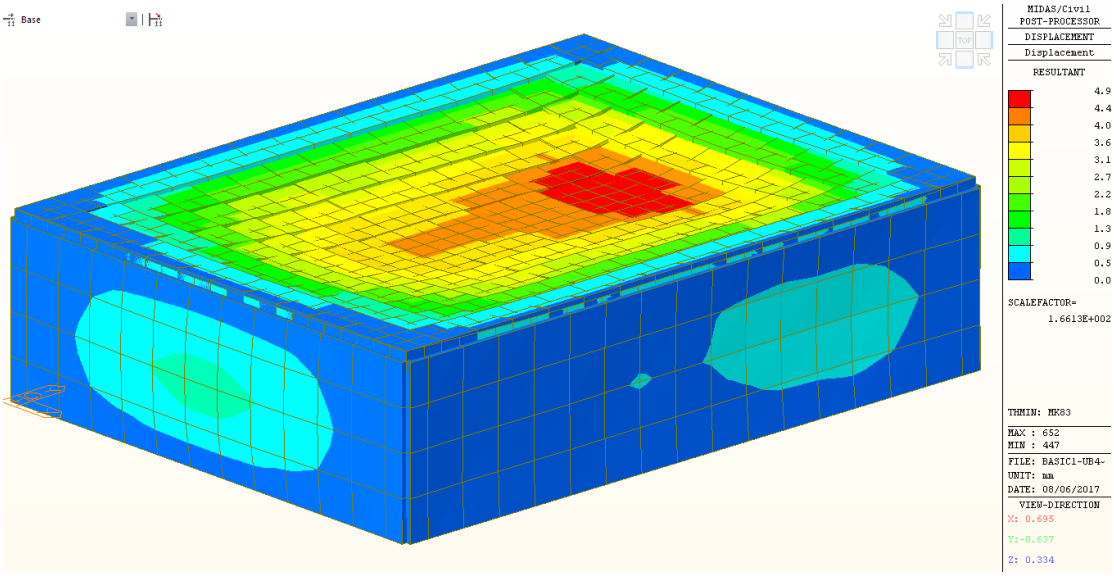

Figure 141 - Post-tensioned slab, 122mm rocket, Maximum Deflection [mm]

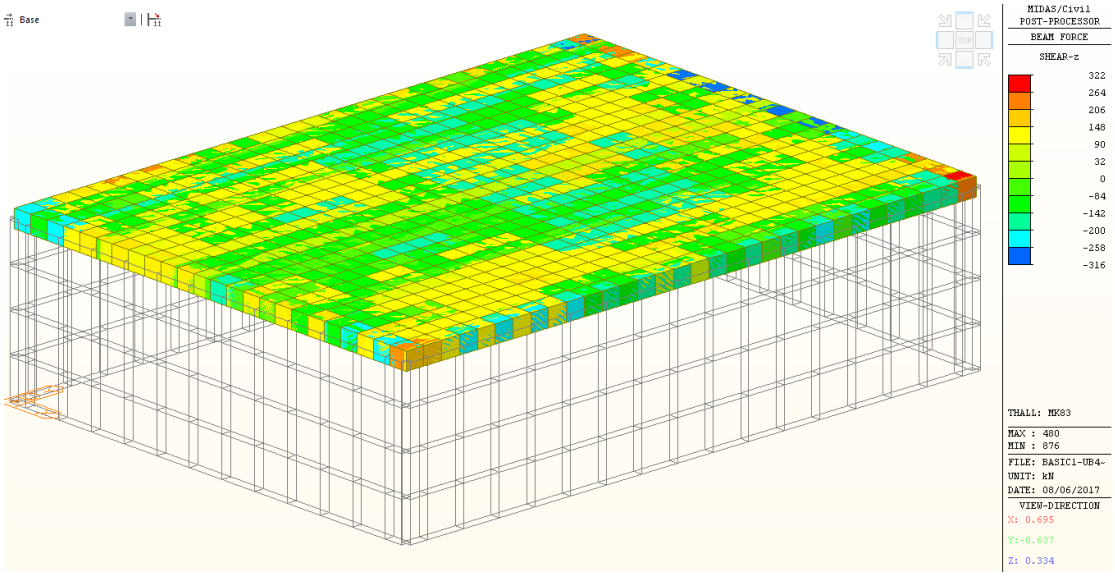

Figure 142 - Post-tensioned slab, 122mm rocket, Shear force envelope [kN]

Input

$b_w := 100cm$ $A_{sl} := 8 \cdot cm^2$ $C_{type} := 40$ $V_d := 322kN$

$h := 45cm$ $f_{sd} := 350 \cdot MPa$ $Aggregate\_Dol := 0$ $N_d := 660 \cdot kN$ Comp = positive

$D := 100cm$ $f_{sk} := 400 \cdot MPa$ $S_{v\_override} := 10cm$ $\theta := 26.5deg$

$ds := 3cm$ $\alpha := 90deg$

$Round\_section := 0$

Calculations

Concrete Table

Output

$Check_1 = "OK"$ $V_{Rd\_max} = 1407 \cdot kN$ $V_{Rd2} > V_d$

design reinforcement minimal reinforcement

$S_v = 10 \cdot cm$ $V_{d\_min} = 263 \cdot kN$

$A_{sv} = 1.32 \cdot cm^2$ $A_{sv\_min} = 1.32 \cdot cm^2$

$V_{Rdc} = 263 \cdot kN$

Figure 143 - Post-tensioned slab, Shear capacity analysis for the 122mm rocket case

Shear resultants show shear reinforcement is necessary to resist the blast load. Consideration of the thickness of the slab at the support and the location of the potential

failure plane make it possible that the slab will be able to resist the loads even without any additional reinforcement.

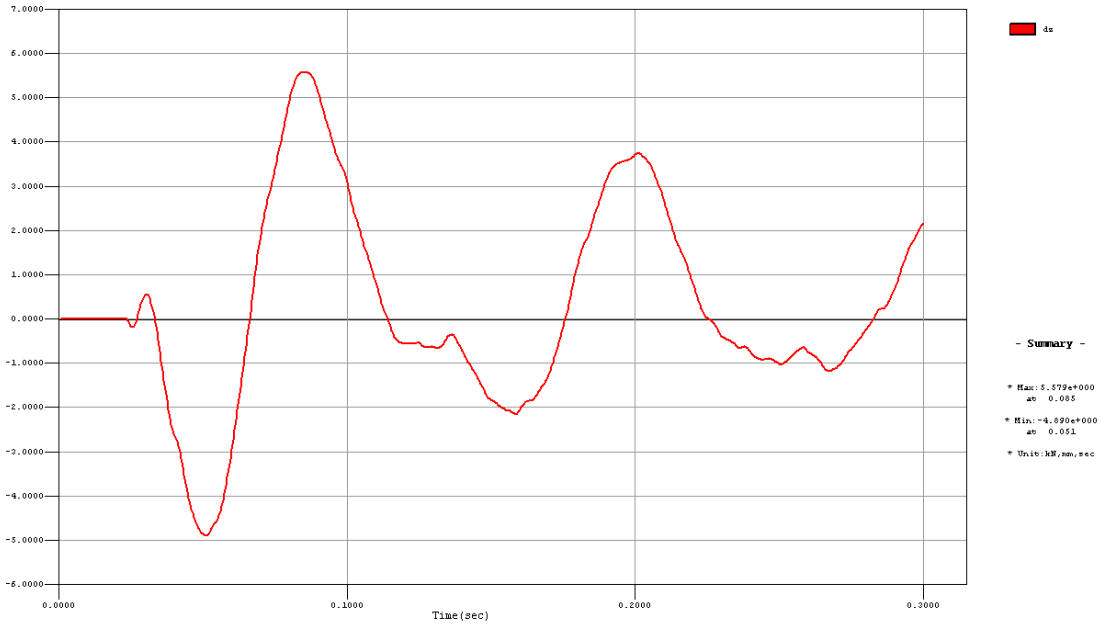

Figure 144 - Time history vertical deflection at mid span. The cycle duration increased to 0.115 sec, a slight increase over the Eigenvalue result.

The analysis results show that provided that shear failure is successfully prevented, the structural system can resist the blast load with the most minor damage caused. In fact, he slab is unlikely to need any repairs and resists the loads extremely well.

Case 3.3 – Post-tensioned slab under 250kg GP bomb blast

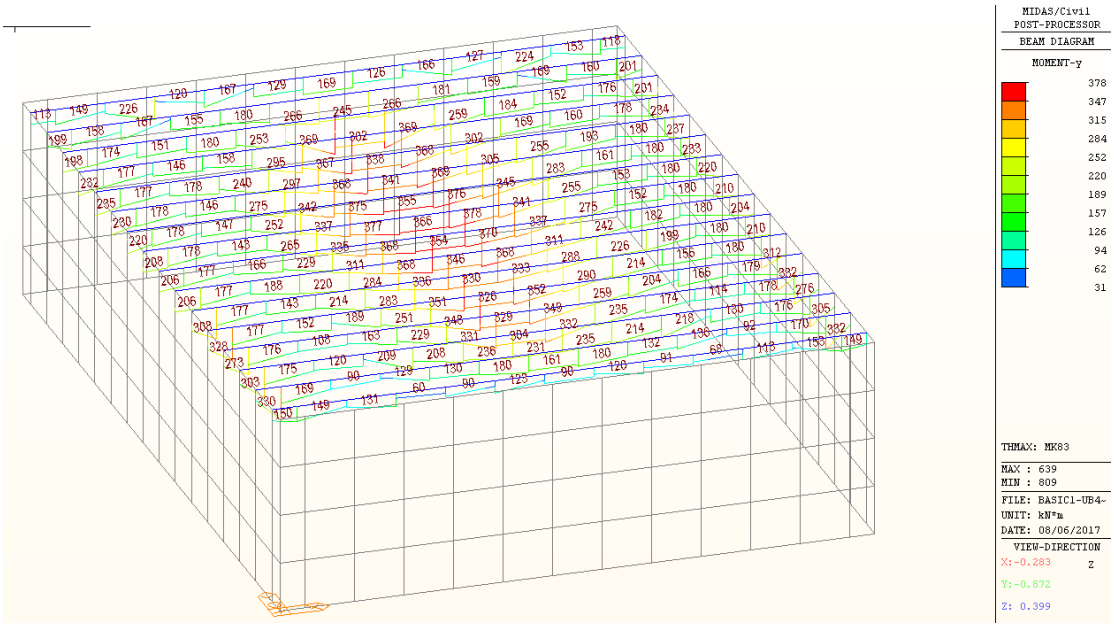

Figure 145 - Maximum positive moment envelope, 250kg GP bomb blast, short span direction [kNm]

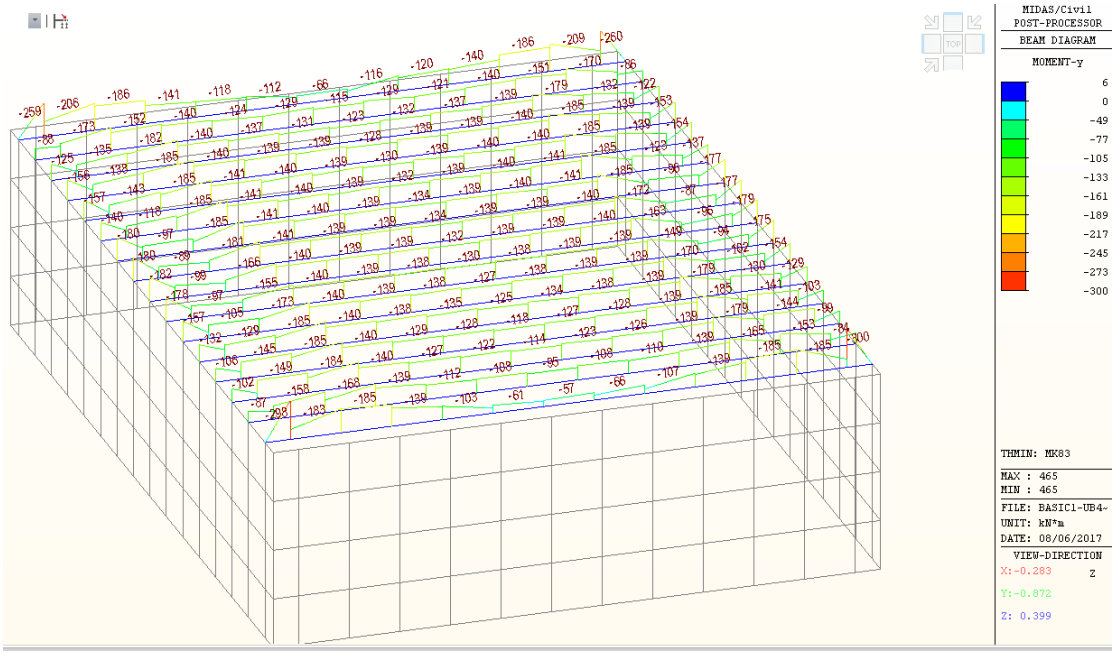

Figure 146 - Maximum negative moment envelope, 250kg GP bomb blast, short span direction [kNm]

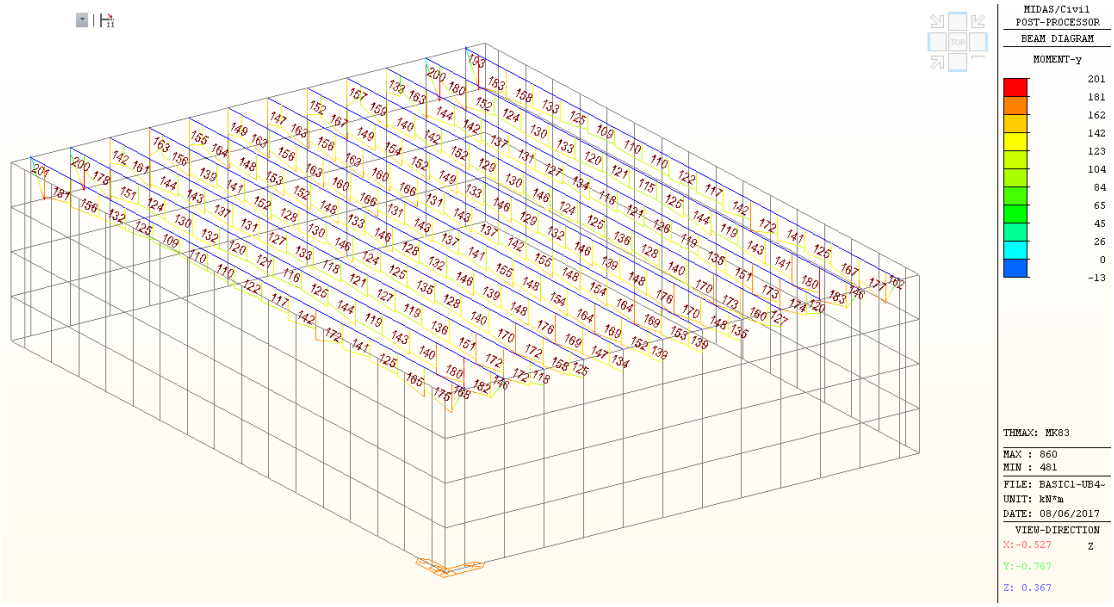

Figure 147 - Maximum positive moment envelope, 250kg GP bomb blast, long span direction [kNm]

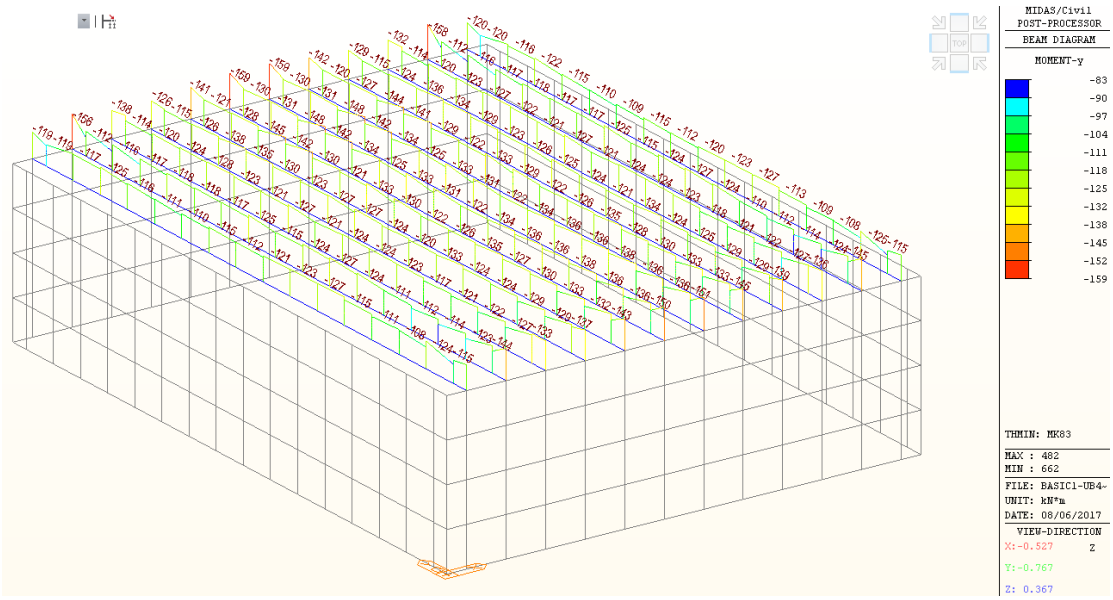

Figure 148 - Maximum negative moment envelope, 250kg GP bomb blast, long span direction [kNm]

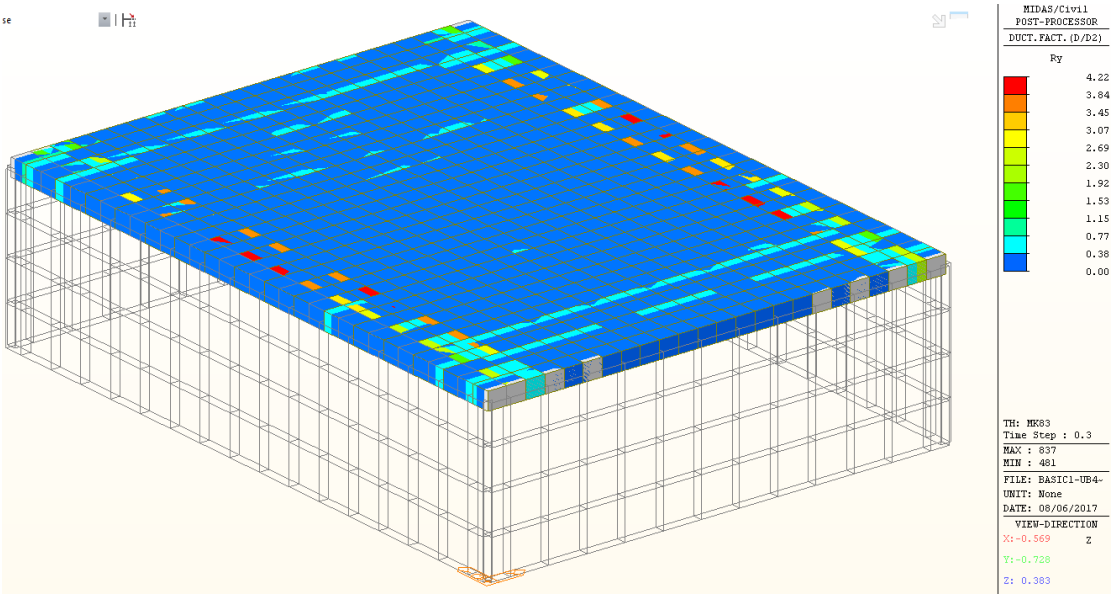

Figure 149 - D2 Ductility factors, 250kg GP bomb blast, positive direction

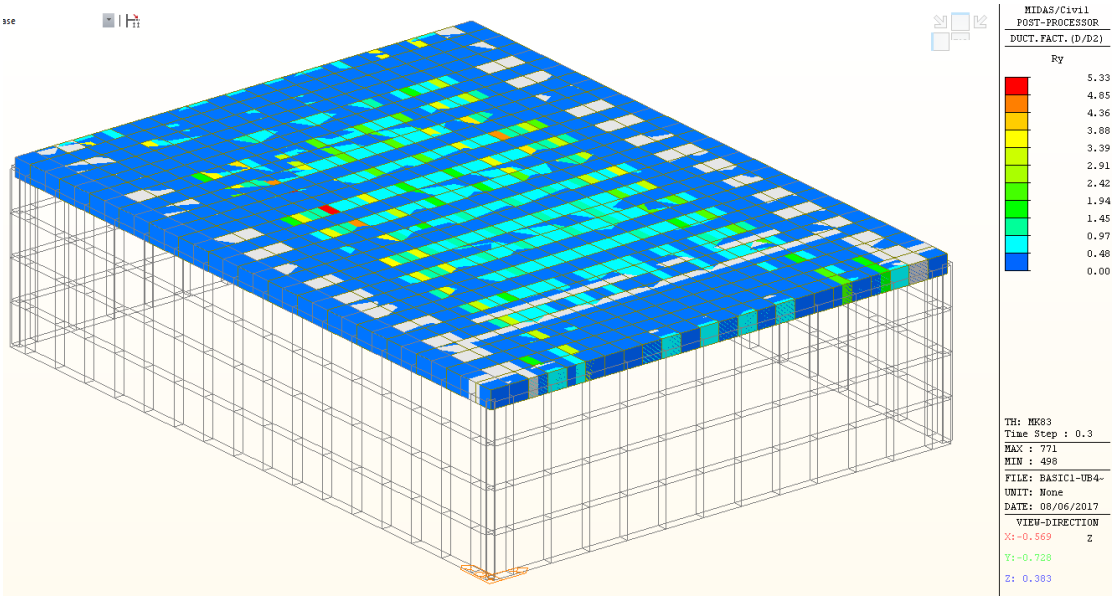

Figure 150 – D2 Ductility factors, 250kg GP bomb blast, negative direction

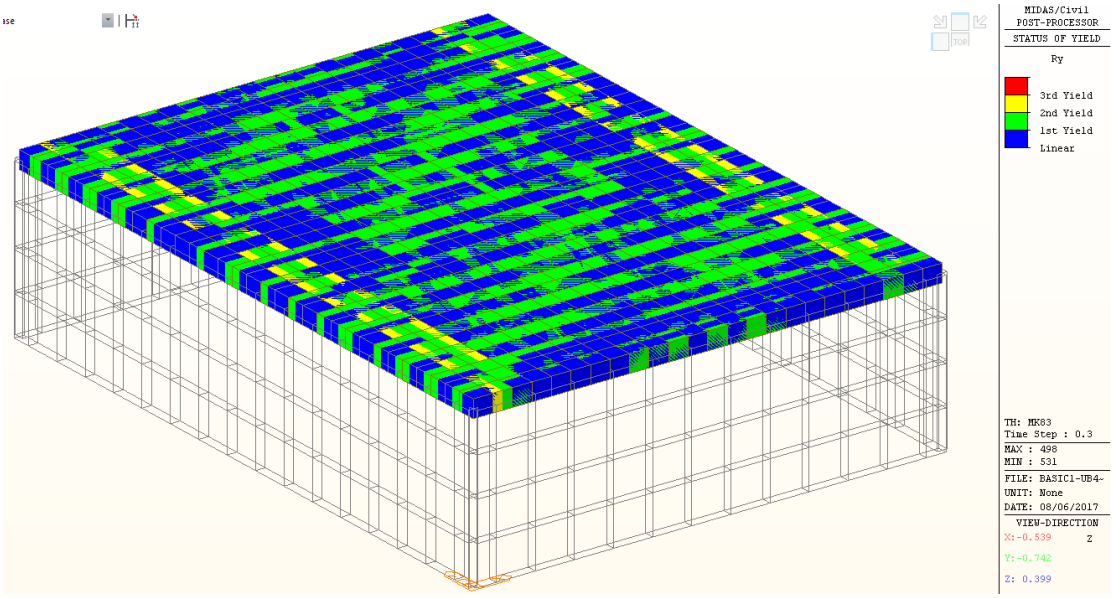

Figure 151 - Yield status output, 250kg GP bomb. Internally cracked regions are marked in green

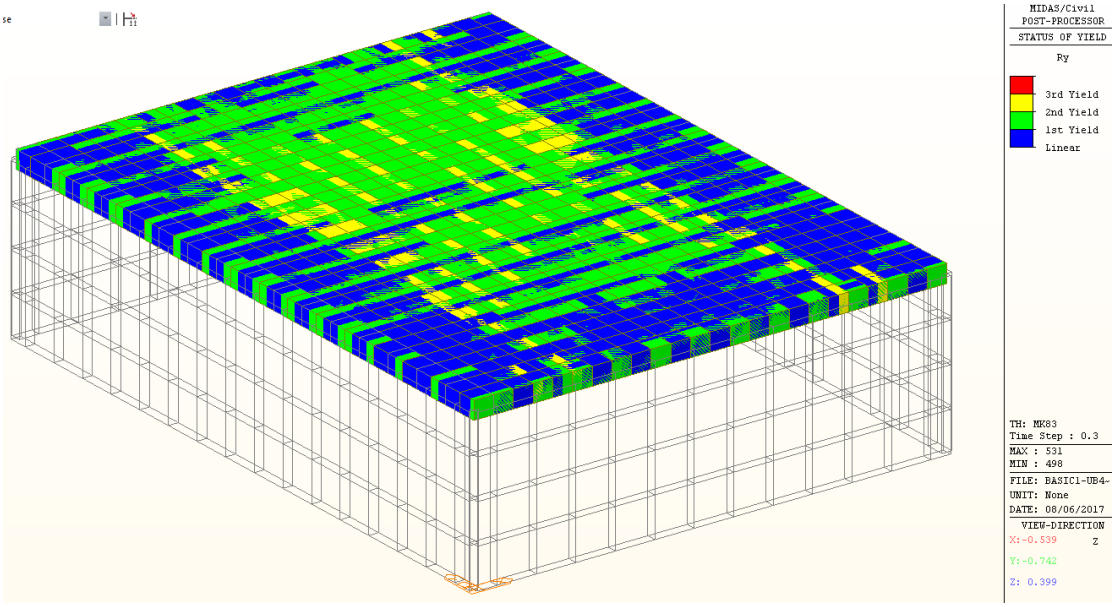

Figure 152 - Yield status output, 250kg GP bomb. Externally cracked regions are marked in green

The results show extensive cracking in both directions, both internally and externally.

Some sections yielded in the short span direction.

The maximum positive curvature is 14.9rad/km, which correlate to bottom fiber cracks that are ~0.28mm wide.

The maximum negative curvature is 8.1 rad/km, which correlate to top fiber cracks that are ~0.14mm wide.

The results indicate extremely good flexural performance of the structure under the extreme load.

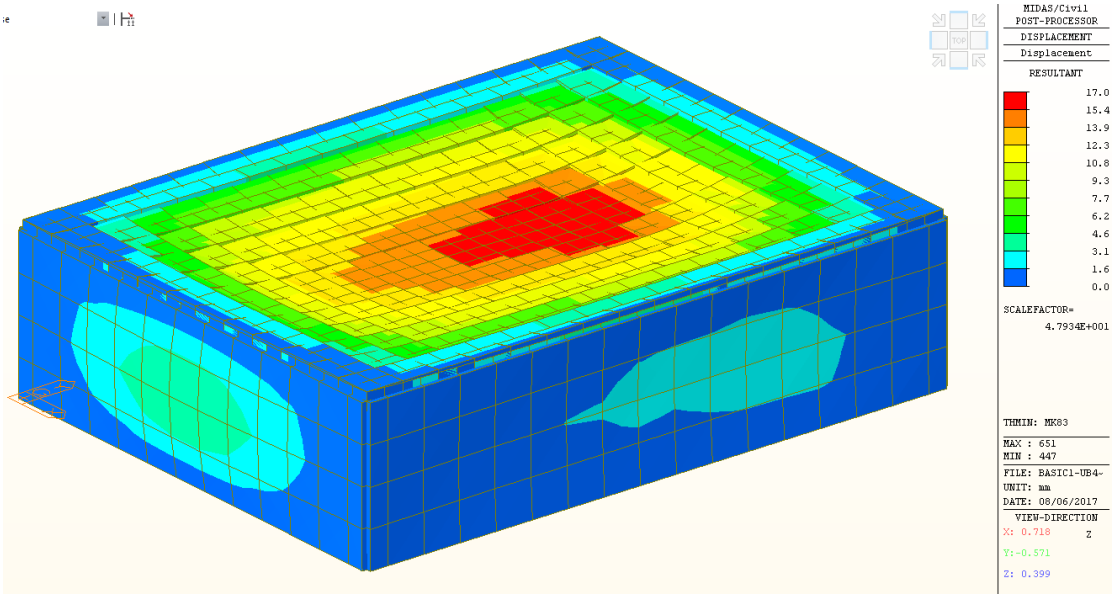

Figure 153 - Post-tensioned slab, 122mm rocket, Maximum Deflection [mm]

The deformation pattern demonstrates a good distribution of the extreme load across the entire slab.

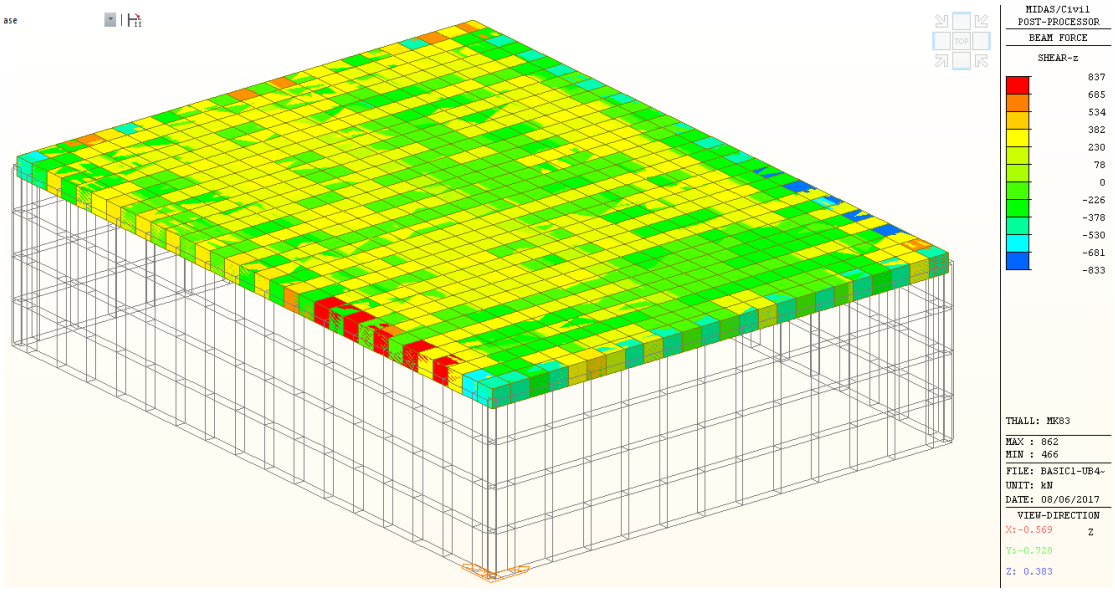

Figure 154 - Post-tensioned slab, 250kg GP bomb, Shear force envelope [kN]

Input

$b_w := 100cm$ $A_{sl} := 8 \cdot cm^2$ $C_{type} := 40$ $V_d := 837kN$

$h := 45cm$ $f_{sd} := 350 \cdot MPa$ $Agregate\_Dol := 0$ $N_d := 660 \cdot kN$ Comp = positive

$D := 100cm$ $f_{sk} := 400 \cdot MPa$ $S_{v\_override} := 10cm$ $\theta := 26.5deg$

$ds := 3cm$ $\alpha := 90deg$

$Round\_section := 0$

Calculations

Concrete Table

Output

$Check_1 = "OK"$ $V_{Rd\_max} = 1407 \cdot kN$ $V_{Rd2} > V_d$

design reinforcement minimal reinforcement

$S_v = 10 \cdot cm$ $V_{d\_min} = 263 \cdot kN$

$A_{sv} = 3.15 \cdot cm^2$ $A_{sv\_min} = 1.32 \cdot cm^2$

$V_{Rdc} = 263 \cdot kN$

Figure 155 - Post-tensioned slab, Shear capacity analysis for 250kg GP bomb

Shear resultants show that with some shear reinforcement, the slab will successfully resist the blast load.

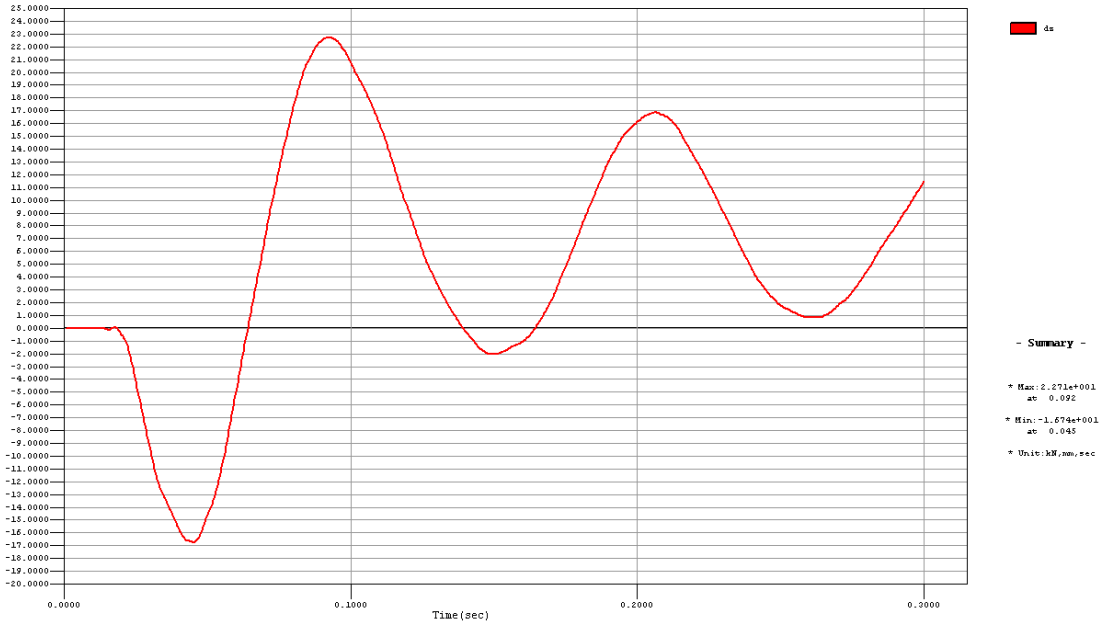

Figure 156 - Time history vertical deflection at mid span. It is possible that the point of equilibrium moves up vertically due to the section being damaged by negative moments.

It is demonstrated by the results that the post tensioned system, when combined with adequate shear reinforcement, can successfully resist the extreme load imposed by the air blast. It is not only predicted to remain intact, but is likely being able to protect against falling debris.

6. Summary

This paper set out to examine the possibility of prestressed concrete systems withstanding blast loads and so to be used in the construction of shelter spaces.

The study compared two commonplace types of prestressed concrete systems to a simple reinforced concrete slab, using 3 types of loads, with a different performance criterion for each load.

The criteria were:

- In the case of the 81mm mortar shell, the structure will not lose serviceability
- In the case of the BM-21 rocket, the structure will not be damaged beyond repair and will offer protection against the down-falling debris
- In the case of the MK82 bomb, there will not be any catastrophic failure and the structure will offer some protection against down falling debris

The following table concludes the findings obtained from the results of the analysis:

Table 4 - Analysis findings summary

	RC slab	Prefabricated hollow slab	Post tensioned slab
81mm Mortar	Pass	Pass	Pass
122mm Rocket	Pass	Pass	Pass
250kg GP Bomb	Pass	Fail	Pass

The results show that there is some plausibility, and even possible advantages to the use of prestressed concrete in protective structures.

Several specific additional conclusions have been achieved from observing the results and from the process in general. It is clear that while overall performance of the reinforced concrete slab was the best, for its superior stiffness, mass and ductility, and despite its lower ultimate bending capacity. However, it is assumed that no splicing was needed. The ductility requirements derived from analysis data may have not been sufficient to sustain the required deformability.

It is also concluded, that while pre-tensioned (and by extension, other bonded tendons or cables) offer the least amount of ductility and deformability of the systems examined, and are perhaps even further crippled by their light weight in the case of hollow core slabs, they may still offer some protection against blast loads.

The higher capacities, both at ultimate and in relation to cracking make up for some of what is otherwise lacking. Provided that the right type of reinforcement and details be put in place, as well as that the proper size of element be used, such elements may be a valid option for quicker, cheaper construction of protective structures.

Such details may include shear reinforcement that protrudes beyond the prefabricated element into the topping layer, to envelop the top reinforcement bars, as well as some sturdy mechanical connection between elements, providing better load distribution between neighboring elements. It may also be desirable to include some form of a very light bottom mesh to limit the danger of spalling concrete.

It is also found that using different amount of tensioning force helps tune the element's performance and that proper balancing between sectional ductility and crack resistance may be achieved this way.

In addition, it is concluded from the results that two-way systems are better suited for use in protective structures in general. They are inherently redundant and able to absorb more energy through the formation plastic deformations in both directions at once. This is both from observing the modulation patterns in the time dependent deformation graph for the two-way systems, as well as from the hinge status results and the general outcomes at large.

Lastly, it has been observed that the un-bonded mono-strand post tensioned slab system's performance was almost as good as that of the RC slab, despite being only 75% in thickness compared to it, and far less heavily reinforced. The inherit deformability of the slab reinforced with un-bonded strands proved an asset when it comes to resisting blast loads, well distributing the energy throughout the element.

The findings of this study, along possible future research of structural systems behavior under blast loads as well as field test may open the gate to better and more efficient design of protective structural systems.

Such future research may include:

- Detailed analysis of prestressed concrete behavior under dynamic loads
- Detailed analysis of RC elements under blast loads, to examine the effects of splicing by using lapped reinforcement bars
- Detailed analysis of prestressed elements under impact/blast combinations, to predict resistance to direct hits by different munitions.
- Field testing of different structural elements to confirm previous findings

Future development work may include:

- Development of dedicated prefabricated pre-tensioned slab systems specifically designed to resist blast loads, as well as other extreme and accidental loads
- Development of special reinforcement detailing methods for the resistance of blast loads, in the case of prestressed elements.

7. Bibliography

(2015). *Analysis for Civil Structures.* MIDAS Information Technology Co.

Ashcrete. (2010). *Ashcrete catalog 2010.* Ashcrete.

Bulcomers. (2014). *81mm Mortar Round AR-M81*. Retrieved 2 12, 2017, from Bulcomers: http://www.bulcomersks.com/index.php/military-products/ammunition/32-amunition/mortal-bombs/246-81mm-mortar-round-ar-m81

Center, The Meir Amit Intelligence and Terrorism Information. (2007). *the rocket threat from Gaza 2000-2007.*

Draganić, H., & Sigmund, V. (2012). BLAST LOADING ON STRUCTURES. Osijek, Croatia.

Dullum, O. (2010). *The Rocket Artillery Reference Book.* Norwegian Defence Research Establishment (FFI).

FEMA 277. (1996). *The Oklahoma City Bombing: Improving Building Performance through Multi-Hazard Mitigation.* Federal Emergency Management Agency.

FEMA 426. (2003). *Reference Manual to Mitigate Potential Terrorist Attacks Against Building.* Federal Emergency Management Agency.

FEMA 427. (2003). *Primer for Designof Commercial Buildings to Mitigate Terrorist Attacks.* Federal Emergency Management Agency.

IDF. (2015). *Rocket Attacks on Israel From Gaza*. Retrieved June 20, 2017, from IDF website: https://www.idfblog.com/facts-figures/rocket-attacks-toward-israel/

IDF Home Front Command. (2012). *A Guide for Constructive Issues for Shelter and Protected Structure Design .*

ISO 6934-4. (1991). *Steel for the Prestressing of Concrete - part 4: strands*.

Karlos, V., & Solomos, G. (2013). *Calculation of Blast Loads for Application to Structural Components.* European Commission Joint Research Centre.

Lablanc, G., Adoum, M., & Lapoujade, V. (2005). *Blast Loads on Structures- Empirical Approach.* Toulouse, France.

Marc, A. (2016). *CONFLICT AND VIOLENCE IN THE 21ST Century.* World Bank Group.

Miller, P. (2004). *TOWARDS THE MODELLING OF BLAST LOADS ON STRUCTURES.* Toronto, Canada: University of Toronto.

Ngo, T., Mandis, P., Gupta, A., & Ramsay, J. (2007). Blast Loading and Blast Effects on Structures – An Overview. *eJSE International*.

Reddiar, M. K. (2009). *STRESS-STRAIN MODEL OF UNCONFINED AND CONFINED CONCRETE.*

Rigby, S. E. (2014, August 27). Blast Wave Clearing Effects on Finite-Sized Targets Subjected to Explosive Loads. Sheffield, UK.

Rigby, S. E. (2014). *Blast Wave Clearing Effects on Finite-Sized Targets Subjected to Explosive Loads.* Sheffield, UK.

Rubin, U. (2007). *The Rocket Campaign against Israel during the 2006 Lebanon War.* Ramat Gan, Israel: The Begin-Sadat Center for Strategic Studies .

Stewart, M. G., & Netherton, M. D. (2006). *Terrorism Risks and Blast Damage to Built Infrastructure.* University of Newcastle.

Swisdak, M. M. (1994). *SIMPLIFIED KINGERY AIRBLAST CALCULATIONS.* Silver Springs MD: Naval Surface Warfare Center.

Teng, H. (2016). *Coupling of Particle Blast Method (PBM) with Discrete Element Method for buriedmine blast simulation.* Livermore Software Technology Corp.

United Nations Office for Disarmament Affairs. (2015). NTERNATIONAL AMMUNITION TECHNICAL GUIDELINE. New York, New York, USA.

US Department of Defense. (1990). *TM 5-1300.* Washington D.C.

US Department of Defense. (2014). UFC 3-340-02 STRUCTURES TO RESIST THE EFFECTS OF ACCIDENTAL EXPLOSIONS.

US DoD. (1990). TM-5-1300. In *Structures to Resist the Effects of Accidental Explosions* (p. chapter 6A). Washington D.C.: US Department of Defense.